QUARTERLY BULLETIN OF THE DIVISION OF MECHANICAL ENGINEERING AND THE NATIONAL AERONAUTICAL ESTABLISHMENT

National Research Council of Canada
Ottawa, Ontario

1968

FOREWORD

The Quarterly Bulletin is designed primarily for the information of Canadian industry, Universities, and Government Departments and agencies. It provides a regular review of the interests and current activities of two Divisions of the National Research Council:

The Division of Mechanical Engineering
The National Aeronautical Establishment

Some of the work of the two Divisions comprises classified projects that may not be freely reported and contractual projects of limited general interest. Other work, not generally reported herein, includes calibrations, routine analysis and the testing of proprietary products.

Comments or enquiries relating to any matter published in this Bulletin should be addressed to the Editor, DME/NAE Bulletin, National Research Council, Ottawa, mentioning the number of the Bulletin.

ETCH TUNNELS
IN
2S ALUMINUM

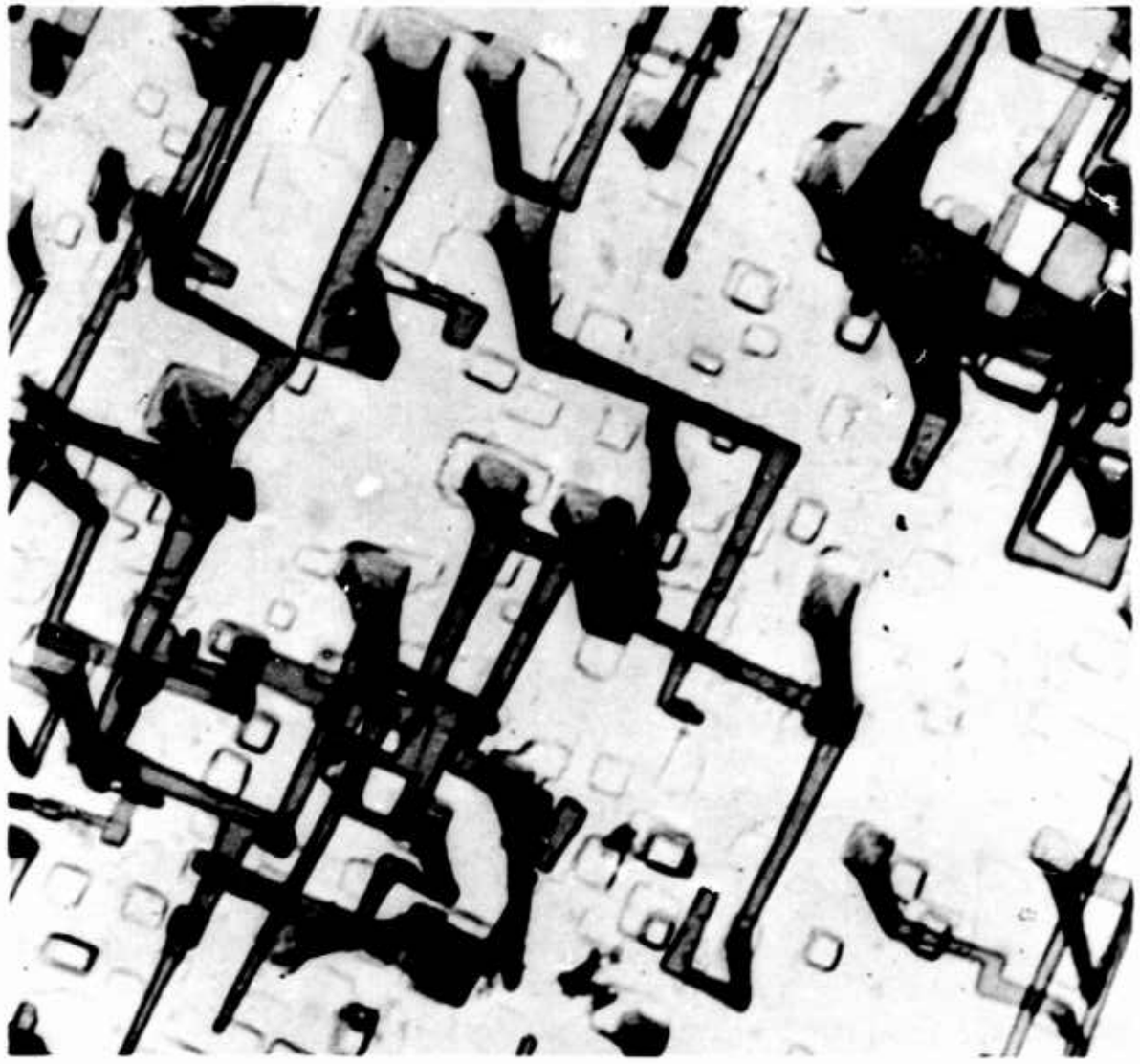

x36,000

AWARD WINNING ELECTRON MICROGRAPH BY W. WIEBE, NAE
AMERICAN SOCIETY FOR METALS, OCTOBER 1967.

STRUCTURES AND MATERIALS LABORATORY
NATIONAL AERONAUTICAL ESTABLISHMENT

A CENTENNIAL PROJECT

The National Aeronautical Establishment was asked by the Aerospace Engineering and Test Establishment (AETE) of the Canadian Forces to manufacture and install a sensitive flow vane to fit in the confined space of an existing CF-104 nose boom. The two photographs depict the vane and its installation on the CF-104. This was the aircraft used in recent altitude record attempts, a Centennial project carried out at AETE. The flight profile consisted of a high speed run up to about Mach 2.4 at 35,000 feet, followed by a zoom to maximum altitude. One critical aspect of the zoom profile was to keep the aircraft angle of attack below certain limits. These limits, if exceeded, could have resulted in the CF-104 entering a flat spin, a manoeuvre from which recovery is almost impossible. Therefore, angle of attack had to be accurately obtained and displayed in the cockpit. The existing angle of attack indicator on the CF-104 proved much too insensitive at the high altitudes reached during the zoom.

A vane had to be designed that would withstand the high dynamic pressure of the Mach run ($q \doteqdot 9200$ psf), yet still be capable of producing accurate angle of attack readouts in the low "q" regimes encountered at the top of the zoom profiles ($q \doteqdot 10$ psf).

The vane shown in these photographs, designed and built by the Flight Research Laboratory, performed extremely satisfactorily throughout more than 30 altitude record attempts flown during the project.

CONTENTS

CONTENTS (Cont'd)

ILLUSTRATIONS

ILLUSTRATIONS (Cont'd)

ILLUSTRATIONS (Cont'd)

Page

CURRENT PROJECTS (Cont'd)

THE EFFECT OF PSYCHOLOGICAL STRESS ON DECISION PROCESSES IN A TRACKING TASK

C.B. Gibbs

Control Systems Laboratory

Division of Mechanical Engineering

1. INTRODUCTION

The human brain is the most complicated control system on Earth, but little is known of the operational methods that are used within the central nervous system. However, recent research on biological control mechanisms has produced findings and inventions of potential social value in reducing accidents.

Many lethal weapons have been produced by intent but none has approached the mortality rate achieved incidentally by the automobile. This mass slaughter may be attributed in part to faults in the design of vehicles and traffic systems, but many forms of psychological stress impair driving ability and are undoubtedly major causes of accidents.

Stress is defined as a force that can produce strain or distortion in a system. Psychological stress can be applied to human beings by the use of alcohol, drugs, or by fatigue, frustration or many other influences. It is extremely difficult to detect impairment in actual performance because increased expenditure of energy or effort may mask the effects of stress upon the aspects of behaviour that are readily observed and measured.

The precision of tracking movements made in a limited time is frequently measured in laboratory studies of stress. Precision is obviously important in driving automobiles, but it is clear that incorrect decisions, rather than lack of precision in executing movements, are major causes of traffic accidents. Reference 1 describes a tracking task wherein subjects had a choice between rapid decisions, which usually produced incorrect responses, and more deliberate judgments, which normally led to appropriate action. Reference 2 shows that the rate of making accurate decisions is often impaired by moderate doses of alcohol, and there can be no serious doubt that impaired judgment is a major cause of the high correlation between drinking and traffic accidents that is described in Reference 3.

2. THE STRESSALYZER

There is a serious shortage of rapid, sensitive tests of the effects of

stress upon those aspects of skill that are known to be important in controlling vehicles. In an effort to provide more sensitive measures, an instrument called the stressalyzer was developed to provide a rapid and simple test of a person's ability to control a machine. A handwheel and pointer are used to track a target that appears equally frequently, at two-second intervals, at one of five different positions. The handwheel and the pointer move in opposite directions, and this arrangement causes the operator to make an appreciable number of tracking errors, i.e., tracking movements that start in the wrong direction.

A target starting from either of the outside Positions 1 or 5 can only move inward, and these steps are termed "unequivocal". There is a 3 to 1 probability that a target starting from Position 2 will next move to the right rather than outward to Position 1; a target at Position 4 is more likely to move left than right. Steps are termed "probable" when the movement actually demanded conforms to the higher probability; steps outward from Positions 2 or 4 are called "improbable". A target starting from Position 3 is equally likely to move in either direction, and these steps are called "equiprobable".

Response latency or reaction time is the period elapsing between the appearance of a target and the beginning of the operator's response. The stressalyzer provides simple, read-out records of response latency, the number of response latencies exceeding 0.4 second, the number of errors, and the number of targets acquired with high precision in one run.

Figure 1 shows the average results of a group of 12 subjects. The height of the solid black bars indicates the percentage of errors on improbable and probable steps, and it is clear that error percentage is far higher on the former than on the latter steps. The height of the circles represents response latency for correct responses, whereas the latency of movements that start in the wrong direction is indicated by the height of the crosses. The graph shows that it takes much longer to reach a correct decision on improbable than on probable steps. On improbable steps, short latency usually produces an error, whereas more delibertate decisions normally lead to a correct response.

3. THE EFFECTS OF SLEEP DEPRIVATION ON SKILL

A tired subject is often stimulated by the challenge of a test situation and may perform well for a limited period. Performance on some tasks is impaired little, if at all, by prolonged sleep loss. Sleep deprivation reduces efficiency in a typical vigilance task of detecting a faint, infrequent signal, but even when subjects have normal sleep, their performance often deteriorates as their time on watch increases. In many tasks, it is difficult or impossible to decide whether sleep loss reduces motivation through the effects of boredom or whether it produces actual impairment of skill. The theoretical issue has important practical implications because reduced motivation can be offset by a

variety of means, whereas the condition of impaired skill can only be remedied by rest and sleep.

Previous studies of sleep deprivation, using conventional methods of testing, have produced a variety of opinions on the cause and effects of impairment by sleep loss. Reference 4 indicates that 30 hours sleep deprivation had little effect on performance when subjects were given knowledge of the results of their performance, but there were adverse results when this information was withheld. In Reference 5, Wilkinson suggested that motivational factors were important determinants of the degree of impairment, and concluded that: "Sleep deprivation reduces the level of arousal or activation of the body. If the incentive is there, however, this can be overcome, so that arousal and therefore performance are maintained at normal levels".

There is an urgent requirement for a rapid test that can detect impairment of skill by fatigue, as distinct from the boredom that may be produced by a lengthy test. The stressalyzer sets a task of brief duration and provides measures of response latency, errors, and the number of response latencies exceeding 0.4 second. These measures relate to the speed and precision of movements and the rate of making correct decisions on improbable events; the long latencies may well reflect or precede potentially dangerous lapses of attention. These are important factors in controlling vehicles and other machines, and the stressalyzer was therefore used in studies of sleep deprivation.

The very different effects of fatigue on various tasks may be due to differences in their inherent interest, as suggested in Reference 5, or to distinctions drawn in References 6 and 7 between the times available to complete different tasks. The stressalyzer presented a paced task wherein targets appeared for a limited time. An unpaced task of mirror tracing was also used in the studies of sleep deprivation. The subjects used a metal stylus to trace over the outline of a star while viewing reflections of the star and stylus in a mirror. The total time taken for tracing and the period wherein tracing was precise were both recorded.

4. SLEEP DEPRIVATION FOR 48 HOURS

Twelve youths, aged between 16 and 19 years, volunteered for the tests and were given preliminary, spaced practice totalling nearly four hours on each task. They were then deprived of sleep for 48 hours, while kept under close supervision. The experiment started at 0900 hours and each subject was tested on both tasks in each subsequent four-hour period. The group had three runs on the stressalyzer in each test session, and a similar time was spent on mirror tracing.

The average scores of the group on three successive runs on the stressalyzer are shown in Figure 2, wherein captions define the meaning of the

plotted symbols. The Figure shows separately the mean response latency (R.L.), the number of targets missed (T.M.), and directional errors (E). The combined effects of these different effects are also shown by a statistic based upon the product of response latency and the sum of targets missed and errors. The actual statistic used, 4 (R.L.) (T.M.+E), was derived to provide sensitive discrimination among the abilities of different subjects, among the effects of different experimental conditions, and to provide a suitable scale for the graphs.

The figures at the foot of Figure 2 show the hours elapsed from the start of the test. There was an appreciable rise in the statistic after sleep deprivation of 20 hours. There was also a rise in the percentage of long response latencies exceeding 0.4 second, denoted by closed circles, some ten hours after starting the test, with another pronounced rise when the group had been deprived of sleep for 28 hours. The detailed results show large differences among individuals in their tolerance of sleep deprivation.

Figure 3 shows the results of Subject 3; the figures at the top of the graph show the time of day, and immediately below this the relative ranking of the individual in a group of 12 subjects, in respect to the various measures that were obtained. In overall ability, as shown by the statistic, Subject 3 began with the worst score in the group but ended the test ranking third, because he maintained a more consistent performance than many other subjects although there was no improvement in his absolute scores.

Figure 4 shows the results of Subject 2 and the considerable deterioration in his overall ability, as denoted by the statistic, only 10 hours after testing began, although his initial ranking was higher than that of Subject 3. There was also a large increase in his percentage of long latencies some 16 hours after testing began.

Figure 5 shows the results of Subject 12 who ranked seventh in overall ability, as denoted by the statistic, when the tests began, but ranked only tenth after 48 hours without sleep. Comparison of Figures 3 and 5 shows a hare and tortoise effect, because the initial ranking of Subject 3 with respect to the statistic was lower than the ranking of Subject 12, but the order was reversed by the end of the test.

Figure 6 shows large fluctuations in the percentage of long latencies produced by Subject 8. This percentage was extremely high between 0900 and 1300, some 28 hours after beginning the test, but at this stage his movements were still rapid and precise, few targets were missed, and few errors were made. In tests conducted between 0100 and 0500 hours, with sleep deprivation of about 44 hours, there was again a high percentage of long response latencies accompanied by considerable impairment of tracking ability.

Sleep deprivation for 48 hours had much less effect on the unpaced task of mirror tracing than on the paced task set by the stressalyzer. In

tracking, the group's percentage time on target was 81% in the first test session, with a slight drop in precision to 77.6% in the last session. In contrast, the average time per run was reduced from 37 seconds to 33 seconds in the first and last sessions, respectively.

5. THE EFFECT OF DISTURBED SLEEP ON SKILL

Reference 5 notes the paucity of studies of partial sleep deprivation, which is probably of greater practical importance than complete deprivation. The previous study was therefore extended. The same 12 youths were again tested over a 48-hour period wherein sleep was permitted, although sleeping subjects were aroused periodically at night and tested some 15 minutes after waking, at the times and intervals used in the previous sleep deprivation experiment.

Figure 7 presents group data for the mean of three runs made during each test session on the stressalyzer, and shows considerable deterioration in group performance in the early morning, between 0100 and 0900 hours. Figure 8 shows the detailed scores of Subject 2 and allows comparisons with his scores shown in Figure 6, which were obtained in the study of complete sleep deprivation. The impairment of Subject 2, soon after waking in the early morning, exceeded the deterioration produced in any one subject by 48 hours complete sleep deprivation in the previous study, or by the highest alcohol dosage tested in studies that are described later. Another subject was found to be impaired, to an even greater degree than Subject 2, when tested soon after waking.

6. THE COMBINED EFFECTS OF SLEEP LOSS AND ALCOHOL

Eight young men in another group were kept awake for 36 hours and had three runs on the stressalyzer at five hourly intervals. The subjects drank spirits before taking the last test and the average breathalyzer reading of the group, in the last test session, was about 0.08%.

A surprising finding is illustrated by Figure 9. In spite of intoxication and sleep deprivation, the average group scores were better on the last run than on the first. Five of the eight subjects had worse scores on their first run than on their last trial. Figure 10 shows the scores of Subject H, who was one of two subjects exhibiting gross impairment in early trials, although all subjects had been awake for at least one hour before their first test began. The scores of this subject and of the group as a whole improved some five hours after testing began, and from then on increasing sleep deprivation, together with alcohol consumption before the last session, produced little or no impairment in respect to response latency, targets missed, or errors. Figures 9 and 10 show a high percentage of long latencies, however, during the last session.

7. A COLLABORATIVE STUDY

A further study was conducted in collaboration with the Human Resources Research Office (HumRRO) of the George Washington University. The HumRRO scientists conducted tests on a simulated driving task, and a task of monitoring four screens in a typical vigilance test in which the subjects were required to report the appearance of a faint light on a screen. The National Research Council (NRC) team conducted tests on the stressalyzer, and the two groups communicated data on a reciprocal basis.

In the HumRRO study, five test booths were provided and two men occupied each booth. One man, termed the driver, used a steering wheel to position a tracking index, in a simulated task of steering along a winding road. The scores termed "time off target" denote the period wherein the tracking index was outside the limits of the simulated road during a test session of 90 minutes. The other man, termed the monitor, watched four large screens and was required to report the appearance of a faint orange light that appeared briefly, at random intervals, on 15 occasions during a test period of 90 minutes. Both tasks, of monitoring and simulated driving, were carried out continuously during each test session. A test session was normally followed by a rest pause of 15 minutes, but there was a longer break of one hour for a meal, beginning at 0700, 1300, 1900, and 0100 hours. Each man had three successive runs on the stressalyzer at intervals of about four hours. The times of testing and the average results of ten men who were tested are shown in Figure 11.

Figure 11 shows the group's average results on the stressalyzer, using symbols already defined. Squares are used in plotting the data kindly provided by HumRRO scientists, and again a rise in the curve indicates worsened performance. The solid squares represent the monitors' scores in a 90-minute session. The number of signals missed is expressed as a proportion of the total number of signals presented. The open squares indicate the drivers' performance; the time off target is expressed as a proportion of the total 90 minutes of the test.

Figure 11 shows a large increase in the proportion of signals missed, about 21 hours after starting the test, but the drivers did not show a comparable increase in time off target until near the 33-hour stage. Over much of the test, the signals missed on the vigilance task and the latencies of 0.4 second or more on the stressalyzer, tended to increase or to decrease together. The results of Subject F, shown in Figure 12, are a striking example of this correlation.

8. THE EFFECTS OF ALCOHOL ON SKILL

Research on the effects of alcoholic stress has been hampered by the lack of an adequate analysis of skill and the absence of rapid and relevant

test procedures that could be standardized. Chemical and physiological tests are available that show the effects of alcohol on the breath or blood of subjects, but such tests do not provide insight into the effects of alcohol on actual behaviour.

Figure 13 shows the effects of alcohol on three individuals, selected from 150 subjects tested to date, to illustrate the wide range of differences among individuals in their innate ability, tolerance of stress, and the strategies they adopt under alcoholic stress. The number of errors is shown by triangles scaled on the left ordinate, and response latency is indicated by circles, scaled in portions of one second, on the right-hand ordinate. The errors and response latencies are plotted separately for each subject when his breathalyzer reading was zero, and after drinking had raised the b.a. level to about 0.05% and then to 0.1% or more, as shown at the foot of the Figure. The first graph shows the average results of three runs by a subject who progressively reduced his response latency with increased intoxication, with a consequent large increase in errors. The third graph is from a subject with a similar preference for rapid reactions rather than slow, accurate decisions. The second graph is from a subject who adopted the opposite strategy by increasing his reaction time as intoxication increased, thereby minimizing his errors. This subject made fewer errors with a breathalyzer reading of 0.11% than the other subjects made when they were sober.

Figure 14 shows the average results of a group of 12 subjects who were first tested when sober, and later after drinking had raised the group's average breathalyzer reading to 0.05% and then to 0.1%. All subjects had three runs on the stressalyzer at all three levels of intoxication. Drinking ceased on reaching the 0.1% level, but the subjects were tested later when the average breathalyzer reading of the group had fallen to 0.05% and then to zero. The two graphs of Figure 14 show results on two consecutive days, and it is clear that increasing intoxication did not increase errors on highly probable steps, whereas there was a large increase of errors on improbable steps. In Figure 14, the circles show average response latency on improbable steps, and the graphs indicate considerable increase in latency with increased dosage. A striking finding is that impairment persisted some seven hours after consuming a dosage that produced a peak reading of about 0.1%, although breathalyzer readings had then fallen to zero. There was little difference between this residual impairment and the deterioration shown with a breathalyzer reading of 0.05%.

9. DISCUSSION

The stressalyzer sets a task that was first developed to analyze perceptual-motor skill, rather than to study stress. In an early study, three of four subjects showed gross impairment compared with their previous performance. This impaired subjects admitted to heavy overnight drinking, although this

had ended ten hours before testing began. These subjects were not given knowledge of results and their performance deteriorated steadily over the test session of 30 minutes.

Another group of 12 subjects slept in the laboratory to permit strict control of drinking. These subjects were tested on the stressalyzer but were not told their scores. Figure 14 shows considerable residual impairment many hours after drinking had ended and breathalyzer readings had returned to zero. At the zero level, 11 of the 12 subjects performed better before drinking began than after drinking had ended; the other subject had equal scores on pre-drinking and post-drinking runs. This study leaves no doubt of the highly adverse after-effects of alcohol.

In all other experiments, subjects were given knowledge of their results and separate tests showed that such information often improved performance and tolerance of stress, compared with test conditions when no knowledge was given. The largest change was that one subject acquired 90 of 100 targets presented when given knowledge of results, but only 58 on his second run after this information was withheld.

Figures 3, 4, and 5 illustrate large individual differences in innate ability and tolerance of sleep deprivation, similar to the variation shown in the alcohol studies. Of the 12 subjects, two showed very high resistance to fatigue and little impairment at the end of 48 hours of sleep deprivation. Figure 4 shows that Subject 2 was definitely impaired eight to twelve hours after testing began, and one other subject also showed very low tolerance of stress. The remaining eight subjects showed intermediate tolerance, and Figure 5 shows representative results of good performance until the 44-hour stage but gross impairment in the final test session.

Figure 7 shows the results of the same group in conditions where subjects slept at night but were awakened in turn at about four hourly intervals through the night and tested 15 to 20 minutes after waking. A comparison at the 24-hour stage, based upon the statistic 4 (R.L.) (T.M.+E) of Figures 2 and 7 shows that the group performed very much better in the condition of complete sleep deprivation than in the test where they slept but were tested soon after waking. A similar comparison at the 44-hour stage shows that impairment from disturbed sleep had a cumulative effect that was certainly not less than the impairment following 44 hours of complete loss of sleep. Figures 4 and 8 show the scores of Subject 2, and similar comparisons, using the statistic, support the above conclusion. The scores of Subject 2 at the 44-hour stage (Fig. 8) were far worse than the results of any subject in the studies of alcohol effects and complete sleep deprivation.

A further group of eight subjects had no sleep for 36 hours, and consumed alcohol before the last test session began. In the interests of realism, the overnight drinking of these subjects was not controlled, but they were asked

to state the amount of alcohol consumed on the night before testing. Cross checks were made within the group. The results of the group are shown in Figure 9, and there was little apparent impairment during their last run, compared with their first. In everyday observation, two sources of stress may tend to cancel rather than compound each other, as in the familiar example of loud noise tending to offset the effects of sleep deprivation. In the present study, the consumption of a limited amount of alcohol did not have the expected effect of lowering group performance, but this result may be due to the introduction of a novel, welcome factor into the test routine, rather than to the beneficial or neutral effects of alcohol per se. Certainly, the poor initial performance of the group, shown in Figure 9, was largely due to the gross impairment of Subject H (Fig. 10) and one other subject in their first test session. This impairment confirms many previous findings of poor initial performance, followed by improvement due to the so-called "warm-up" effect, but the gross degree of initial impairment of two subjects suggests that overnight drinking was an additional cause of their extremely poor performance. This suggestion is compatible with the impressions received from cross-questioning within the group.

Some results of the experiments conducted in collaboration with HumRRO scientists are shown in Figures 11 and 12, and the most striking finding is the close correlation between signals missed in the HumRRO test of vigilance and the number of long response latencies found in the NRC stressalyzer experiment. Complete identity of results was not expected, nor found, because subjects were under direct observation and supervision in the stressalyzer test but were isolated in a booth during the tests of vigilance and simulated driving. Despite large differences in the degree of coercion employed, it is clear that increases of long latencies in the stressalyzer test lasting one or two minutes, were reflecting the lowered attentiveness that increased the number of missed signals in the vigilance test lasting 90 minutes. In the former, unlike the latter test, increased impairment could not be attributed to boredom or to withdrawal from the task.

Figure 1 shows that long latencies on improbable steps usually produce correct responses, and an increased number of long latencies could result from increased stress and a compensatory increase in the effort expended to maintain an adequate standard of overt tracking performance on the stressalyzer test.

This explanation is compatible with data presented in Figure 2. At the 28-hour stage, there was a large increase in the percentage of long latencies, although the statistic, reflecting overall tracking ability, did not show a similar abrupt rise until the 36-hour stage. With further sleep deprivation of 44 hours, and then 48 hours, long latencies increased and there was a concurrent deterioration in overall tracking ability as shown by the statistic. Figure 7 illustrates a general group tendency to perform worse by night than by

day; the well-known effect of the circadian rhythm. Subject 8, as shown in Figure 6, had an abnormally large increase in long latencies about 28 hours after starting the test, but this was associated with slight improvement in overall tracking scores as denoted by the statistic. A large increase in his long latencies and serious impairment of tracking ability occurred about 44 hours after commencing the test. He was the only subject who developed a psychosomatic disability, and who failed to complete the second part of the test wherein sleep was disturbed.

Figure 9 shows little difference in scores in the first and last session of a group, although they were intoxicated and had been deprived of sleep for about 32 hours when the last runs were made. However, there was a high percentage of long latencies in the last session, and in other groups and individuals such increases immediately preceded deterioration in tracking performance. Many writers have considered that these so-called blocks or lapses reflect brief periods of sleep, or a condition like sleep. In sharp contrast, the present view is that, at least on their first appearance, these blocks probably reflect periods wherein considerable energy is expended in an effort to maintain adequate tracing performance. The traditional explanation may be valid at a later stage in sleep deprivation, when tracking performance indicates considerable impairment.

Williams et al report in Reference 7 that in their experiments, using subject-paced tasks, sleep deprivation produced a decrease in speed but little or no change in accuracy. In contrast, both speed and errors increased with sleep loss in the present experiment, using the subject-paced task of mirror tracing. It is possible that the relative effect of sleep loss upon speed and error is greatly affected by the degree of continuity of tasks.

Differences in the vulnerability of various tasks to sleep deprivation have been attributed to differences in experimental conditions such as the interest, complexity, and duration of a task, or the presence or absence of monotony or knowledge of results. For some purposes, Broadbent and Williams et al, in Reference 6 and Reference 7 respectively, found it useful to distinguish between paced tasks wherein the experimenter controls the onset and timing of a stimulus, as in a vigilance test, and unpaced tasks such as mirror tracing where the subject determines his own speed and timing.

In the NRC and HumRRO studies, there were large differences of impairment in tasks of equal duration when full knowledge of results was given in all cases. The considerable impairment on the stressalyzer cannot be attributed to monotony because the test lasted only two minutes. There was severe impairment in two paced tasks, of vigilance and stressalyzer tracking, but comparatively little deterioration on the paced task of simulated driving. The distinction proposed by Wilkinson in References 2 and 5, to account for such differences between tasks, is based on the mentalistic, qualitative term and concept of relative interest, but in conflict with this hypothesis, the opinion

of all subjects was that the stressalyzer was more interesting than mirror tracing. The distinctions proposed to date are not valid for classifying tasks according to their vulnerability to fatigue.

The real basis for differences in the vulnerability of various tasks to stress, is the relative amount of external information that must be processed for efficient performance, the continuity of the task, and the amount of advance information on response requirements that is available in the task. No information is conveyed by a statement of the obvious, and more information is conveyed by the occurrence of an improbable than a probable event. Figure 14 shows that stress affects decisions on improbable rather than probable events. The NRC unpaced task of mirror tracing, and the HumRRO paced task of simulated driving, were continuous and gave anticipatory information on the responses required. The tasks did not demand unexpected responses and little external information had to be processed for efficient performance. In sharp contrast, the stressalyzer and the vigilance task required responses to improbable events or to signals that appeared at random, unpredictable intervals; the occurrence of such stimuli presented considerable information.

An important finding, reported by Wilkinson in Reference 4, was that knowledge of results reduced the adverse effects of sleep deprivation. In contrast to Wilkinson's interpretation, however, it is concluded by this writer that the major effect of knowledge of results is to enhance objective information, rather than subjective interest, thus compensating for the reduction by stress, of the rate at which a subject can process information. Experiments on knowledge of results are continuing and analysis is not yet complete, but at this stage it seems highly probable that the different effects of alcohol-induced stress on the scores of two groups, illustrated by Figure 13 and Figure 9, are due mainly to the effects of knowledge of results. The rapid recovery of Subject H, shown in Figure 10, was probably also due to the immediate information he was given on his scores; no recovery occurred in an earlier test, where the hangover effect was observed and no relevant knowledge was given.

10. ACKNOWLEDGEMENTS

Mr. G. Rowlands of the Royal Aeronautical Establishment, Farnborough, U.K., provided capable assistance on some of the tests, while seconded to the Division of Mechanical Engineering. Doctor L.D. Cannon, Mr. E.H. Drucker and Mr. J.R. Ware, all of HumRRO, kindly provided data on the experiments that they conducted on vigilance and simulated driving. Mr. D. Gibbs, and Mr. R. Hughes made valuable contributions to the design of instruments used in the studies. Thanks are also due to members of the Defence Research Board of Canada, and of the Armed Services of Canada and the United States of America for considerable help in arranging and conducting the experiments.

11. REFERENCES

1. Gibbs, C.B. — Probability Learning in Step-Input Tracking. Brit. J. Psychol., Vol. 56, Nos. 2 and 3, 1965, pp. 233-242.

2. Gibbs, C.B. — The Effect of Minor Alcohol Stress on Decision Processes in a Step-Tracking Task. I.E.E.E. Trans. on Human Factors in Electronics, Vol. HFE-7, Number 4, Dec. 1966, pp. 145-150.

3. Borkenstein, R.F. Crowther, R.F. Ziel, W.B. — The Role of the Drinking Driver in Traffic Accidents. Dept. of Police Administration, Indiana University, U.S.A., 1964.

4. Wilkinson, R.T. — Interaction of Lack of Sleep with Knowledge of Results, Repeated Testing and Individual Differences. J. Exp. Psychol., Vol. 62, Number 4, 1961, pp. 263-271.

5. Wilkinson, R.T. — "Sleep Deprivation" in "The Physiology of Human Survival". Editors, V.G. Edholm and A.L. Bacharach, Academic Press, London, 1965.

6. Broadbent, D.E. — Noise, Paced Performance and Vigilance Tasks. Brit. J. Psychol., Vol. 44, 1953, pp. 295-303.

7. Williams, H.L. Lubin, A. Goodnow, J.J. — Impaired Performance with Acute Sleep Loss. Psychol, Mono., Vol. 73, Number 14, 1959.

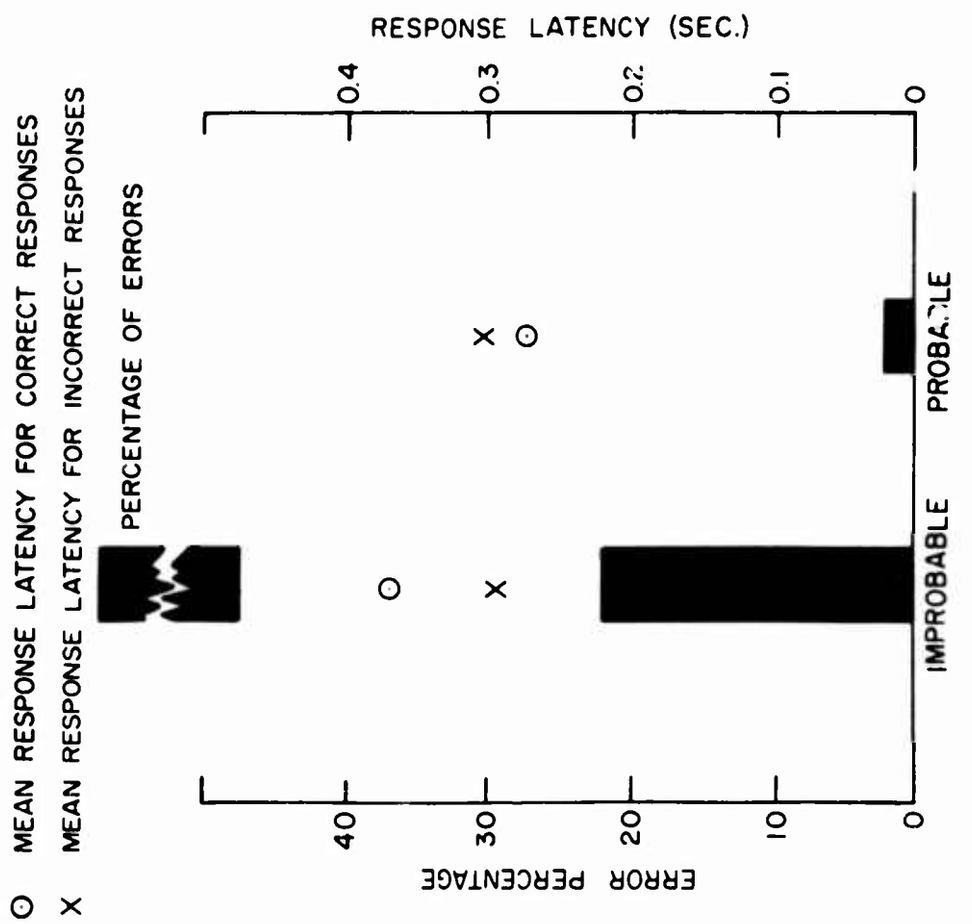

FIG. 1 MEAN RESPONSE LATENCY FOR CORRECT AND INCORRECT RESPONSES AND PERCENTAGE OF ERRORS ON STEPS OF DIFFERENT PROBABILITY

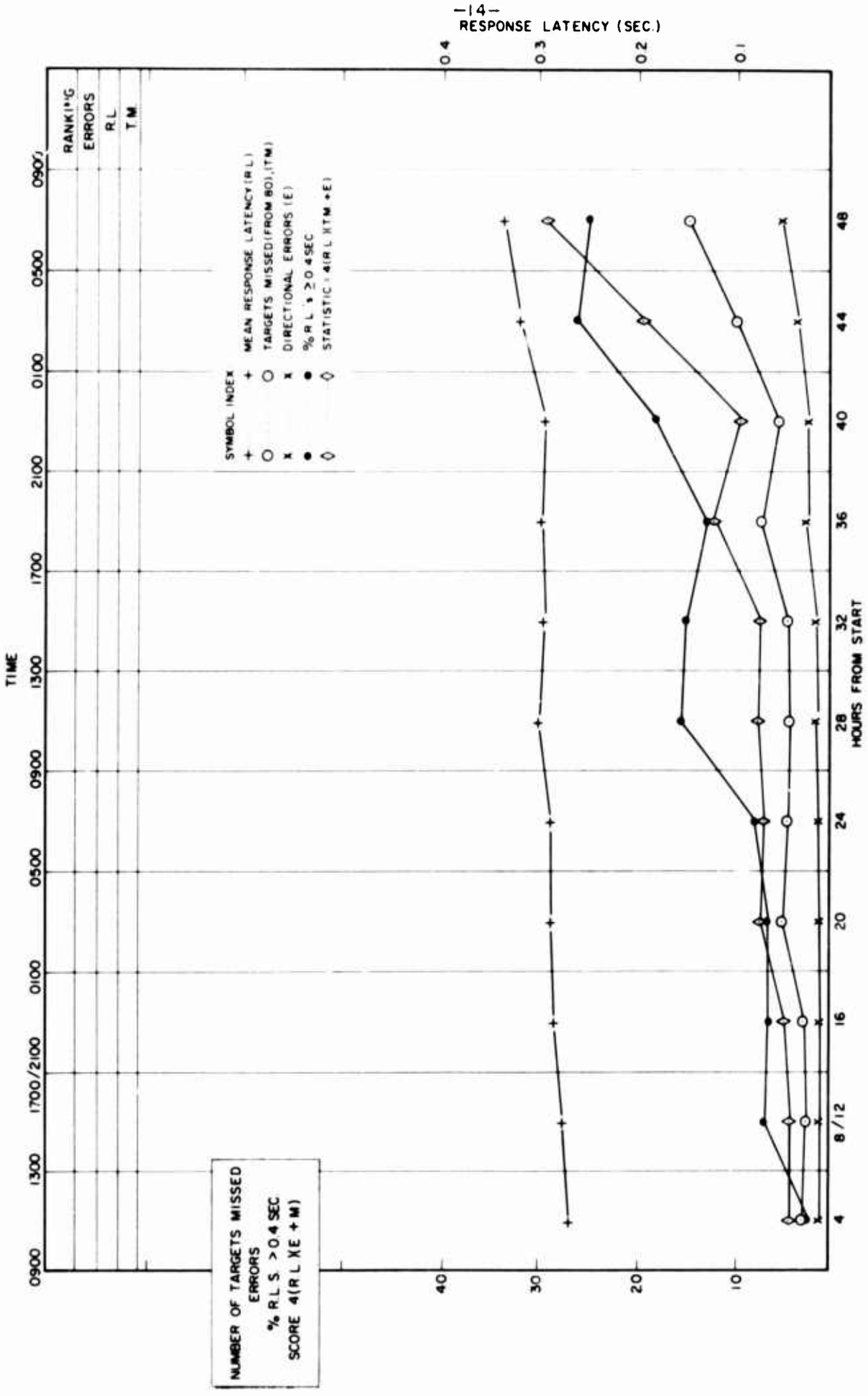

GROUP RESULTS 15/7/66

FIG. 2

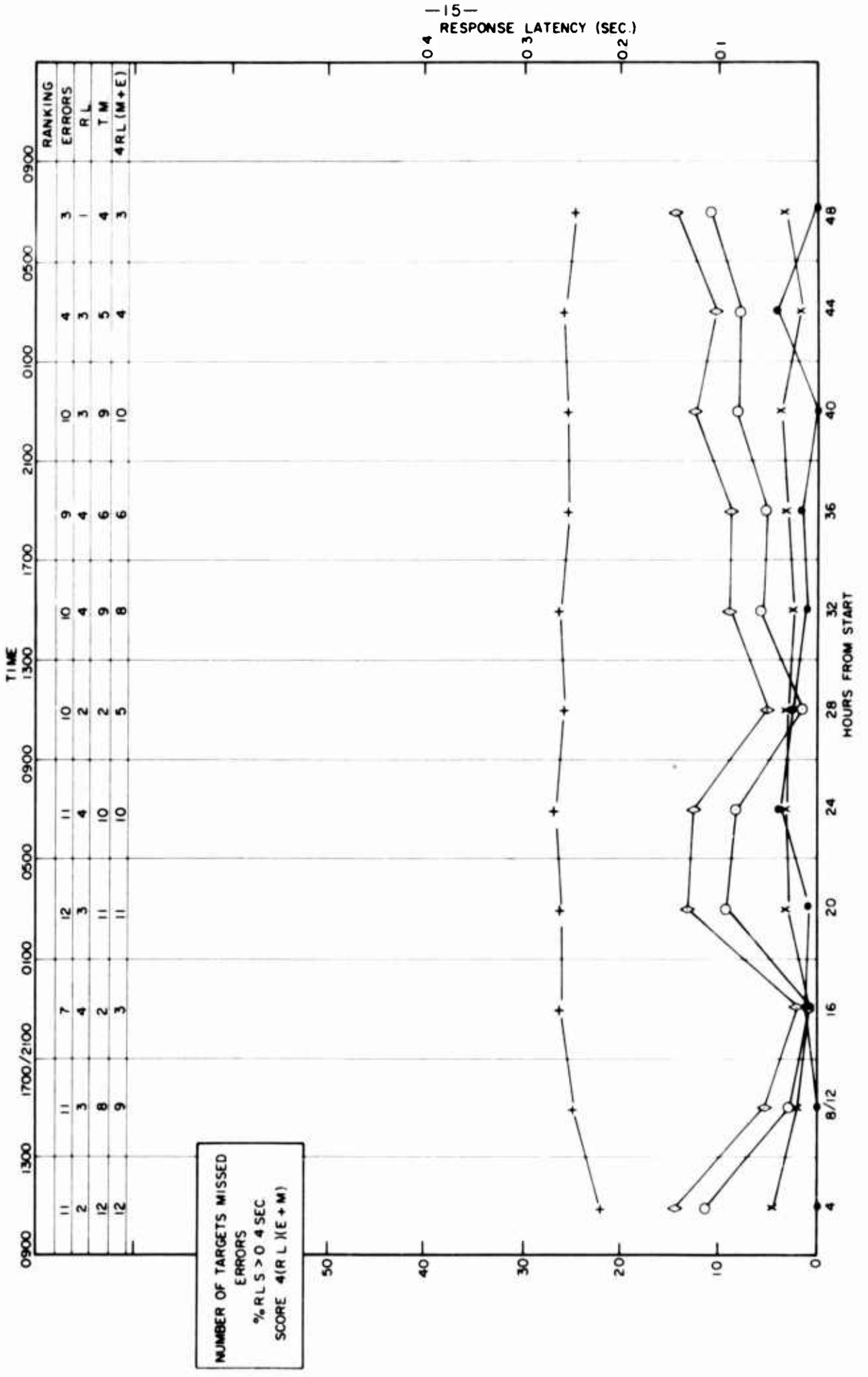

FIG. 3

SUBJECT 3

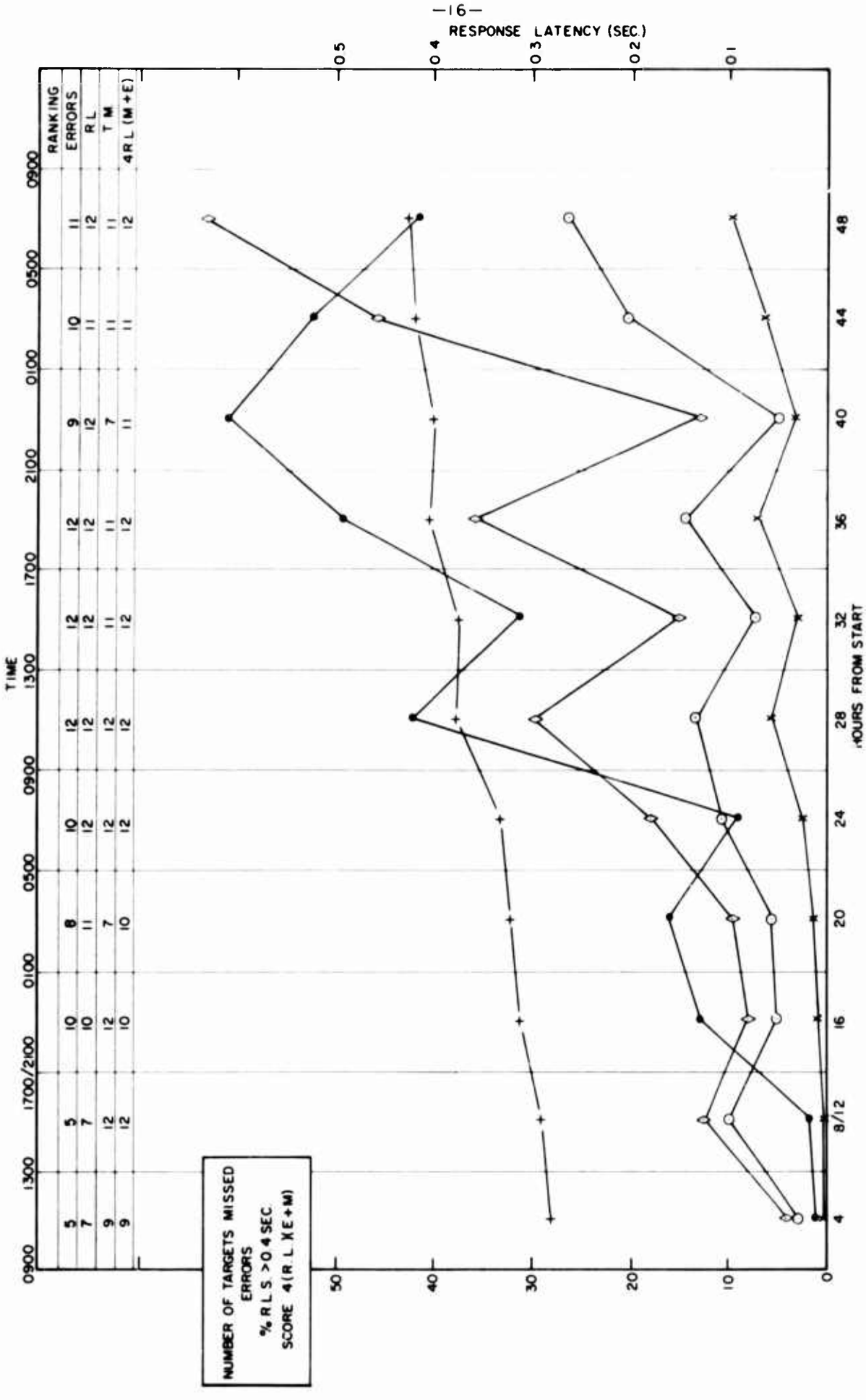

SUBJECT 2

FIG. 4

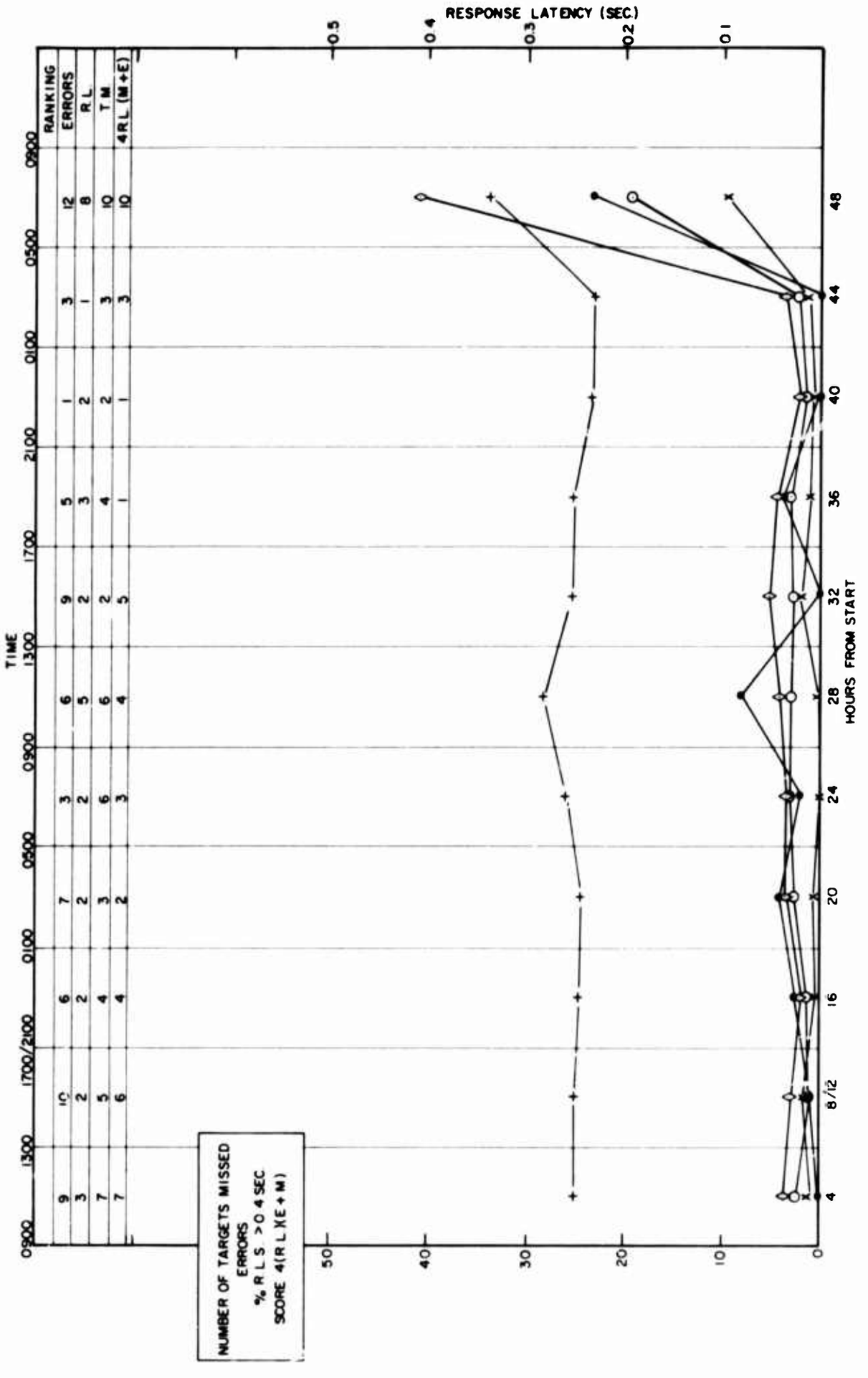

SUBJECT 12

FIG. 5

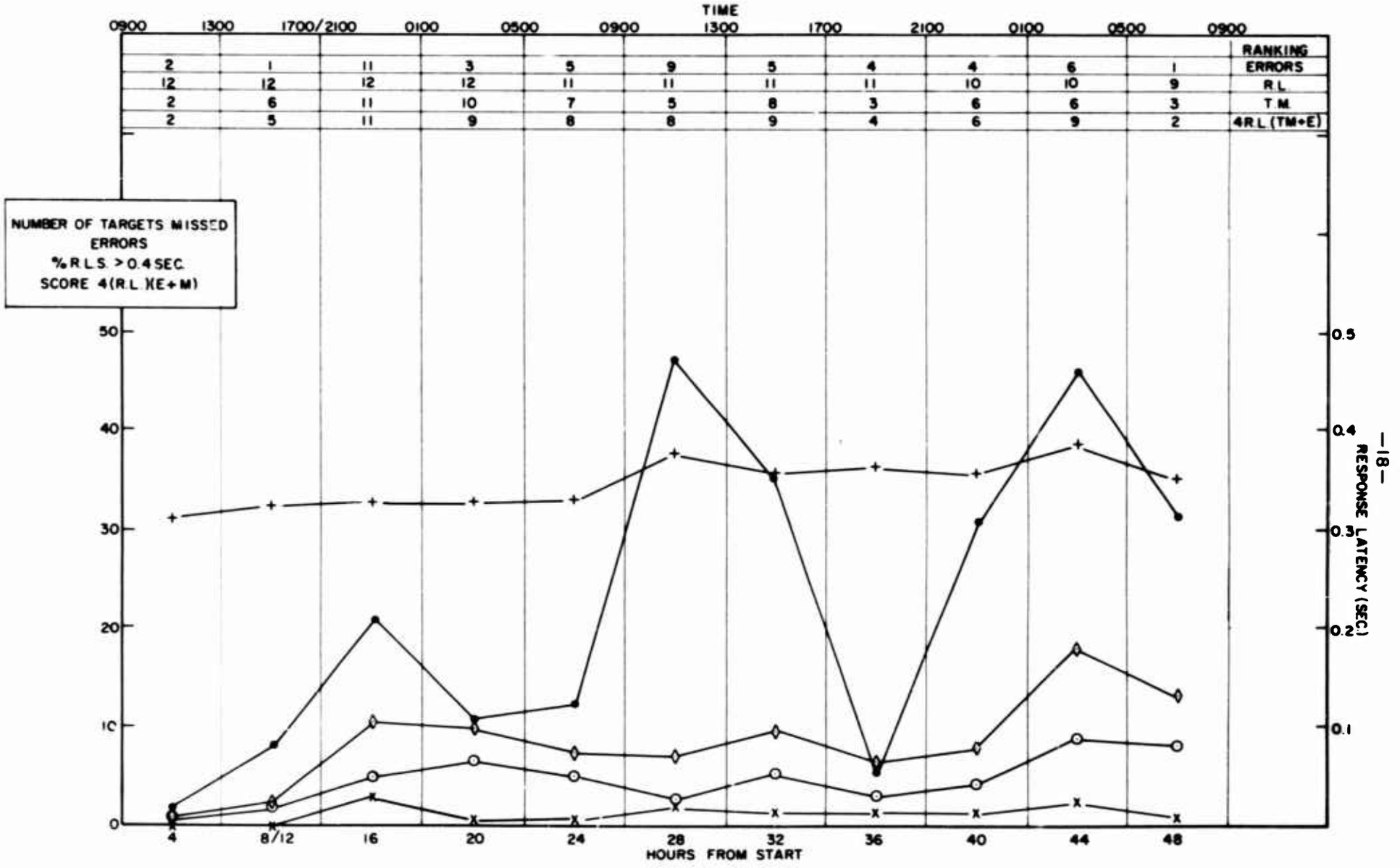

FIG. 6

SUBJECT 8

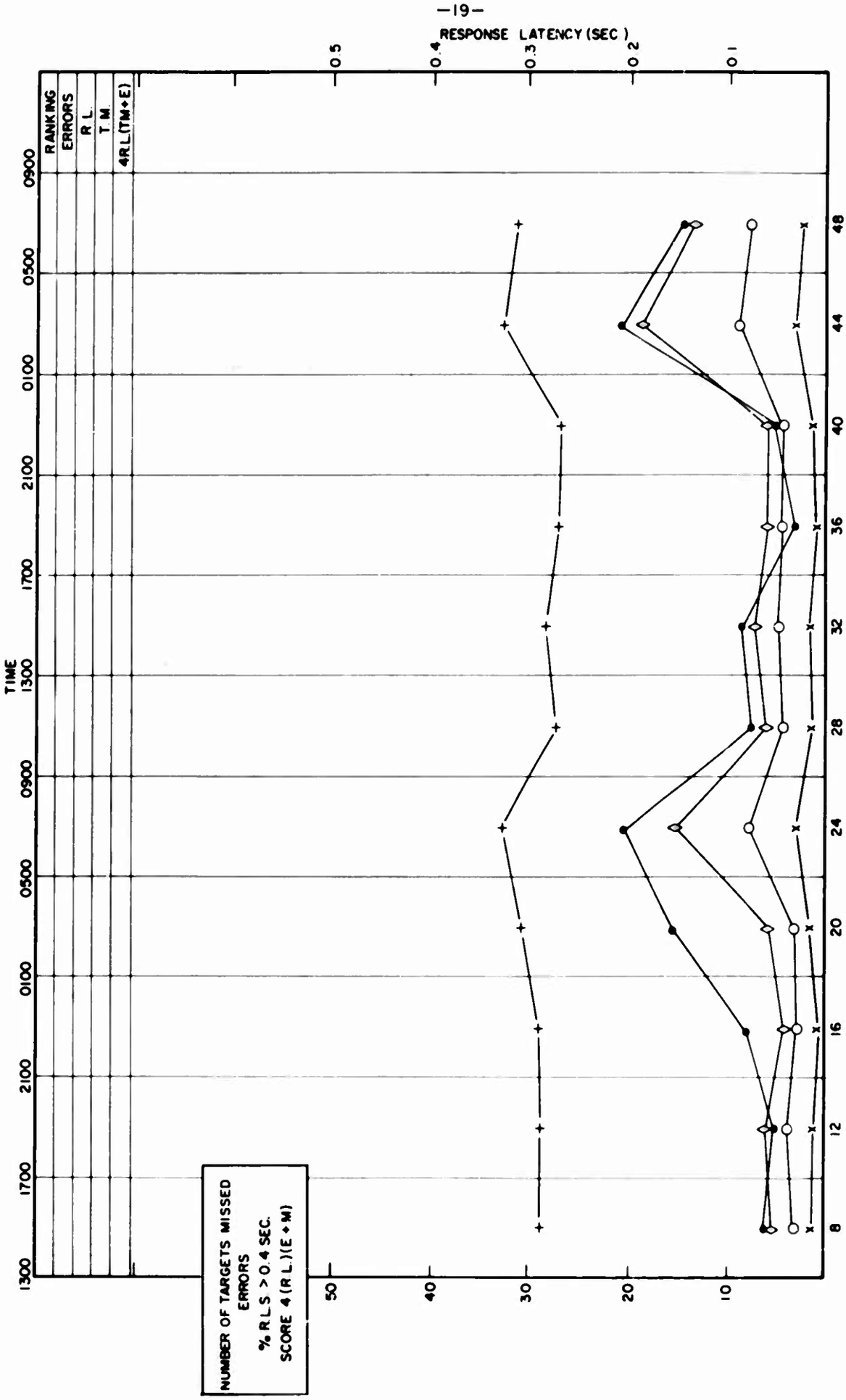

GROUP RESULTS 22/7/66

FIG. 7

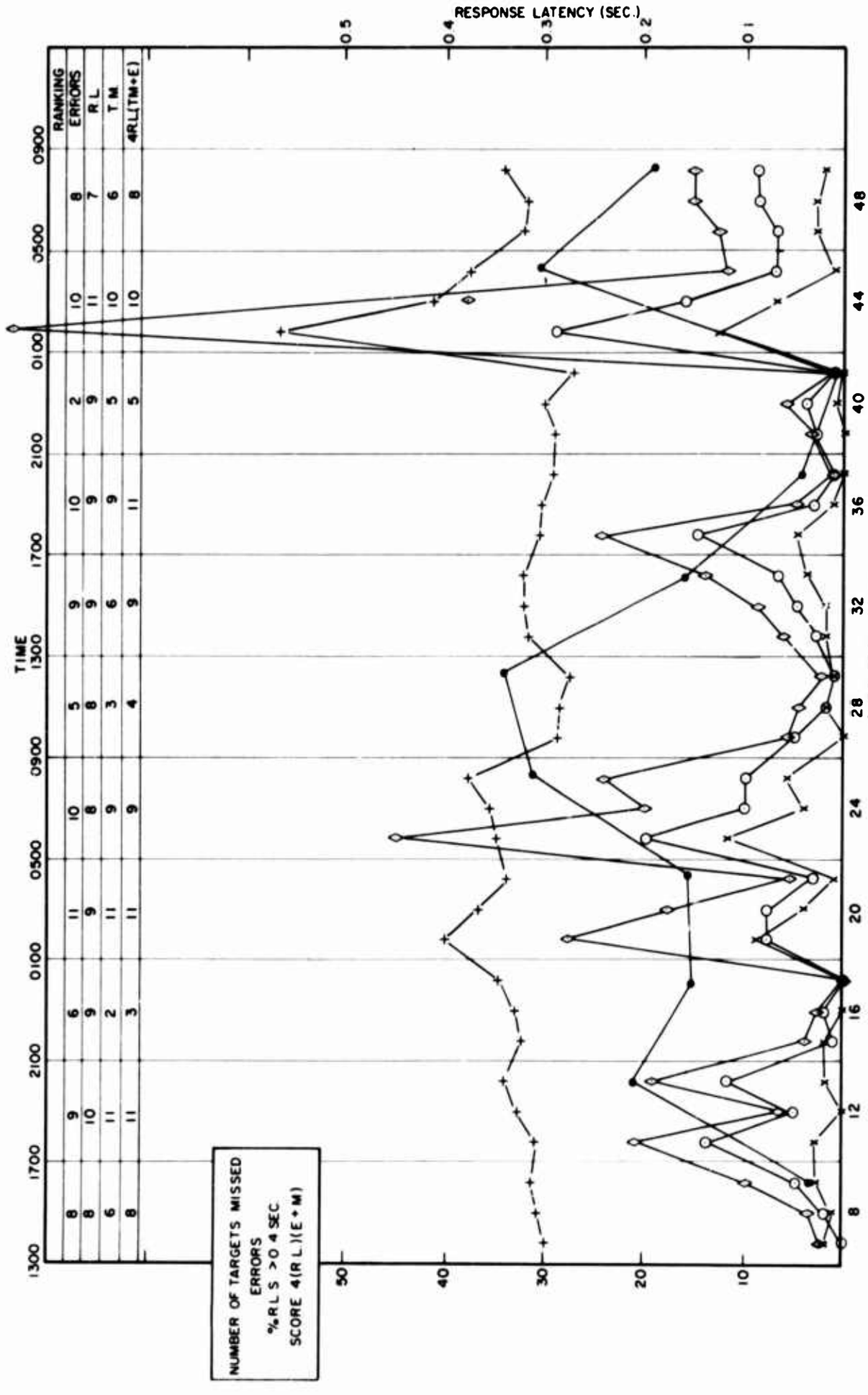

SUBJECT 2

FIG. 8

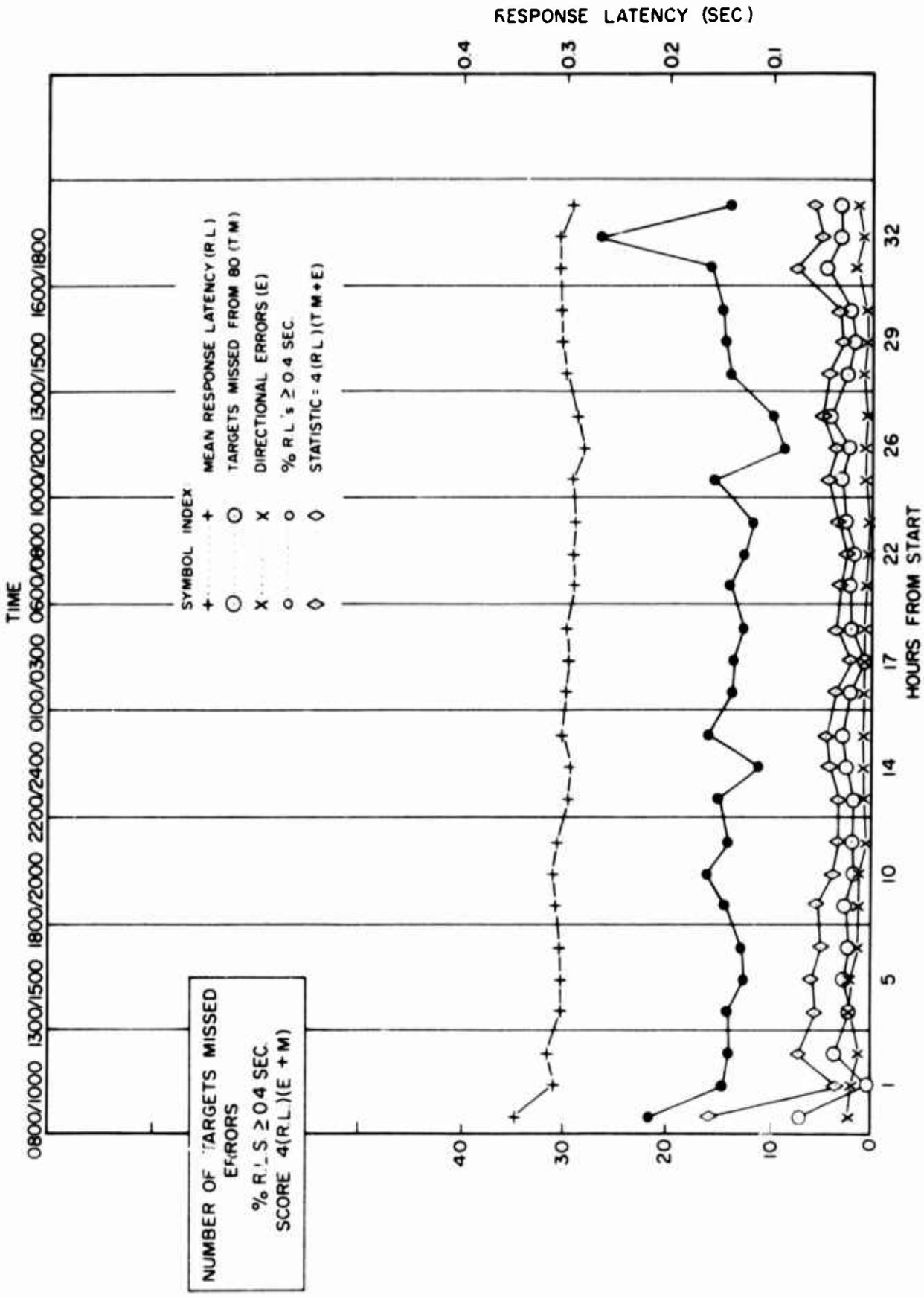

FIG. 9 GROUP RESULTS 36-HOUR TEST

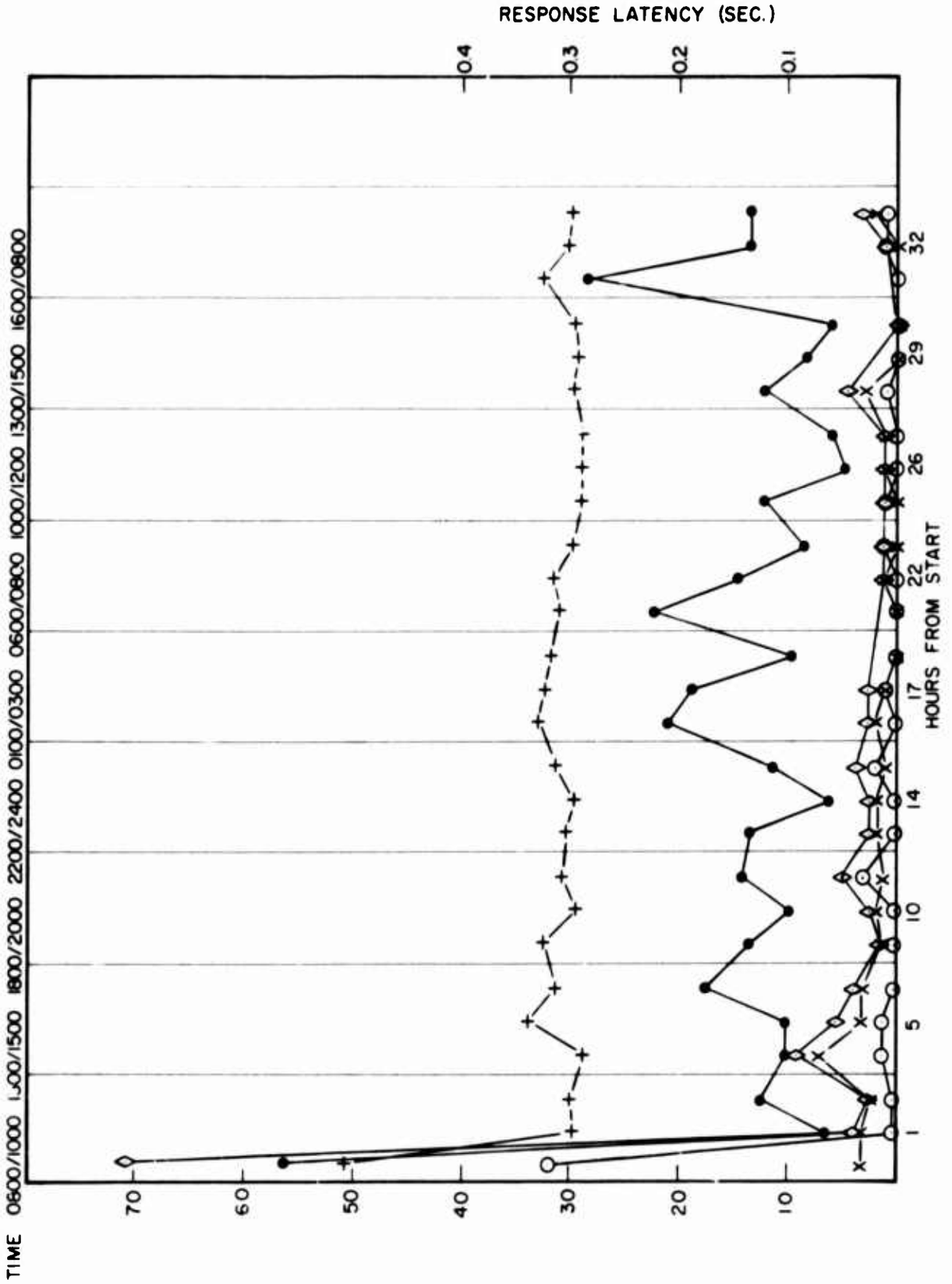

SUBJECT H

FIG. 10

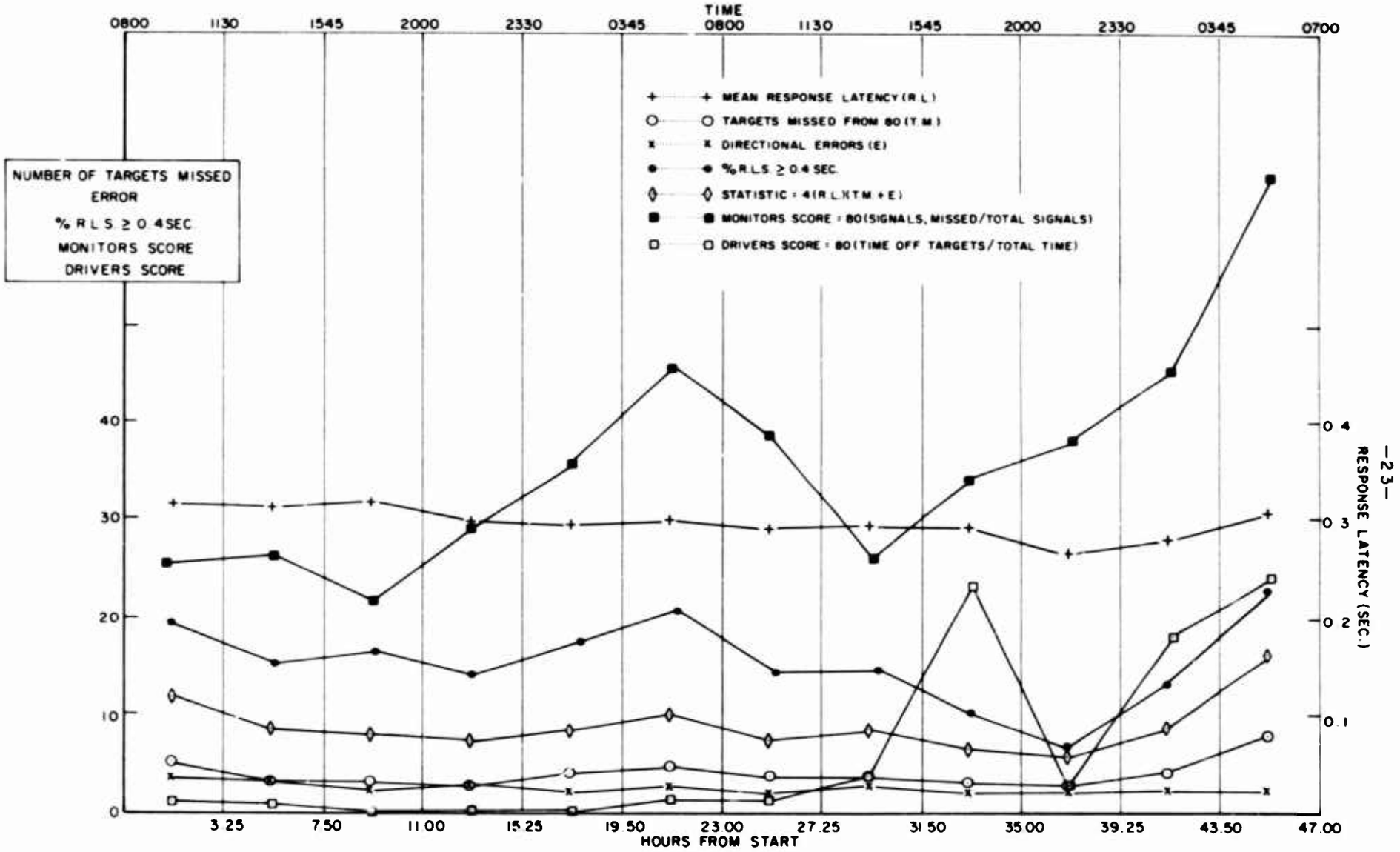

FIG 11

U.S.A., GROUP I, RESULTS

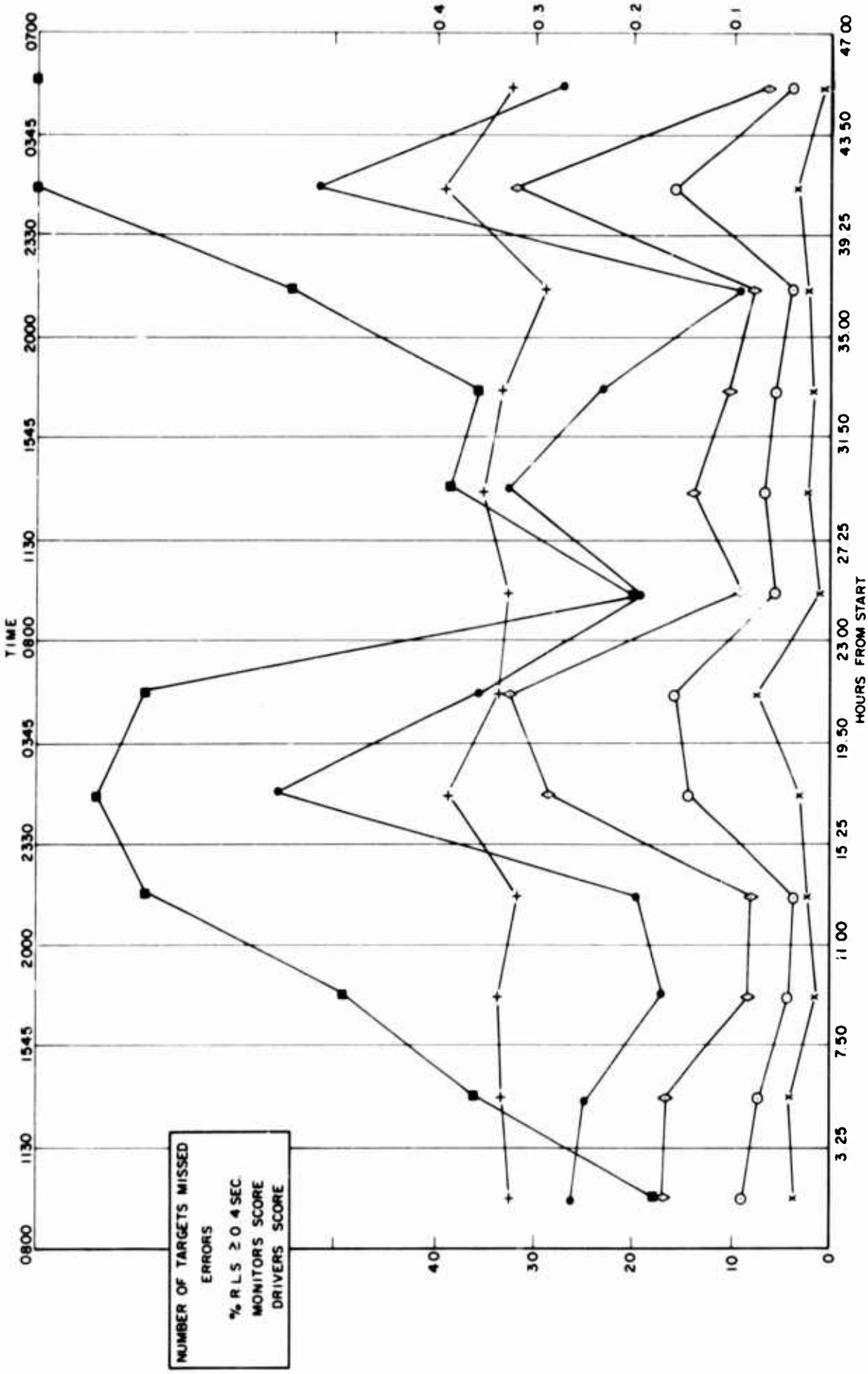

SUBJECT F, U.S.A, GROUP I, MONITOR

FIG. 12

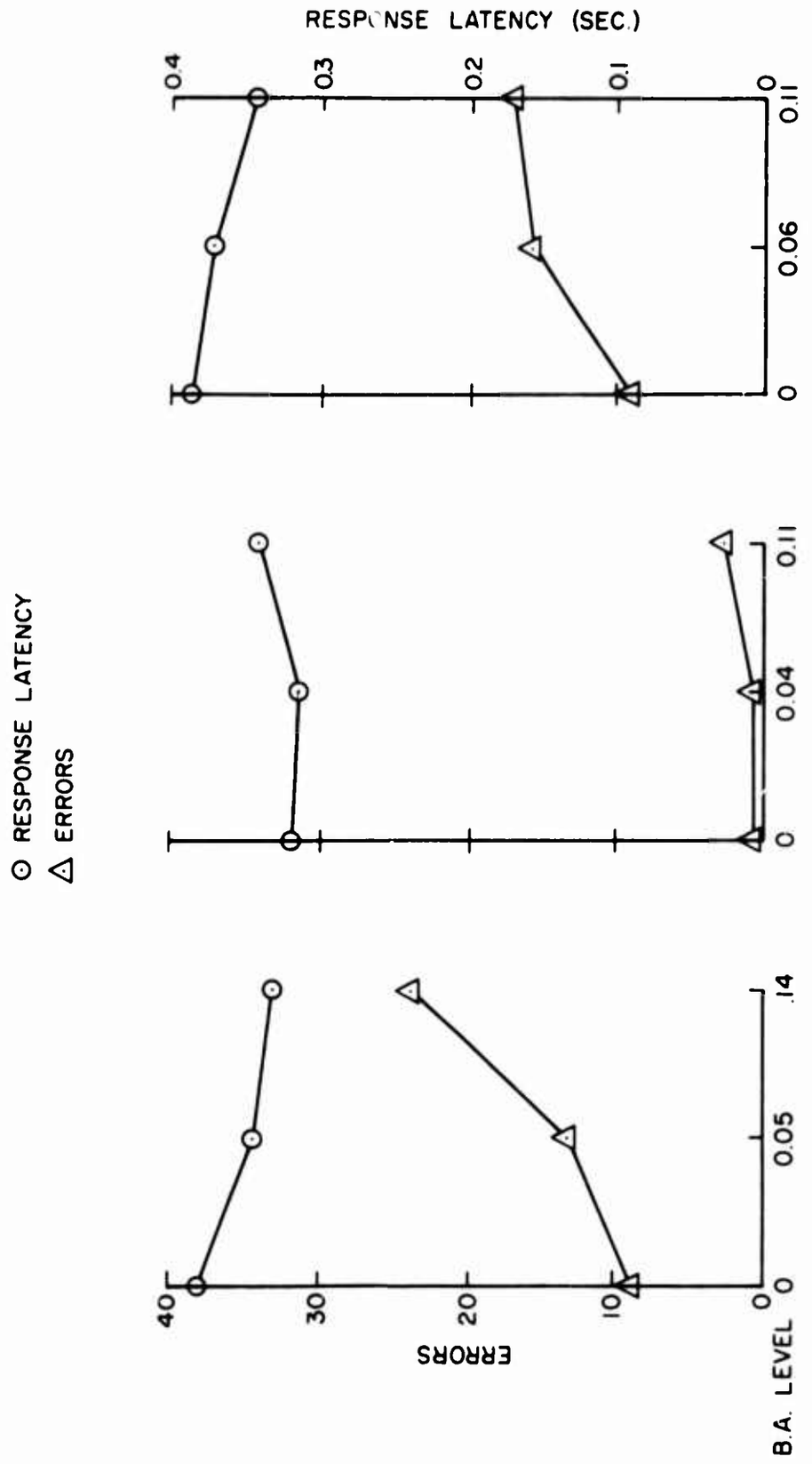

FIG. 13 INDIVIDUAL REACTION TO ALCOHOL

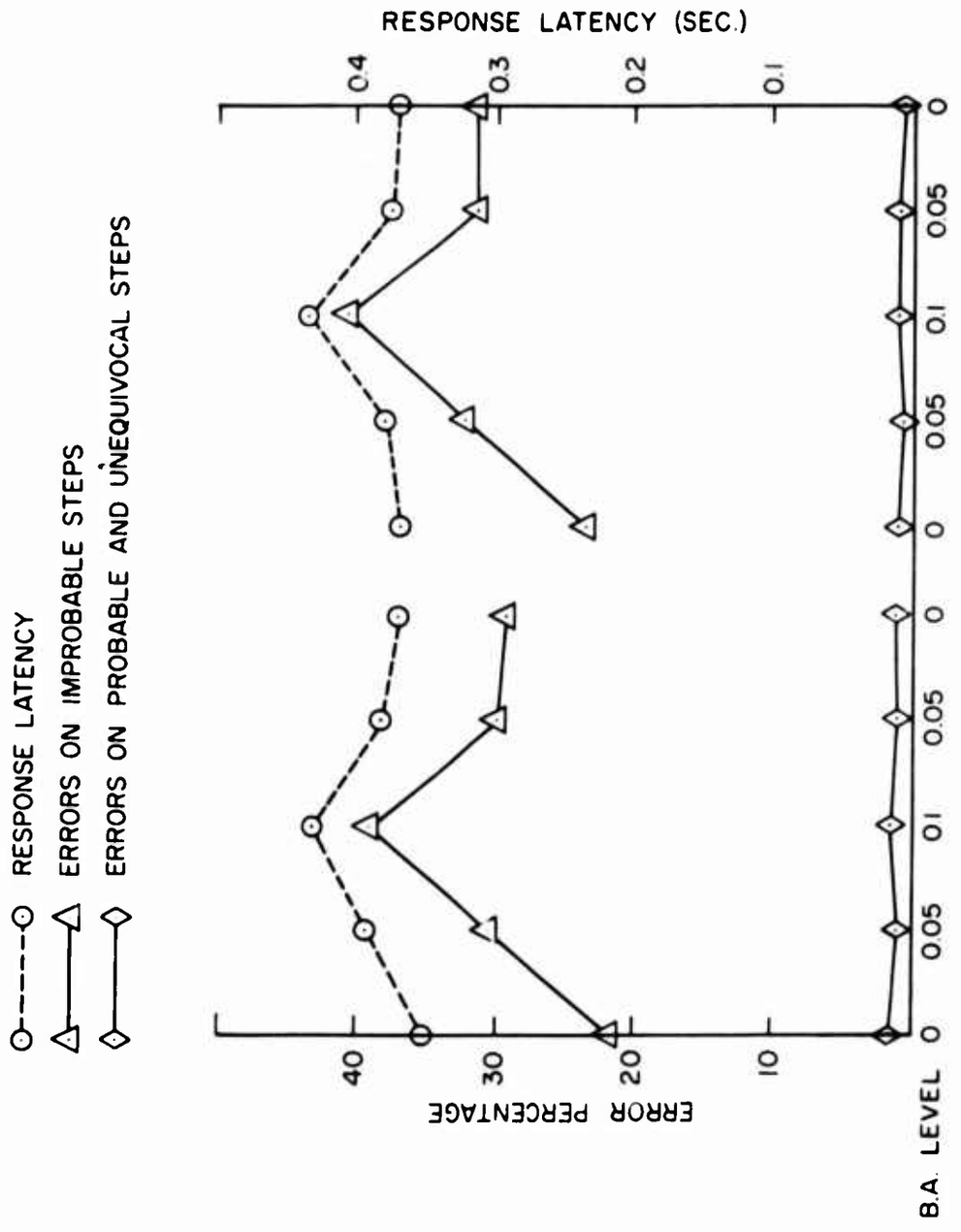

FIG. 14 EFFECT OF ALCOHOL ON RESPONSE LATENCY AND ERRORS ON PROBABLE AND IMPROBABLE STEPS

THE NAE ACOUSTIC TEST FACILITY

Structural Response to Random Noise

G.M. Lindberg, R. Westley and M.D. Olson

Structures and Materials Laboratory

National Aeronautical Establishment

1.0 INTRODUCTION

High intensity noise fields produced by modern propulsion systems and high speed flight have significantly increased the extent of sonic induced fatigue and equipment malfunctions. Control of the effects of noise upon aerospace structures and prevention of sonically induced fatigue are important design goals requiring careful attention during development of modern flight vehicles. The problem facing the designer is to achieve greater fatigue resistance for more severe loadings, while simultaneously reducing the weight of the vehicle components.

At present, theoretical predictions of the response of structures to noise and the prediction of acoustical fatigue lives are possible for special, idealized cases only. The designer of a complicated structure must resort to testing at the development stage as well as for the final proof test. Hence there is a continuing need for test facilities and for research into panel response and acoustical fatigue.

This article describes the NAE Acoustic Test Facility, which was built in 1965, and outlines current research being carried out in the laboratory on structural response to random noise and the investigation of choked jet noise.

2.0 GENERAL LAYOUT OF ACOUSTIC TEST FACILITY

The NAE Acoustic Test Facility was designed to be as adaptable as possible, so that many different types of tests could be performed. The main types envisaged were:

(a) Structural response tests and acoustical fatigue studies

(b) Sound transmission loss and noise attenuation studies

(c) Aerospace environmental military specification testing.

The general layout is shown in Figure 1. Air from a compressed air supply passes through a siren or some type of noise generator. The noise created propagates through the small exponential horn, thence through a constant cross-section progressive wave tube (for panel response testing), and finally through a large exponential horn and into a reverberation room (for environmental military specification testing). A concrete plug or window at the far side of the reverberation room can be removed to connect the anechoic termination room to the reverberation room. Panels for transmission loss studies can be placed in this opening.

The modes of operation of the facility are summarized as follows:

(1) Concrete plug in place

Electronic equipment packages can be suspended in the reverberation room and subjected to intense noise to satisfy environmental testing requirements.

(2) Concrete plug open

(a) Panel response and acoustical fatigue tests can be carried out by placing panels in the progressive wave tube.

(b) Transmission loss or noise attenuation studies can be carried out by placing test panels in the plug opening.

2.1 Air Supply

Air is supplied from the air storage bottles of the NAE Supersonic Blowdown Wind Tunnel. The supply system can operate at pressures up to 300 psig, although the normal operating pressure range is 0 - 30 psig. Operating pressures are automatically selected and maintained by a pneumatic servo-control system. An emergency shut-off valve and extensive interlocks ensure that the system is fail-safe.

2.2 Noise Sources

The facility is equipped with two main intense noise generators - a random noise siren, and a discrete frequency siren (Fig. 2). Both sirens are air-chopping devices. The discrete frequency siren can operate in the range 20 - 850 cps; a typical 1/3 octave spectrum of its output is shown in Figure 3.

The random siren has four overlapping rotors that chop the same airstream. Each rotor has a different pattern of holes or slots and each is driven at a different speed of rotation. This arrangement ensures that the airstream is randomly chopped, thus generating broad band noise similar to jet engine noise. A typical 1/3 octave spectrum of the random noise generated

is shown in Figure 4. Figure 5 indicates typical noise levels that can be achieved in various parts of the facility, using these sirens.

A loudspeaker is also used for generating low intensity noise, and two experimental sirens are under development. The addition of an electro-pneumatic air modulator is planned.

2.3 Progressive Wave Tube

The progressive wave tube is designed for studies of the response of panels excited by grazing incidence sound. It has a constant cross-section 1 ft wide by 4 ft high by 8 ft long; either side can be removed and replaced by a test panel. Figure 6 illustrates the tube with a side removed.

One purpose of a test could be to simulate the noise environment encountered by many structural sections on a modern jet aircraft. In particular, the rear fuselage, horizontal stabilizer, and vertical rudder are usually immersed in this type of noise field, which is induced by the jet engine exhausts.

Typical sound pressure levels that can be achieved in the progressive wave tube are shown in Figure 5. Higher levels may be obtained by reducing the cross-sectional area of the tube. If tests with varying incidences of sound are desired, test specimens may also be placed in the throat of the large horn at an angle to the propagating sound.

Ideally, the sound field over a test specimen situated in the side wall of the progressive wave tube should be uniform and propagated by normal waves that travel axially down the tube. The frequency band of particular interest for structural testing is approximately 50 to 500 cps, and efforts have been made to investigate and improve sound distribution in the tube for this frequency range. The sound distribution, generated by a loudspeaker instead of the siren, was measured with a microphone that could be traversed axially in the tube (Fig. 6). A reference microphone was mounted in the side wall near the upstream end. Complete sound measurements were taken for various modified versions of the tube.

Figure 7 shows a few typical sound level profiles after some of these modifications. The curves were obtained with the loudspeaker driven by a discrete frequency signal, and represent sound levels in the tube versus axial position down the tube. The top row in the Figure gives the results for the untreated tube. The profiles are typical of a complex standing wave pattern and exhibit very large differences between lowest and highest levels over the 8-foot length.

The low frequency profiles were improved by adding a termination wedge lined with several layers of 1-inch thick etched polyurethane foam. The size and position of the wedge are shown schematically in Figure 8. The

resulting low frequency profiles, shown in the second row of Figure 7, were greatly improved, but the higher frequency profiles were not. It appeared that the patterns at higher frequencies were associated with cross modes and that a modification of the horn - tube junction shape, or treatment of the upper and lower walls of the tube, might be beneficial. The effect of adding four layers of polyurethane foam to the upper and lower walls is shown in Row 3 of Figure 7. This addition of absorption material eliminated the sharp dips in Row 2, but caused the sound level to fall.

The addition of short, wedge-shaped wood plates to the upper and lower walls reduced this fall-off significantly, as shown in Row 4 of Figure 7. The addition of the rectangular shaped wood plates near the downstream end of the tube, as shown in Figure 8, resulted in the final sound level profiles given in Row 5 of Figure 7. It is felt that sound level distributions obtained in the modified progressive wave tube will be satisfactory for testing structural panels in the side wall of the tube.

A report on the complete details of the sound level measurements in the progressive wave tube, is in preparation.

2.4 Reverberation Room

The reverberation room, roughly 15 ft × 15 ft, by 10 ft high, is built in the shape of a pentagon, with no two sides parallel and with a minimum of acute angles. This shape prevents standing wave patterns from forming and diffuses the sound in the room. The epoxy-coated, 12-inch thick concrete walls of the room are almost totally reflective and their sound absorption coefficient is about 0.025.

Figure 9 shows the reverberation times for various values of air humidity, as indicated by dew point temperatures. The dry air curve was obtained by extrapolating the sound absorption curves to zero humidity. The high frequency reverberation times drop because of air absorption of the sound energy. The low frequency times are not shown, since the wave lengths of sound at low frequencies are as great as the dimensions of the room, and large standing wave patterns and system resonances occur.

Electronic equipment can be suspended in the centre of the reverberation room and subjected to intense, uniform, broad-band noise to satisfy military environmental test specifications for aerospace equipment. Test levels vary from 140 db to 165 db overall sound pressure level for a duration of 30 minutes.

2.5 Termination Room

The termination room is constructed of sand-filled concrete blocks and is located adjacent to the reverberation room. The anechoic termination

inside consists of sets of panels of etched polyurethane foam. Each set of six foam panels is randomly spaced to a depth of 6 ft from the wall, and has a coefficient of absorption of about 0.8. Complete studies of the sound absorption characteristics of these polyurethane foam panels have been made and are reported in Reference 1. The room is designed to permit the entry of a trolley for removal or replacement of the concrete plug or window.

2.6 Transmission Loss Studies

Test panels for transmission loss studies can be placed in the concrete plug opening. The sirens are used to generate intense noise in the reverberation room, and the noise attenuation properties of the test panel can be found by measuring the difference in sound levels in the reverberation room and the anechoic termination room. The termination room is structurally isolated from the reverberation room, so that only noise transmitted by the test panel is present in the termination room.

2.7 Instrumentation

Sound level measurements are generally made with condenser microphones, although piezoelectric microphones are used for very intense noise measurements. Response measurements and strain measurements of panels are generally made with strain gauges and non-contacting inductance displacement pick-ups. A variety of other transducers are available when needed.

Panoramic analyzers or third-octave and octave analyzers, together with level recorders, are used for "quick look" analysis. Transducer outputs are also tape-recorded for more detailed data processing. This processing includes spectral analysis using constant percentage and narrow-band analogue spectrum analyzers, probability density analysis, and auto- and cross-correlation analysis. Analogue data can also be converted to digital form for processing on a high speed digital computer.

3.0 STRUCTURAL RESPONSE TO RANDOM NOISE

Most aerospace structures incorporate some sort of panel-rib-stringer configuration. One of the more common is that in which a thin continuous panel is attached to closely spaced, flexible stringers and relatively stiffer and wider spaced ribs running at right angles to the stringers. The number and complexity of possible vibration modes in such a configuration increase rapidly with the number of bays. As a result, the work required to analyze the random response of this kind of structure, using the customary modal methods, soon becomes prohibitive. Furthermore, the modal frequencies are not widely separated, but rather become squeezed together into distinct bands, the number of frequencies in each band usually being equal to the number of panel bays. This fact implies that the correlations between different modes will no longer be negligible, thereby further increasing the complexity of the modal analysis.

One alternate approach to these problems, successfully developed by several authors, is the method of transfer matrices. This method is somewhat limited, however, in that it is based on the assumption that the panel is simply supported along the ribs.

Another approach, which can account for other boundary conditions (e.g. clamped edges) along the ribs, is to use finite element techniques. This method is developed and illustrated with a sample application in Reference 2. A brief description of the analysis and the results obtained is presented below.

3.1 Theoretical Formulation

A typical configuration used in many aerospace structures is depicted in Figure 10. The design incorporates a thin, continuous panel either bonded or riveted to a framework of ribs and stringers running at right angles to each other. The example illustrated is especially simple in that all panels are identically constructed.

The analysis of the complete structure shown in Figure 10 is beyond present day capabilities and, hence, some simplifying approximations must be introduced. It has been found in practice that the stringers are generally much more flexible than the ribs, and are usually spaced much closer to each other. These conditions suggest the now well-known approximation of neglecting all interactions between panels across the ribs. This leaves only the problem of analyzing a single row of panels and stringers, as depicted in Figure 11.

In the case of clamped boundaries an exact solution is unattainable and approximate techniques must be employed. The approach taken here, which is proving most efficient, is the use of finite plate elements. These are the well-known twelve degree of freedom models derived from virtual work principles (Ref. 3). The panel stringers, which are assumed infinitely stiff in bending, are represented by beam-torsion elements.

The stiffness and mass matrices for an approximate representation of the multi-bay panel are generated from the sub-matrices associated with each plate and beam-torsion element. Once these matrices are established, the panel vibration modes are calculated from the eigenvalue problem

$$(K - \lambda M)\ \vec{X} = 0 \qquad (1)$$

where K and M are the system stiffness and mass matrices and λ is the non-dimensional eigenvalue. These stiffness and mass matrices are also used in determining the panel response to a random excitation field. The structural damping in the panel is assumed equal to igK, where g is a small constant to

yield the matrix equation

$$kM \frac{d^2 \vec{x}}{dt^2} + (1 + ig) K \vec{x} = \vec{f}(t) \qquad (2)$$

where $\vec{x}$ and $\vec{f}$ are the nondimensional displacement and load vectors for the system, respectively. In this case, $\vec{f}$ will be a discrete set of random loads that approximates the distributed load acting on the panel. The solution to equation (2) is determined by a generalized harmonic analysis, and the power spectral densities for each degree of freedom are calculated at particular frequencies. The mean square responses are then determined by numerically integrating the power spectra over frequency.

3.2 Sample Application

The complete analysis for the five-bay, stringer-stiffened panel illustrated in Figure 11 is presented in Reference 2. The edges $y = 0$ and $y = W$ represent the ribs and are considered to be clamped. The overall length L is divided into five equal bays by the stringers, as shown. The edges $x = 0$ and $x = L$ are also assumed to be clamped. The numerical calculations are carried out for a typical panel having the following properties

$$E = 10^7 \text{ psi}, \quad \nu = 0.3, \quad L = 45.0 \text{ in}$$

$$W = 16.5 \text{ in}, \quad d = 1.0 \text{ in}, \quad e = 0.75 \text{ in} \qquad (3)$$

$$\rho = 0.000259 \text{ lb sec}^2/\text{in}^4, \quad h = 0.052 \text{ in}$$

The two finite element representations used to approximate the five-bay panel are illustrated in Figure 12.

3.2.1 Results

The numerical results for the panel vibration modes are shown in Table I. This table gives a comparison of the results obtained from the 3×3 grid/bay representation and the 4×4 grid/bay representation, with the effect of stringers included in both. The corresponding mode shapes (eigenvectors), as obtained from the 4×4 grid/bay representation, are plotted in Reference 2.

The vibration modes occur in distinct groups of five each because there are five bays in the panel. These groups are labelled arbitrarily A, B, C,

etc., for identification purposes, as shown in Column 1 of Table I. The symmetry character of each mode is indicated in Columns 4 and 5, where the symbols S and A stand for symmetric and antisymmetric, respectively. The predominant number of half waves present in the mode shapes in each direction are also indicated by the numbers in these columns.

As shown in Reference 2, the fifth mode in each group has a mode shape with zero slope across each stringer. Hence, in these modes each bay vibrates effectively as though the stringers were clamped edges, and the frequencies may be compared with those predicted for a clamped plate the size of each bay. Such a prediction is shown in Column 6 of Table I, as obtained from Warburton's Rayleigh solutions (Ref. 4).

The comparison of the fifth frequency in each group, with the Warburton results, is very interesting. For the mode groups A, D, E, and G, these frequencies appear to converge towards the Warburton result as the finite element modelling is increased from the 3 × 3 to the 4 × 4 grid/bay representation. On the other hand, for groups B, C, and F, they appear to diverge slightly from the Warburton results. Presumably, a finer grid work of elements would be required to make these latter groups converge to the correct result. However, it may be noted that the maximum error in these frequencies, as predicted by the 4 × 4 grid/bay representation, is only 15 percent. It is expected that the accuracy of the other four frequencies in each group would be the same or better than that of the fifth. Hence, it appears that the first 35 vibration frequencies for the five-bay panel are predicted to within 15 percent by the 4 × 4 grid/bay finite element representation.

Only the fifth frequency in each of the higher groups H to N are presented in Table I. It is clear that these predictions are far less accurate than the lower ones, although they are the correct order of magnitude.

The calculation of the panel response to a random pressure loading is also carried out using the finite element representations. Numerical results are presented in Reference 2 for the particular excitation known as plane wave propagation of acoustic white noise. This type of random loading is of special interest because it may be considered as an idealization of the pressure fields induced downstream by jet engine exhausts.

A typical response power spectral density for the five-bay panel is shown in Figure 13. The three relatively wide peaks exhibited are clearly recognizable as being associated with modal groups A, C, D, and G of Table I. Furthermore, some of the small individual peaks may be associated with particular modes. For example, the five small peaks from 103 to 141 cps are associated with the five individual modes in Group A.

The mean square response for each degree of freedom was also

obtained by numerical integration of its power spectral density curve, using Simpson's rule. This was done simultaneously with the calculation of the power spectra. The results in terms of root mean square amplitude are shown in Figures 14 and 15. Figure 14 shows the longitudinal distribution of the rms panel response. It is interesting to note that this response is not symmetric with respect to the centre bay and, in particular, the maximum amplitude occurs in the last downstream bay. These results are a consequence of the directionality of the excitation field. Figure 15 shows the lateral distributions of the rms panel response in the centre and last bays. These curves indicate that the panel response is dominated by modes with one half wave parallel to the stringer. The relative flatness of the top of these curves is evidence of the presence of higher modes, even though their contribution is small.

A model of the five-bay panel has been constructed and is illustrated in Figure 16. The vibration modes for this panel will be determined experimentally for comparison with the theoretical predictions. The panel will then be subjected to random noise excitation in the progressive wave tube, and its response will be compared with that predicted in the theory.

4.0 CHOKED JET NOISE

In the past it was generally accepted that the noise field from jet engine exhausts was caused predominantly by random turbulent mixing processes, and that no marked change occurred when the pressure ratio across the nozzle exceeded the critical value. A standing shock wave system appears in a jet when the critical pressure ratio is exceeded, and model studies, e.g. Powell (Ref. 5), indicated that screech noise sources could accompany this shock wave system.

Screech noise was not detected on full-scale engines until quite recently, perhaps because of the customarily low pressure ratios across the nozzles. Clarkson (Ref. 6) and McElhinney (Ref. 7) have now pointed out that choked jet noise, or screech, is present on some current jet aircraft, and that it may be a contributing factor in aircraft acoustic fatigue.

The object in measuring the sound fields of a 2.25-inch diameter choked jet is to provide fuller information on choked jet noise. Powell's earlier work was confirmed by preliminary investigations, but more details are required if structures are to be tested or their response predicted when in choked jet noise fields.

Typical screech frequencies and corresponding pressure levels are shown in Figures 17 and 18, respectively. The measuring microphone was located one jet diameter downstream from the nozzle exit and four diameters away from the jet axis. The abscissae in the Figures represent the internal exit static pressure of the nozzle. The ambient pressure around the jet was atmospheric.

Figure 17 indicates that three screech frequencies are present, and that the frequencies decrease with increase of pressure ratio. The fundamental frequency, labelled A_1, and its first harmonic, labelled A_2, both display a discontinuity at one pressure ratio that may be related to a change in the shock wave pattern. Note that the notations A_{11}, A_{12}, etc. merely serve to differentiate between the different branches of the frequency curves. The third screech frequency, B_1, is predominant at the lower pressures (Fig. 18), and may be the one most likely to be associated with full-scale engines. At higher frequencies, the fundamental screech becomes predominant and sound pressure levels of about 150 db are encountered. As noted by Powell, the presence of local reflecting surfaces may cause significant changes in the screech mechanism and the associated sound levels. There is also some evidence that the screech mechanism can be accompanied or replaced by broad-band noise amplification at higher frequencies. The first harmonic component can become predominant at measuring positions further along the jet.

Research into choked jet noise is continuing. The actual shock wave patterns in the jet and the manner in which they change with pressure ratio, jet size, and the presence of reflecting surfaces will be investigated.

5.0 REFERENCES

1. Westley, R.
   Woolley, J.H.
   Sound Absorption Studies of an Anechoic Treatment for Noise Termination Chambers.
   NRC, NAE Aero. Report LR-466, National Research Council of Canada, Ottawa, Ont., Jan. 1967.

2. Lindberg, G.M.
   Olson, M.D.
   Vibration Modes and Random Response of a Multi-Bay Panel System Using Finite Elements.
   NRC, NAE Aero. Report LR-492, National Research Council of Canada, Ottawa, Ont., Dec. 1967.

3. Zienkiewicz, O.C.
   The Finite Element Method in Structural and Continuum Mechanics.
   McGraw Hill Publishing Co., Ltd., London, England, 1967.

4. Warburton, G.B.
   The Vibration of Rectangular Plates.
   Proc. Inst. Mech. Eng., Vol. 168, Institute of Mechanical Engineers, London, England, 1954, pp. 371-381.

5. Powell, A.
   On the Mechanism of Choked Jet Noise.
   Proc. Physical Society, Vol. 66, Sect. B, 1953, p. 1039.

6. Clarkson, B.L. — The Development of a Design Procedure for Acoustic Fatigue. Institution of Sound and Vibration Research, ISAV Report No. 198, University of Southampton, Southampton, England, Sept. 1967.

7. McElhinney, D.M. — Designing to Combat Fatigue. Aircraft Engineering, Vol. 39, No. 10, Oct. 1967, p. 6.

TABLE I

FIVE-BAY PANEL VIBRATION FREQUENCIES

(Effect of Stringers Included)

Mode Group	3 × 3 grid/bay 68 deg of freedom (cps)	4 × 4 grid/bay 147 deg of freedom (cps)	Symmetry and half waves in y dir'n	Symmetry and half waves/bay in x dir'n	Warburton result (cps)
	103.42	105.06	S - 1	S - 1	
	112.35	114.36	S - 1	A - 1	
A	124.60	127.17	S - 1	S - 1	
	136.14	139.38	S - 1	A - 1	
	141.18	144.77	S - 1	S - 1	152.4
	177.37	174.82	A - 2	S - 1	
	180.70	178.21	A - 2	A - 1	
B	185.11	182.71	A - 2	S - 1	
	188.97	186.66	A - 2	A - 1	
	190.53	188.25	A - 2	S - 1	207.2
	288.42	281.41	S - 3	S - 1	
	294.78	282.47	S - 3	A - 1	
C	295.88	284.18	S - 3	S - 1	
	299.67	287.01	S - 3	A - 1	
	299.17	287.03	S - 3	S - 1	303.4
	273.84	280.37	S - 1	A - 2	
	303.23	304.16	S - 1	S - 2	
D	317.01	332.59	S - 1	A - 2	
	330.42	358.89	S - 1	S - 2	
	335.23	370.60	S - 1	A - 2	391.1
	558.78	454.61	A - 4	S - 1	
	558.90	454.83	A - 4	A - 1	
E	559.02	455.02	A - 4	S - 1	
	559.09	455.13	A - 4	A - 1	
	559.12	455.17	A - 4	S - 1	439.8
	354.97	346.39	A - 2	A - 2	
	364.68	356.11	A - 2	S - 2	
F	376.94	368.47	A - 2	A - 2	
	387.22	378.97	A - 2	S - 2	
	391.26	383.16	A - 2	A - 2	444.2
	410.50	454.08	S - 3	A - 2	
	415.96	459.54	S - 3	S - 2	
G	426.96	466.84	S - 3	A - 2	
	443.00	473.88	S - 3	S - 2	
	452.64	477.45	S - 3	A - 2	534.0
H	-	738.51	S - 5	S - 1	614.2
I	-	578.94	A - 4	A - 2	663.1
J	-	662.65	S - 1	S - 3	749.8
K	-	629.30	A - 2	S - 3	803.3
L	-	861.35	S - 5	A - 2	831.4
M	-	800.87	S - 3	S - 3	891.1
N	-	831.58	A - 4	S - 3	1016.0

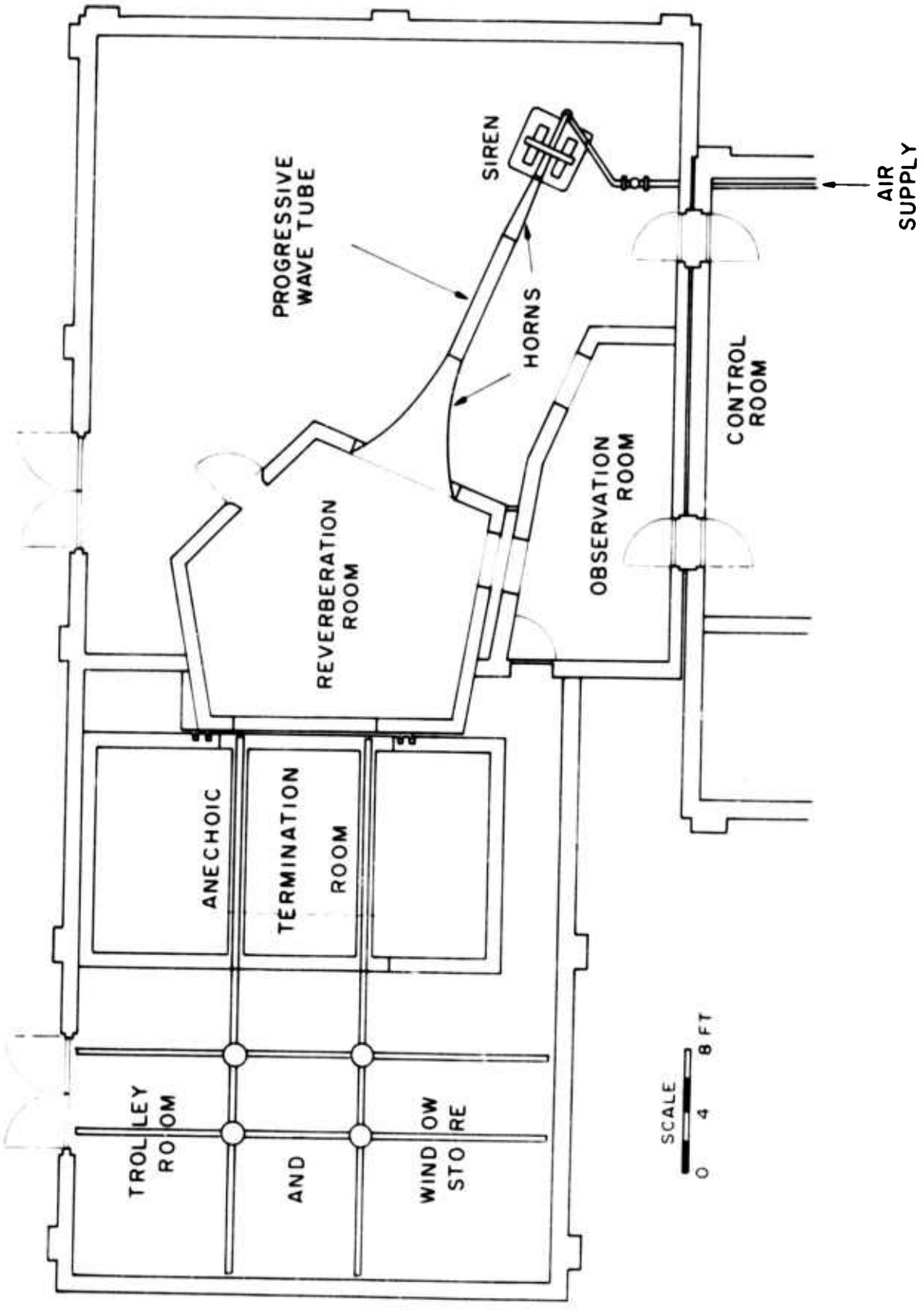

FIG. 1

ACOUSTIC TEST FACILITY

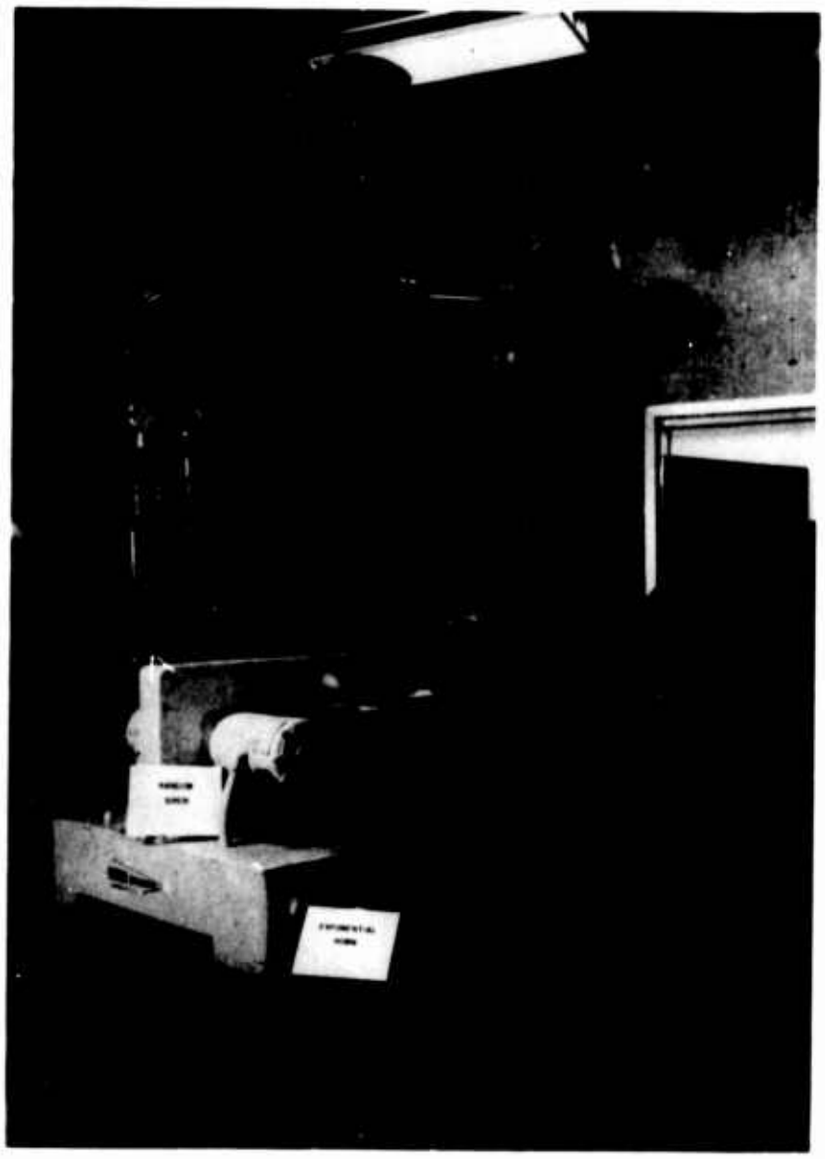

FIG. 2 SIREN

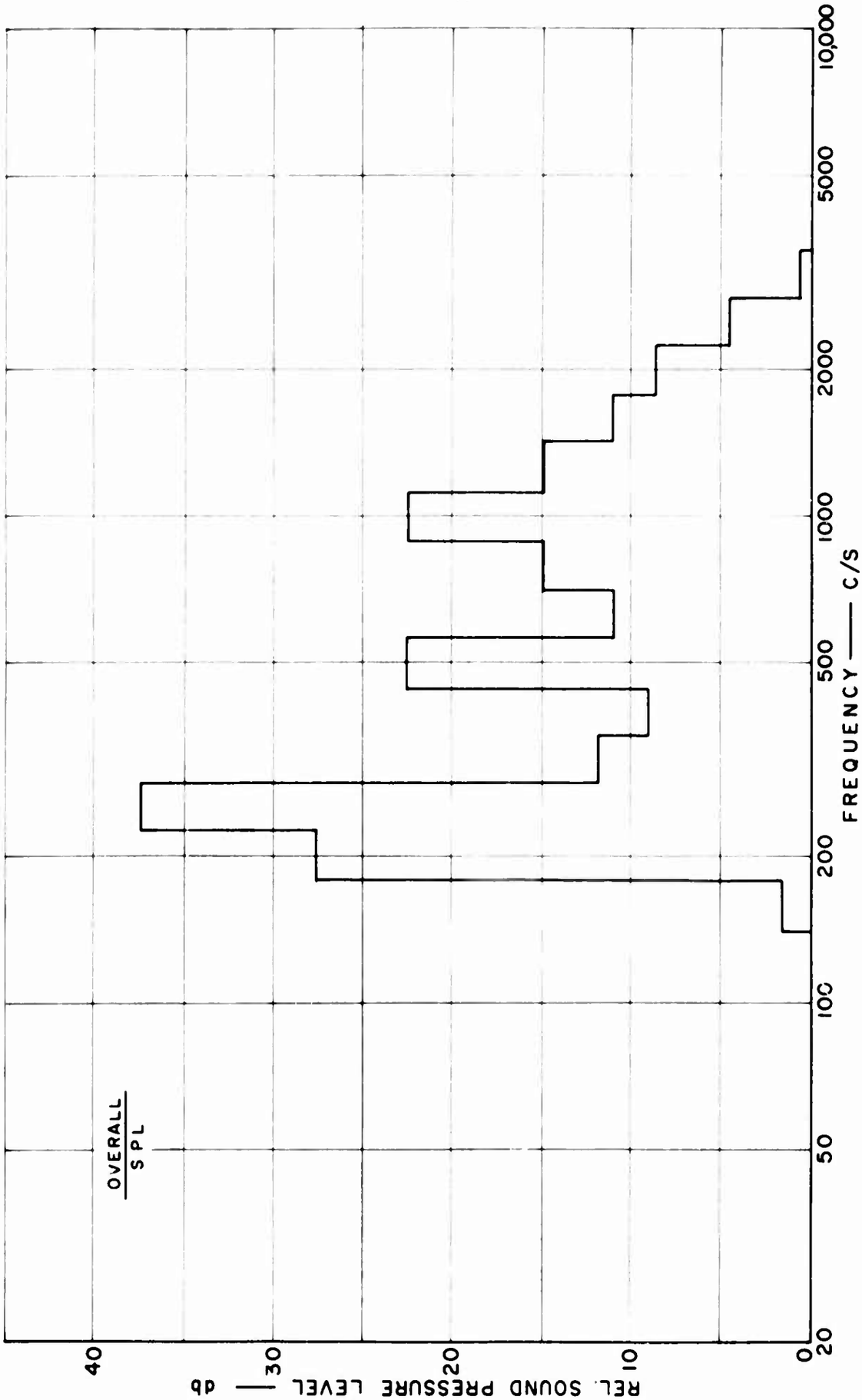

DISCRETE SIREN SPECTRUM

FIG. 3

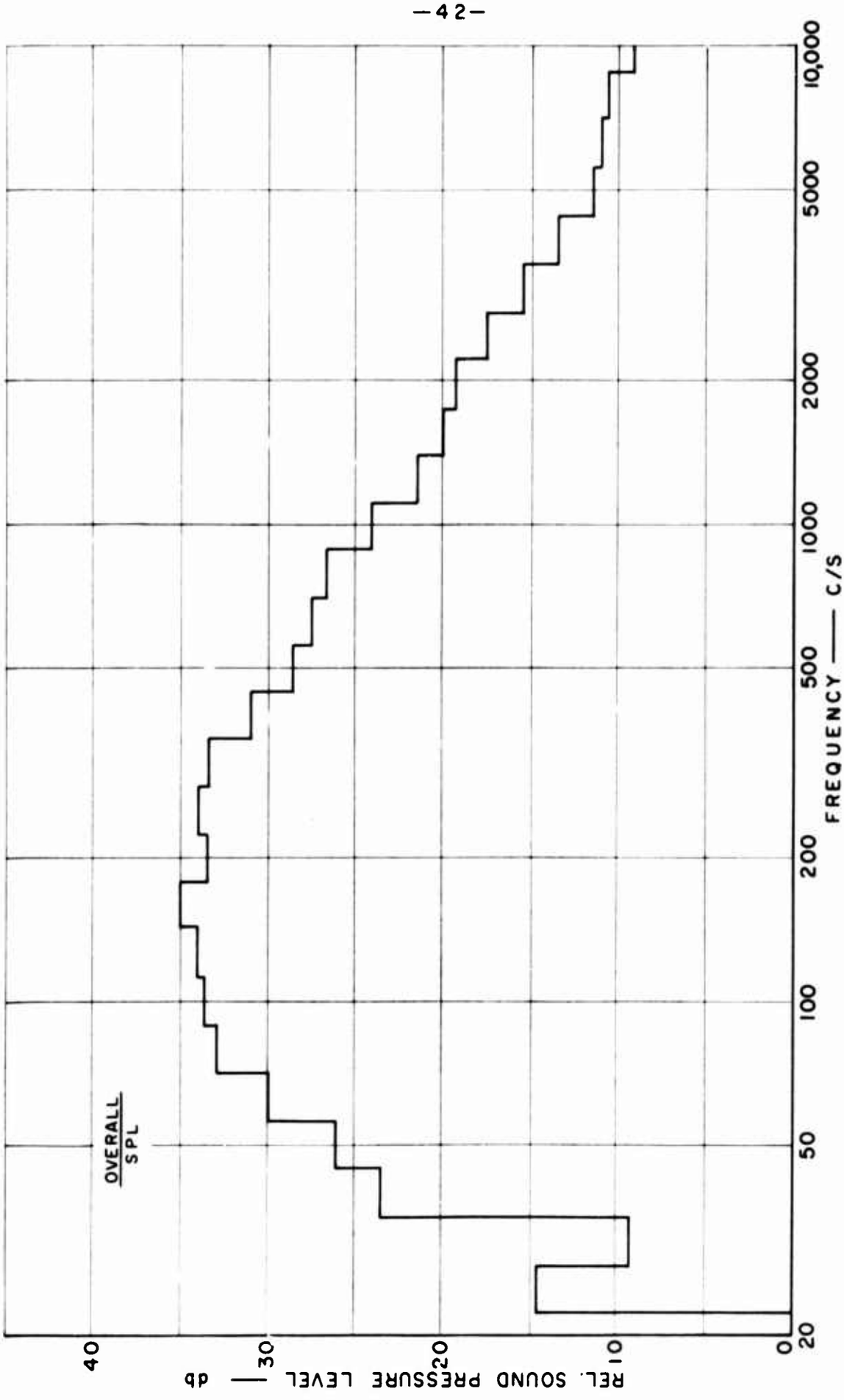

FIG. 4 RANDOM SIREN SPECTRUM

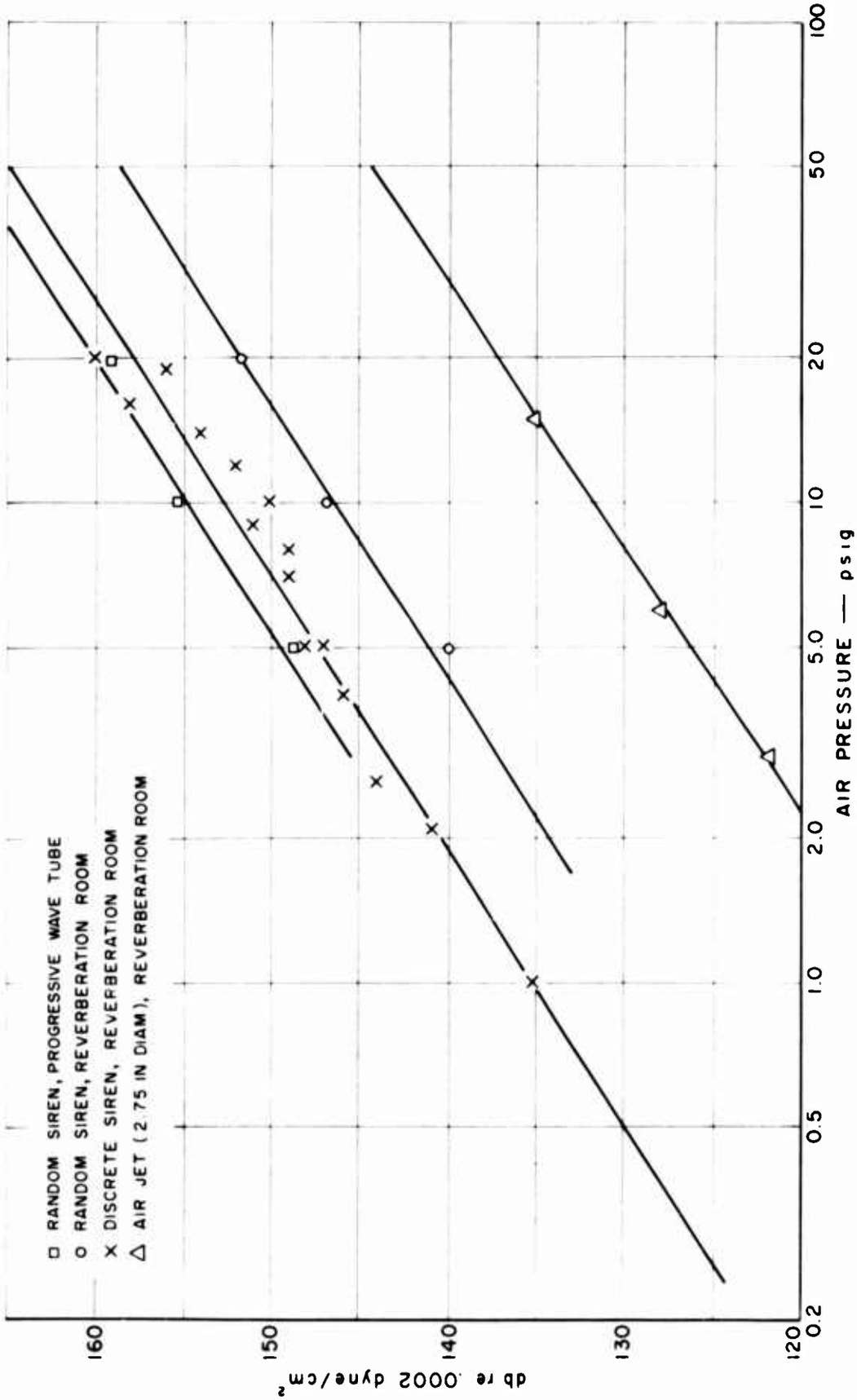

FIG. 5 SOUND PRESSURE vs SIREN AIR PRESSURE

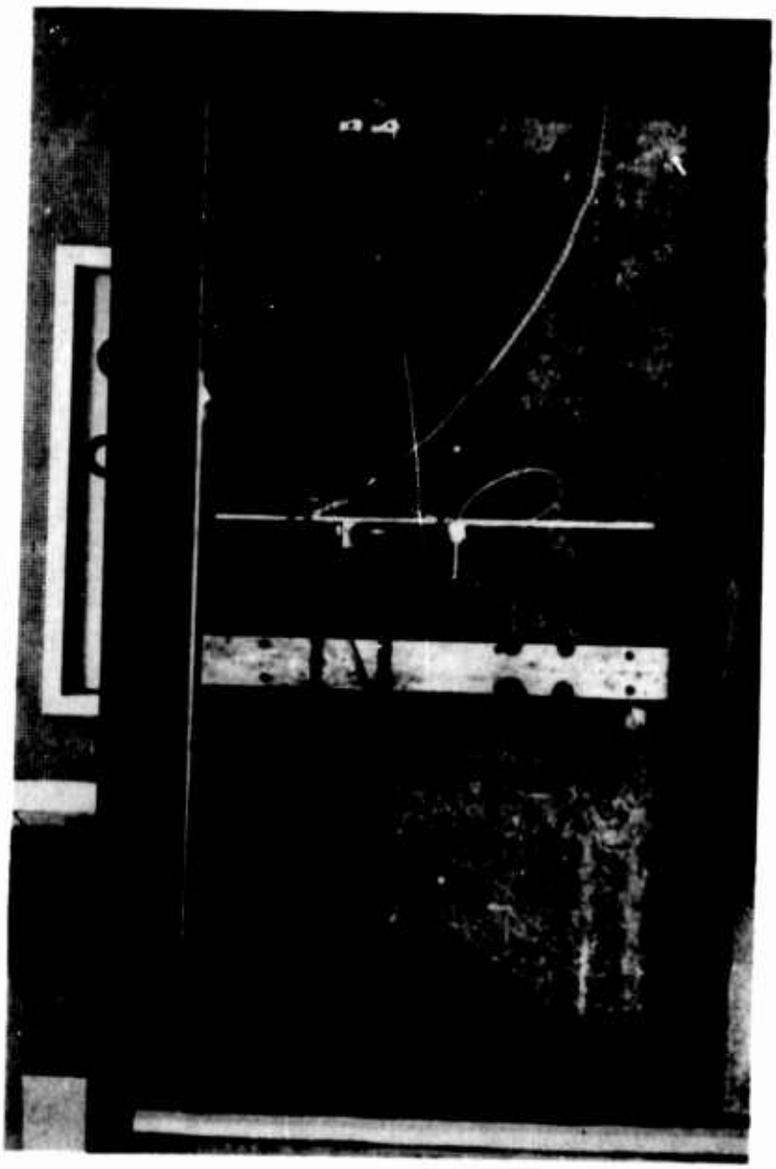

FIG. 6 TRAVERSING MICROPHONE IN PROGRESSIVE WAVE TUBE

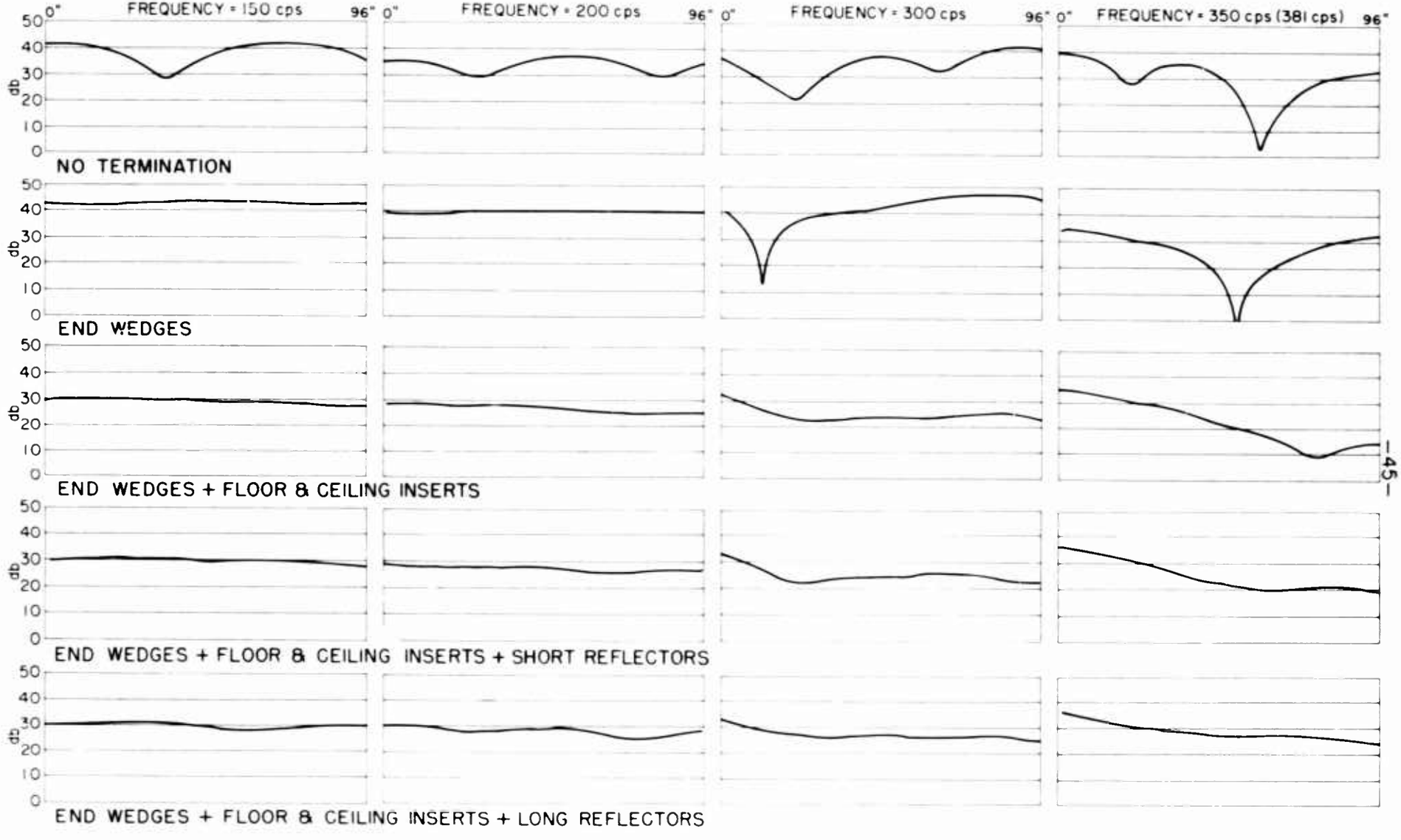

FIG 7 SOUND LEVEL TRAVERSES IN PROGRESSIVE WAVE TUBE

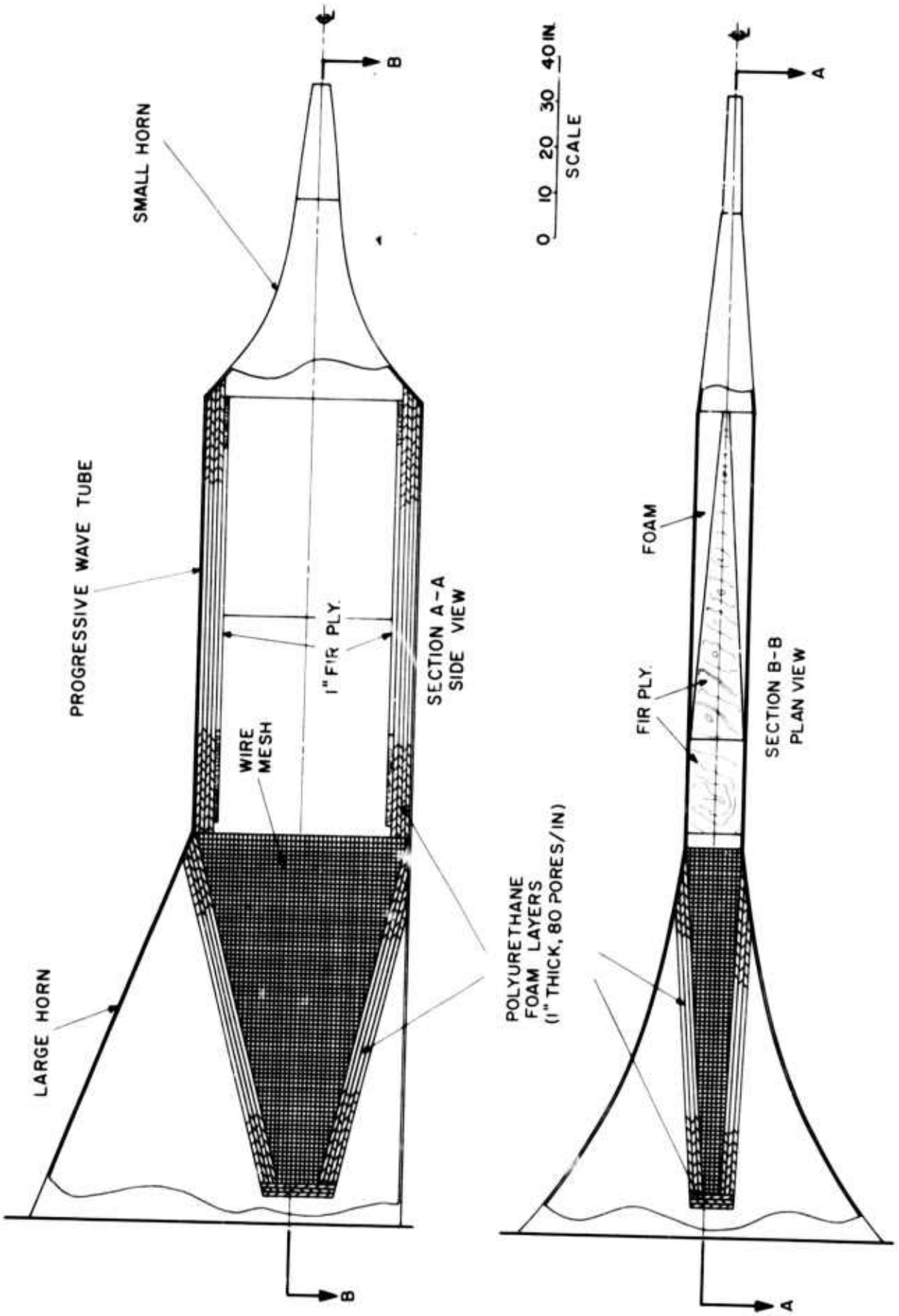

FIG. 8 PROGRESSIVE WAVE TUBE WITH ACOUSTIC TERMINATION

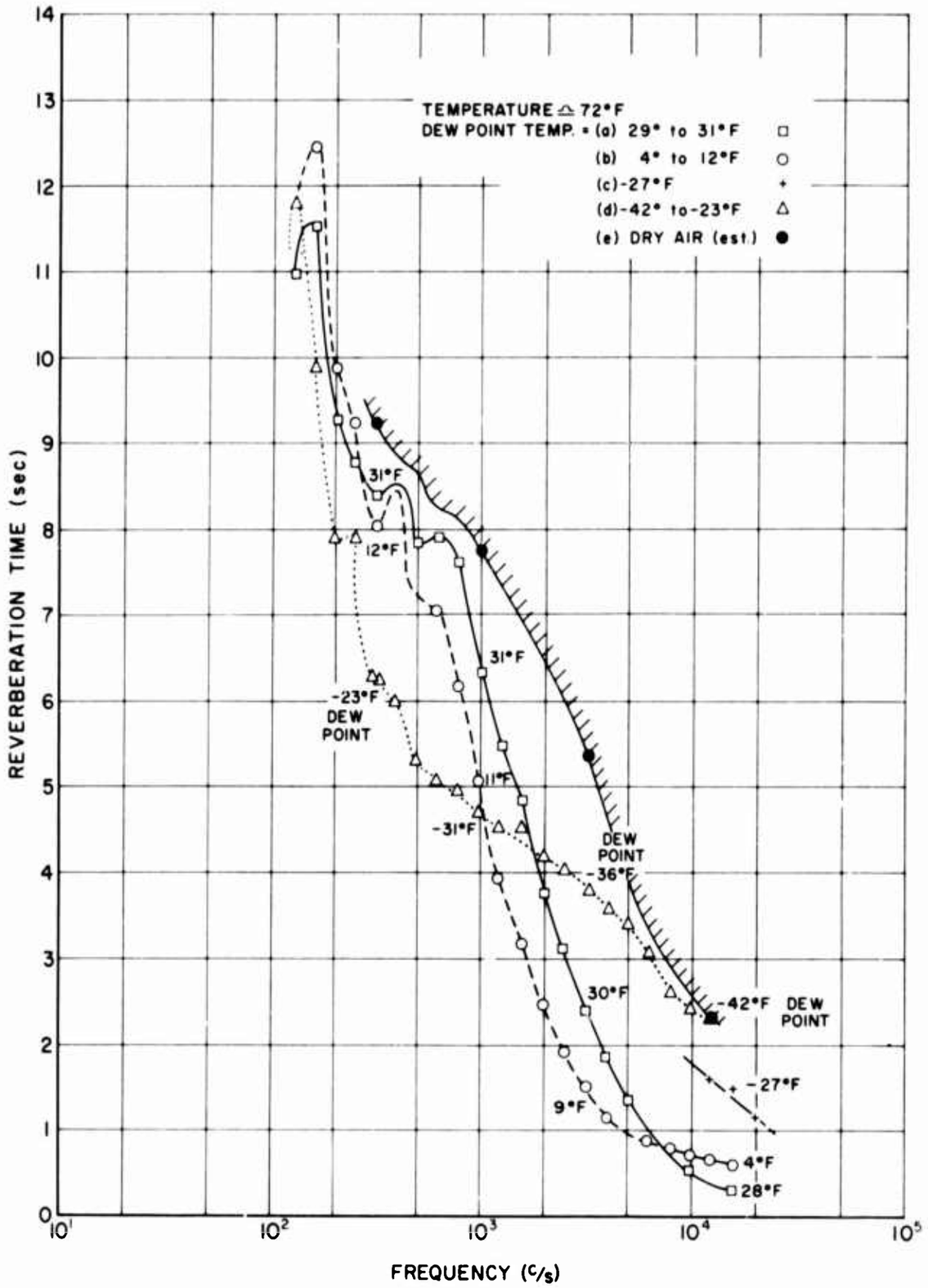

N.A.E. STRUCTURES ACOUSTIC TEST FACILITY

FIG. 9

REVERBERATION TIMES IN "CLEAN" REVERBERATION ROOM

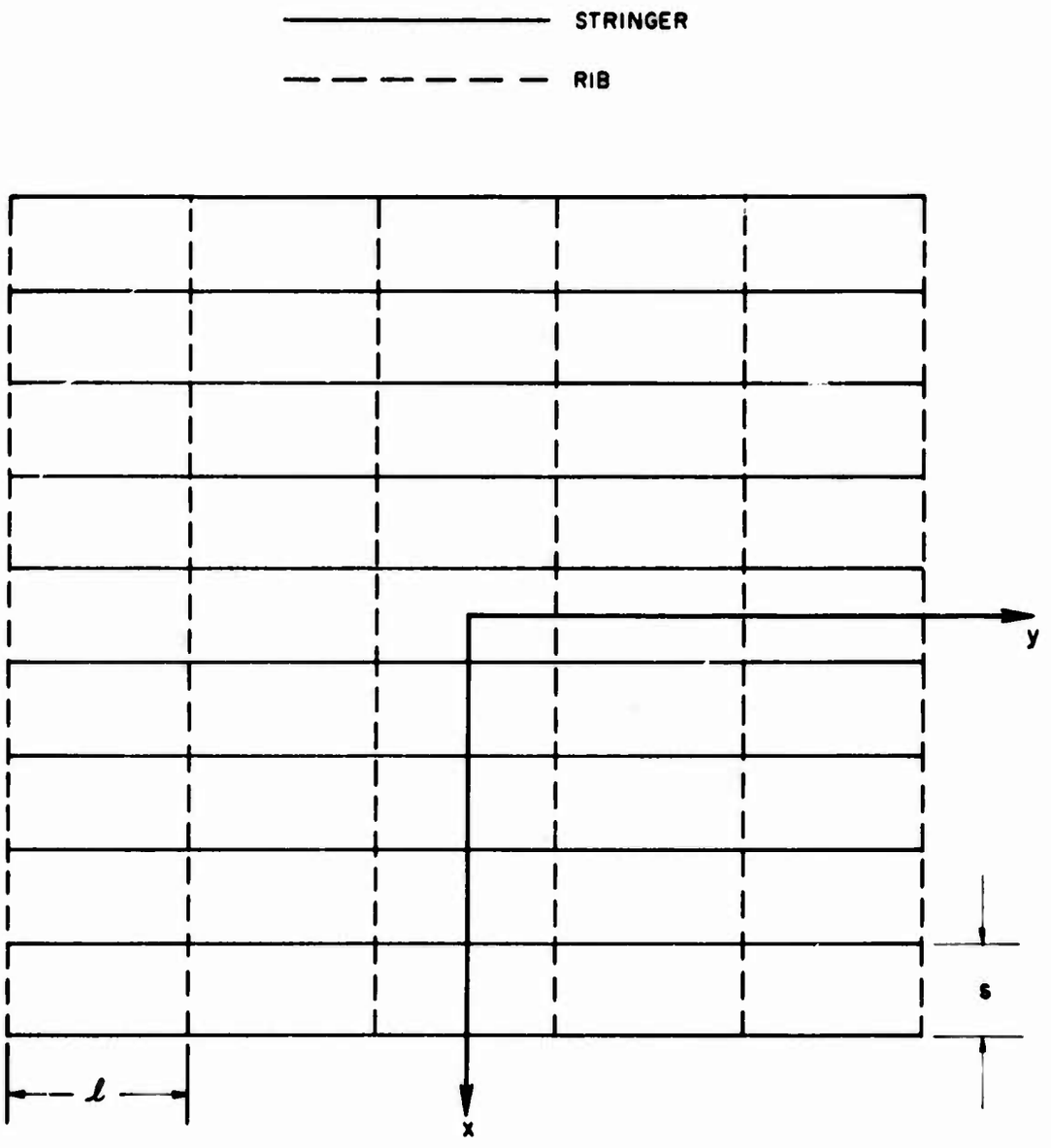

FIG. 10 IDENTICALLY CONSTRUCTED PANELS

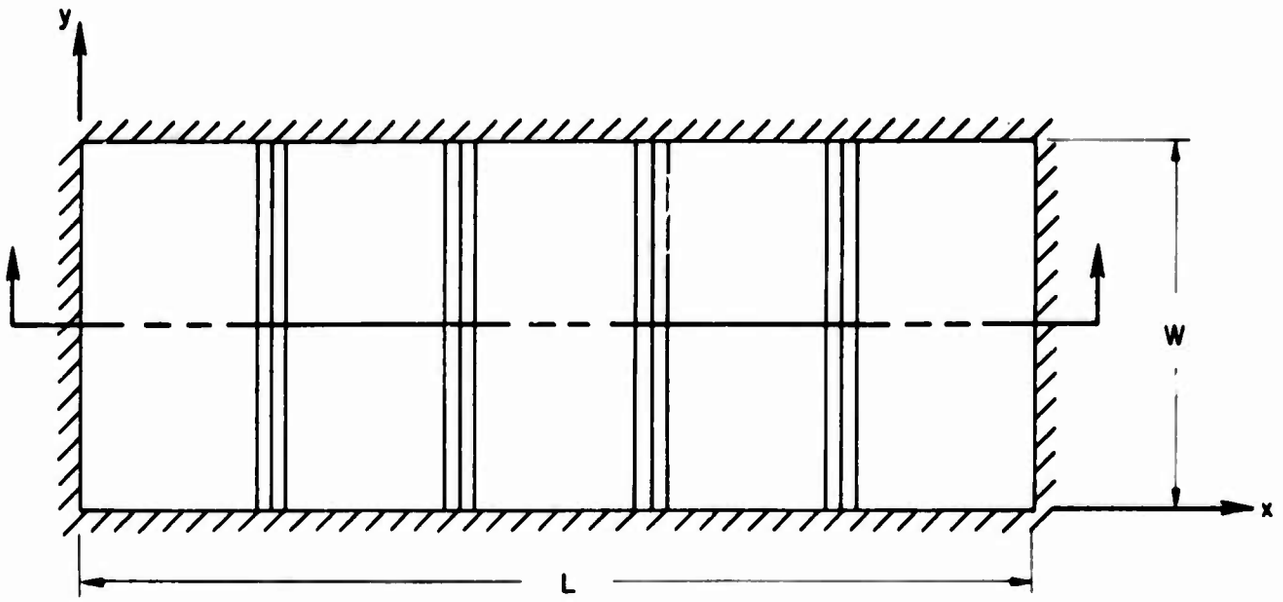

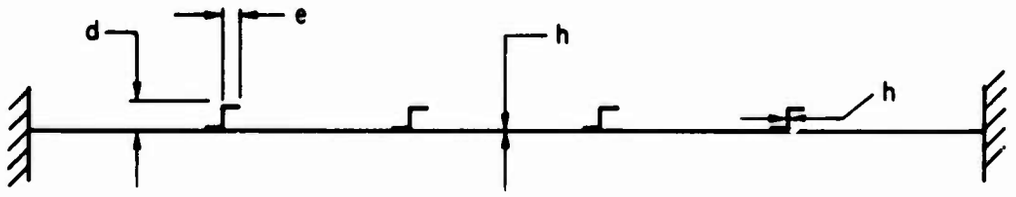

FIG. 11

FIVE-BAY STRINGER STIFFENED PANEL

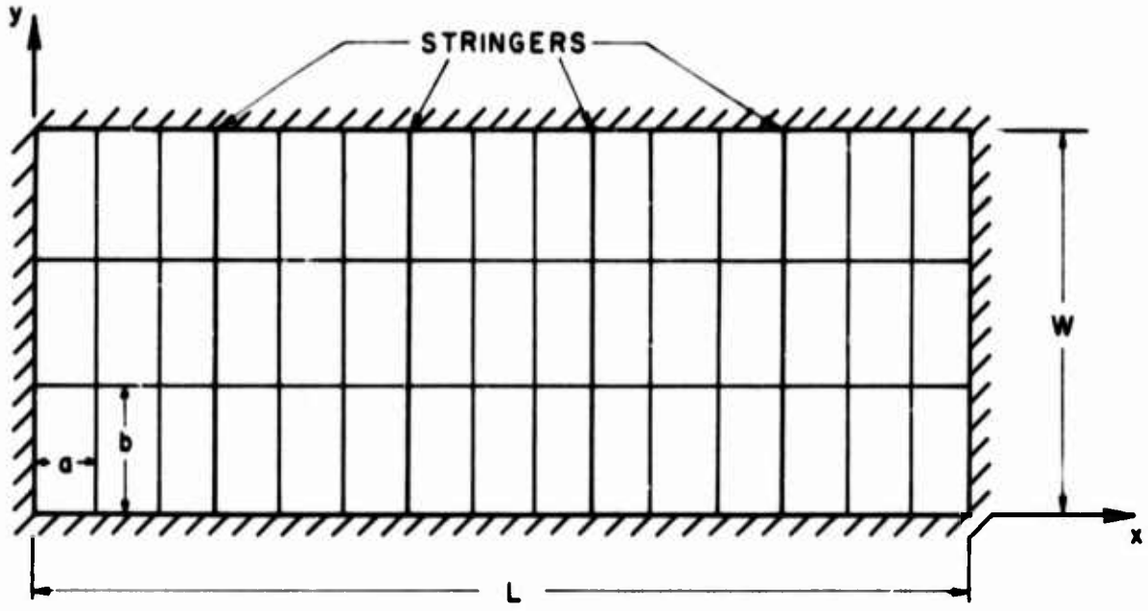

(a) 3x3 GRID PER BAY REPRESENTATION

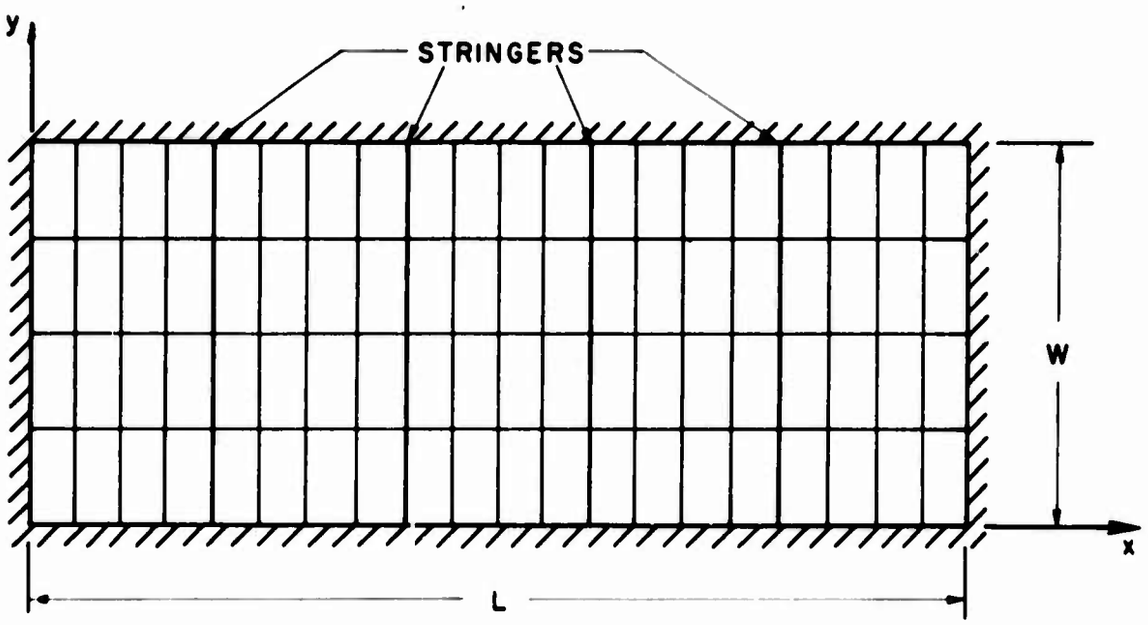

(b) 4x4 GRID PER BAY REPRESENTATION

FIG. 12
FINITE ELEMENT REPRESENTATIONS FOR FIVE-BAY PANEL

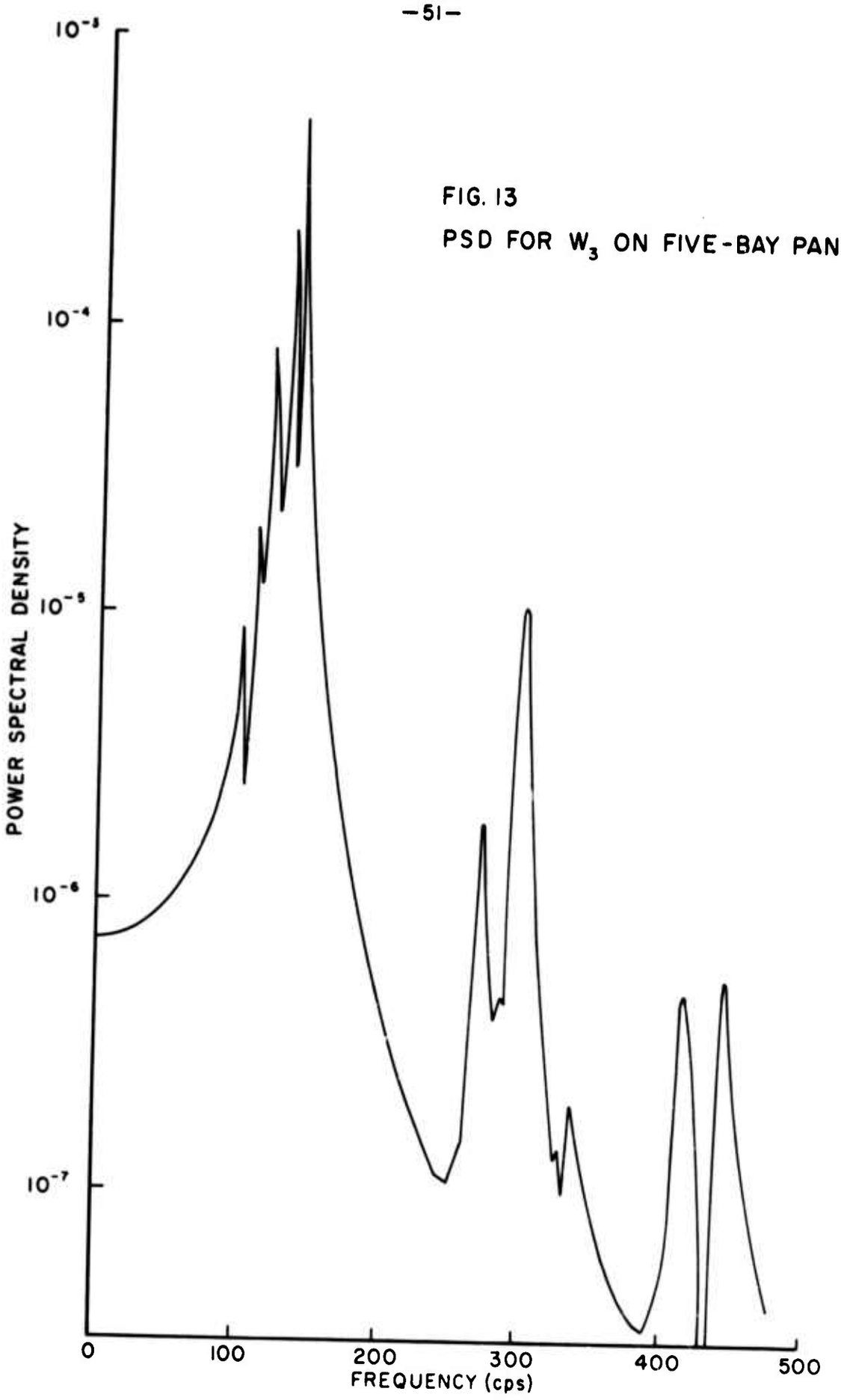

FIG. 13
PSD FOR W_3 ON FIVE-BAY PANEL

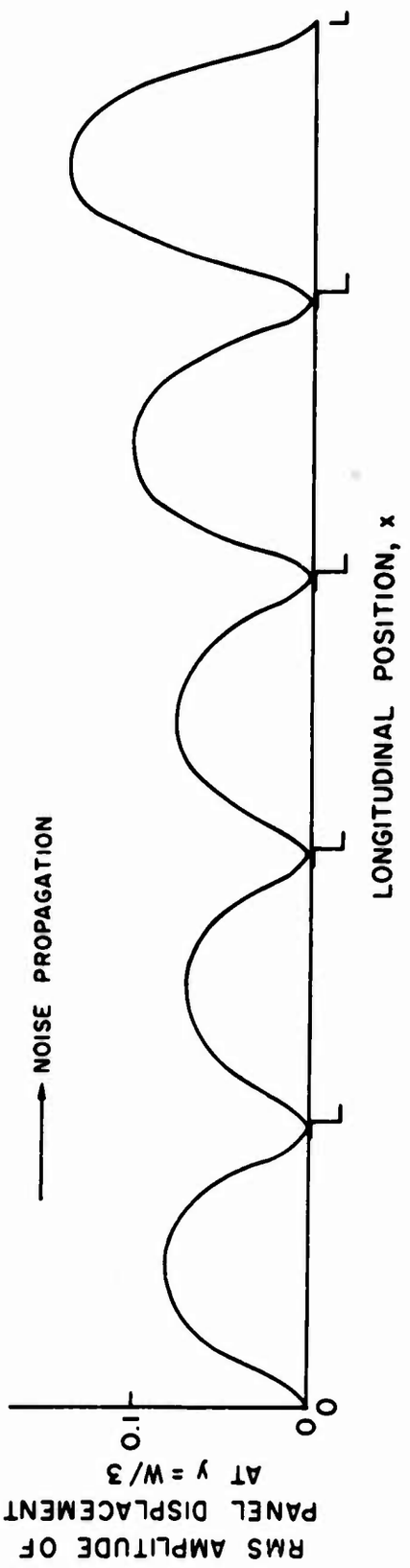

FIG.14 LONGITUDINAL DISTRIBUTION OF RMS PANEL RESPONSE

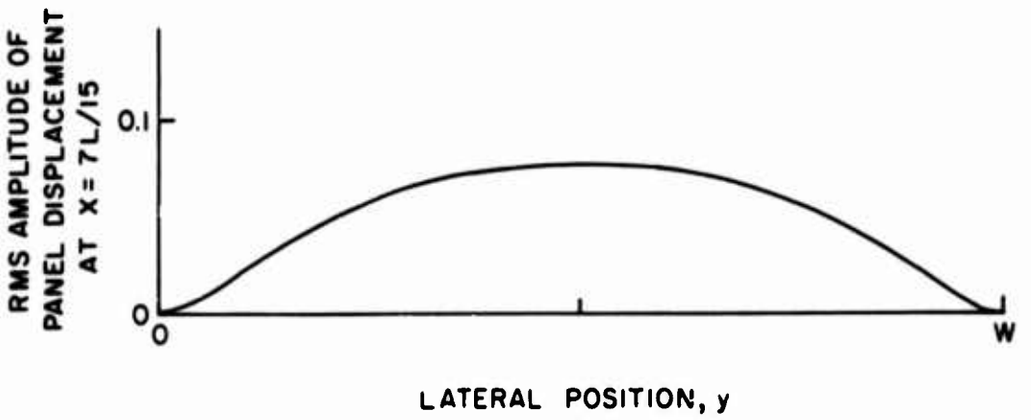

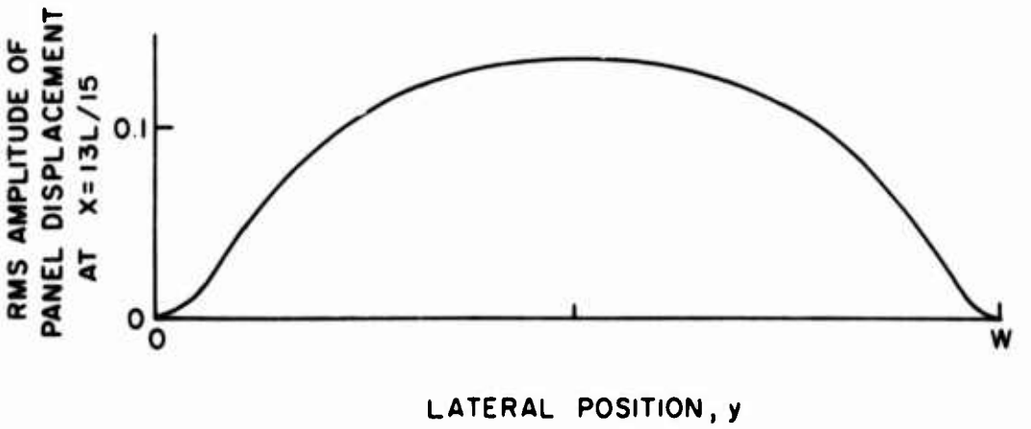

FIG. 15

LATERAL DISTRIBUTIONS OF RMS PANEL RESPONSE

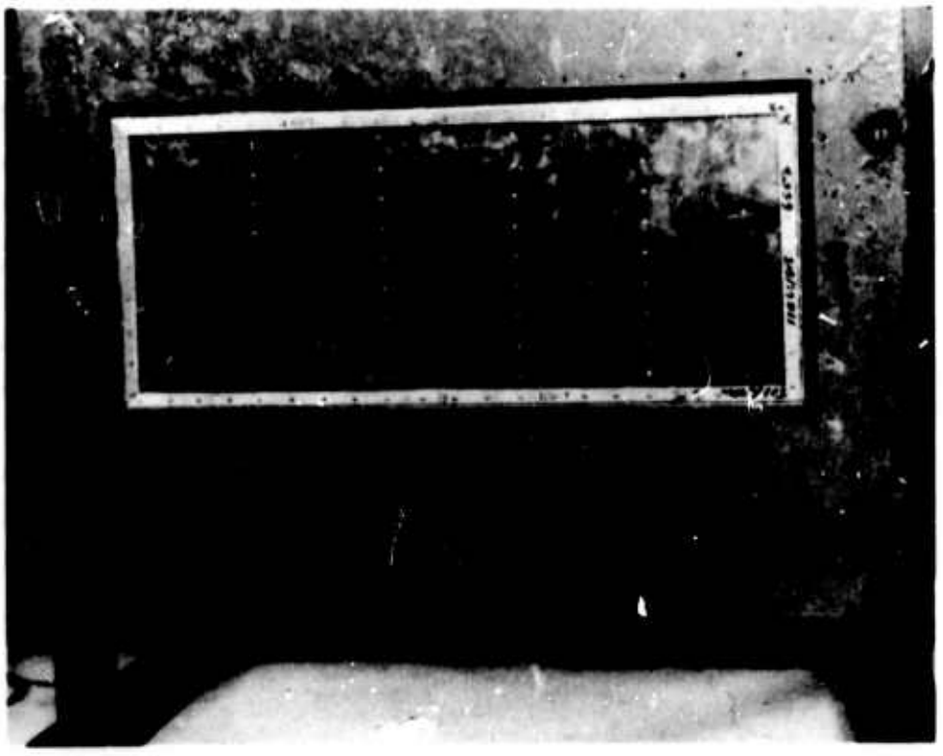

FRONT VIEW OF PANEL

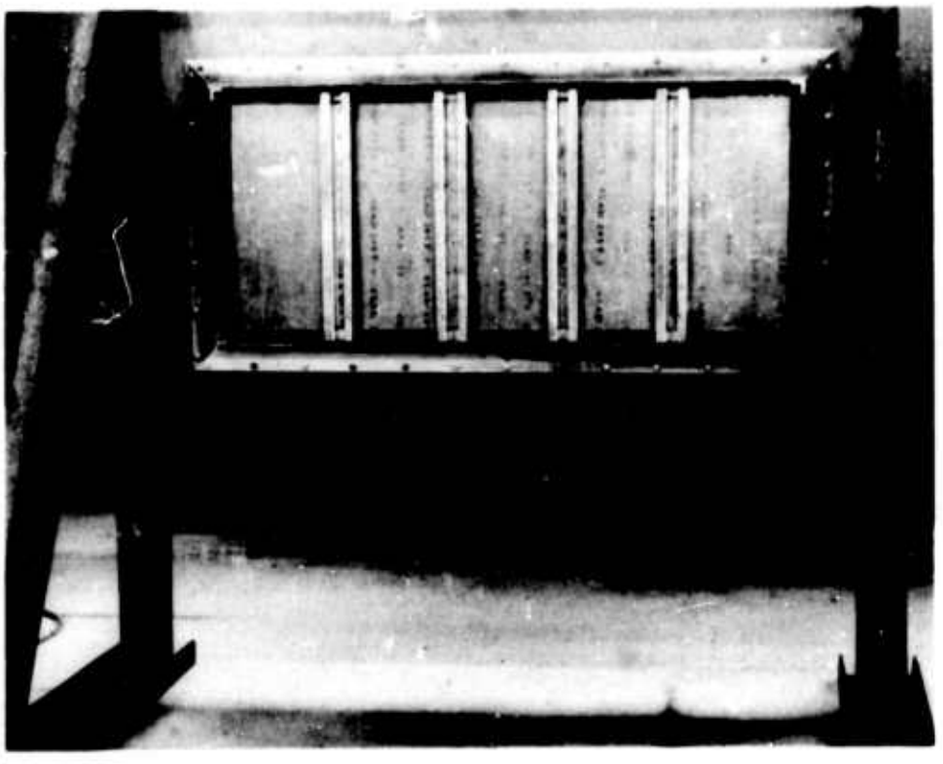

BACK VIEW OF PANEL

FIG. 16 FIVE - BAY PANEL EXPERIMENTAL MODEL

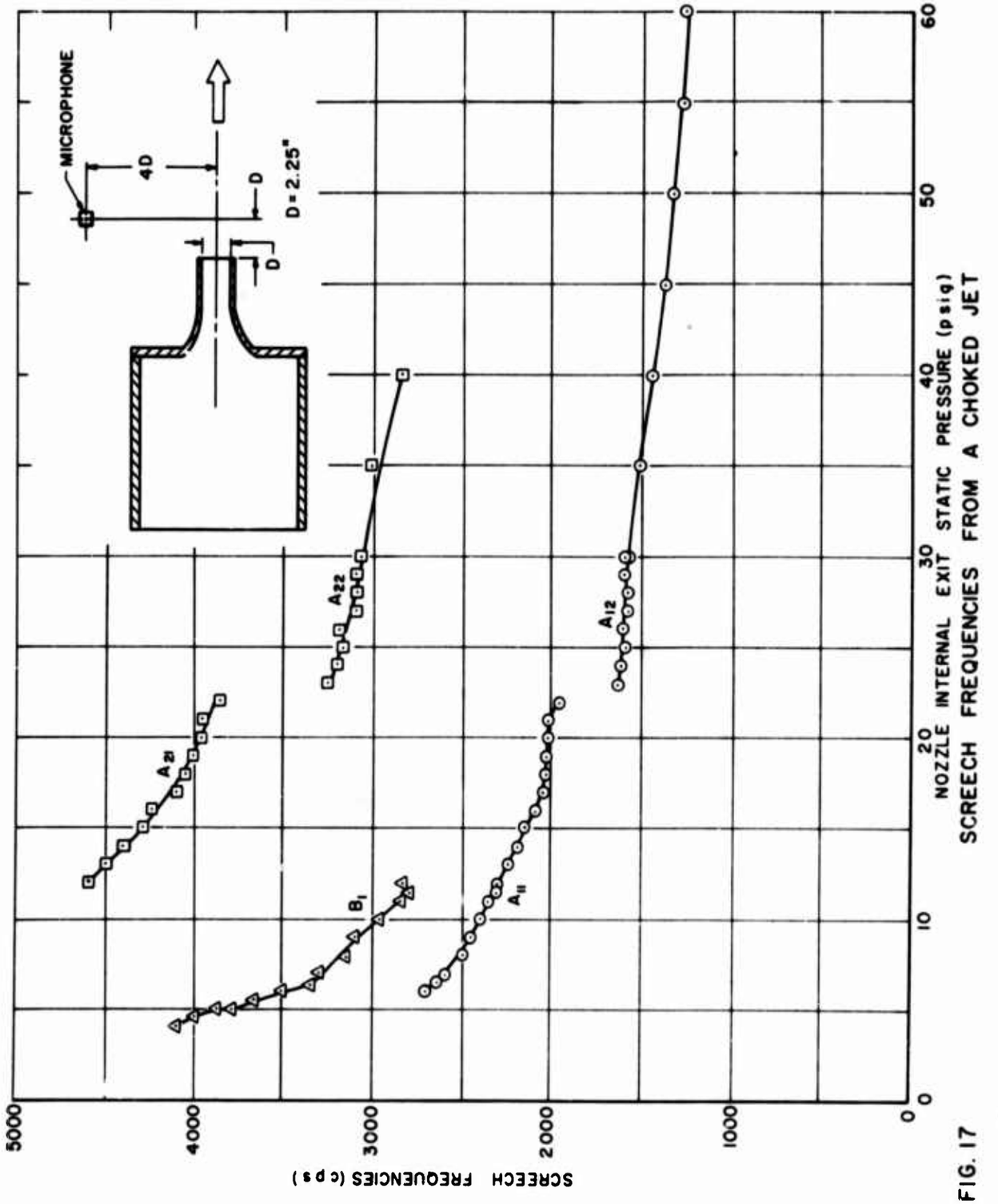

SCREECH FREQUENCIES FROM A CHOKED JET

FIG. 17

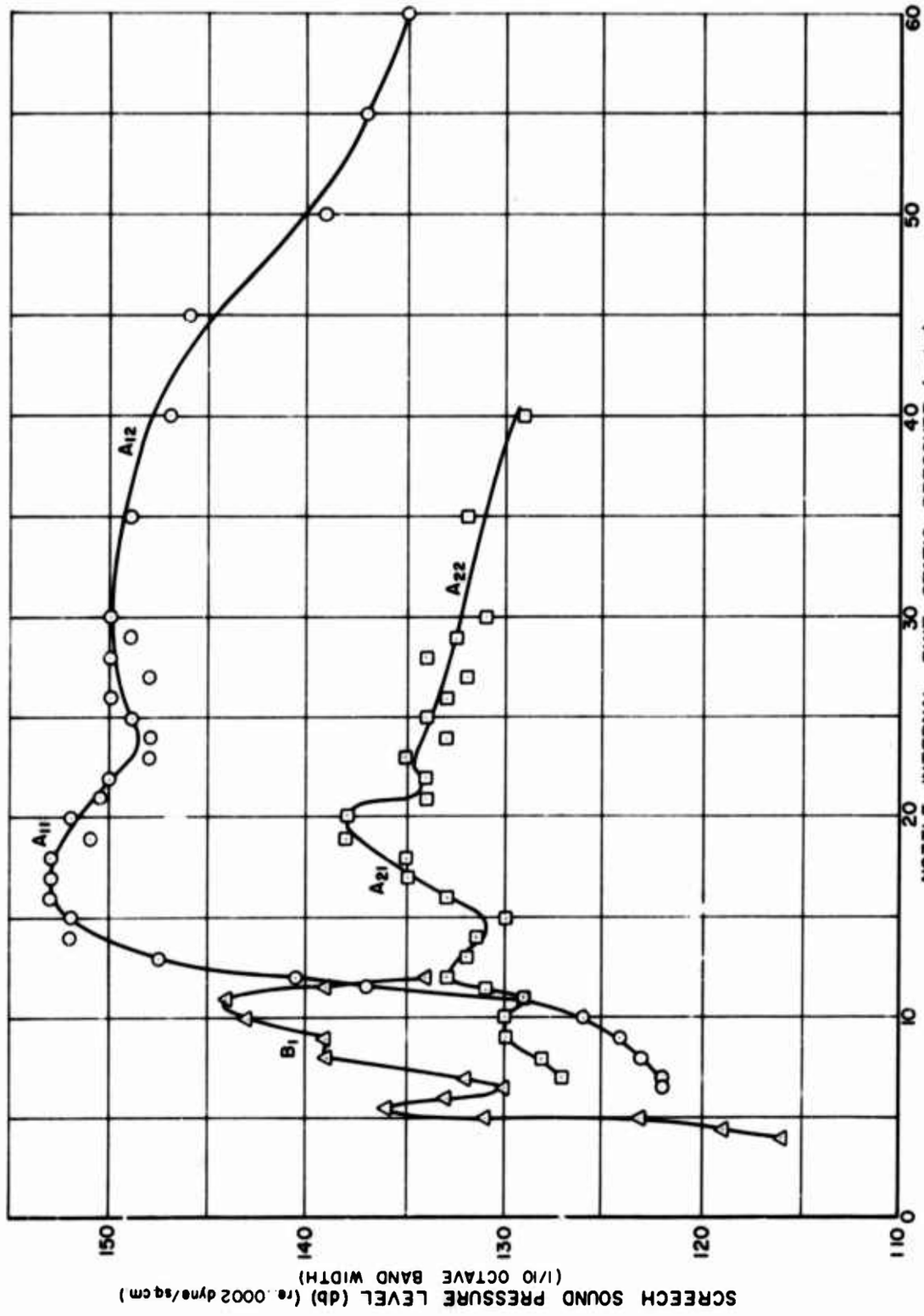

FIG. 18 SOUND PRESSURE LEVELS OF SCREECH FREQUENCIES

MAIN HULL GIRDER LOADS ON A GREAT LAKES BULK CARRIER*

S.T. Mathews

Ship Laboratory

Division of Mechanical Engineering

The importance of the bulk cargo trades on the Great Lakes and Gulf of St. Lawrence, the specialized nature of the Carriers, and the trend to build these in ever-increasing sizes for certain routes, are factors that have given impetus to research in connection with the strength of the large vessels in this trade.

Ship owners, shipbuilders, designers, research groups, regulating authorities, and classification societies have carried out investigations, and a joint technical committee, under the auspices of the Load Line Regulatory Groups, has been formed to co-ordinate this work.

The present work was stimulated by the interest and requirements of the Marine Regulations Branch of the Department of Transport, who are sponsoring a continuing full-scale research program at the National Research Council. They are also sponsoring an extensive full-scale study into the prevailing wave conditions on the Great Lakes and Gulf of St. Lawrence.

Model and full-scale data have been obtained to date for the S.S. Ontario Power (Fig. 1). Similar work is in progress for the M.V. Saguenay, which is a modern, large vessel of lower and more conventional strength. An important part of the model program involves experiments for a proposed 1000-ft. ship.

Although the Ontario Power has main dimensions typical of the Great Lakes vessels, she and her sister ship are especially strengthened for ocean operation during the winter season.

It is difficult to obtain data in waves on the Great Lakes because of the low probability of a vessel being caught in a storm area while transiting the Seaway system. For this reason, advantage was taken of the opportunity to obtain these data on the Ontario Power in the Atlantic Ocean.

FULL-SCALE STUDIES

Stress Gauges

The vessel was equipped with stress gauges at positions one quarter

---

* Taken from paper presented to The Society of Naval Architects and Marine Engineers, read at Expo, Montreal, July 1967.

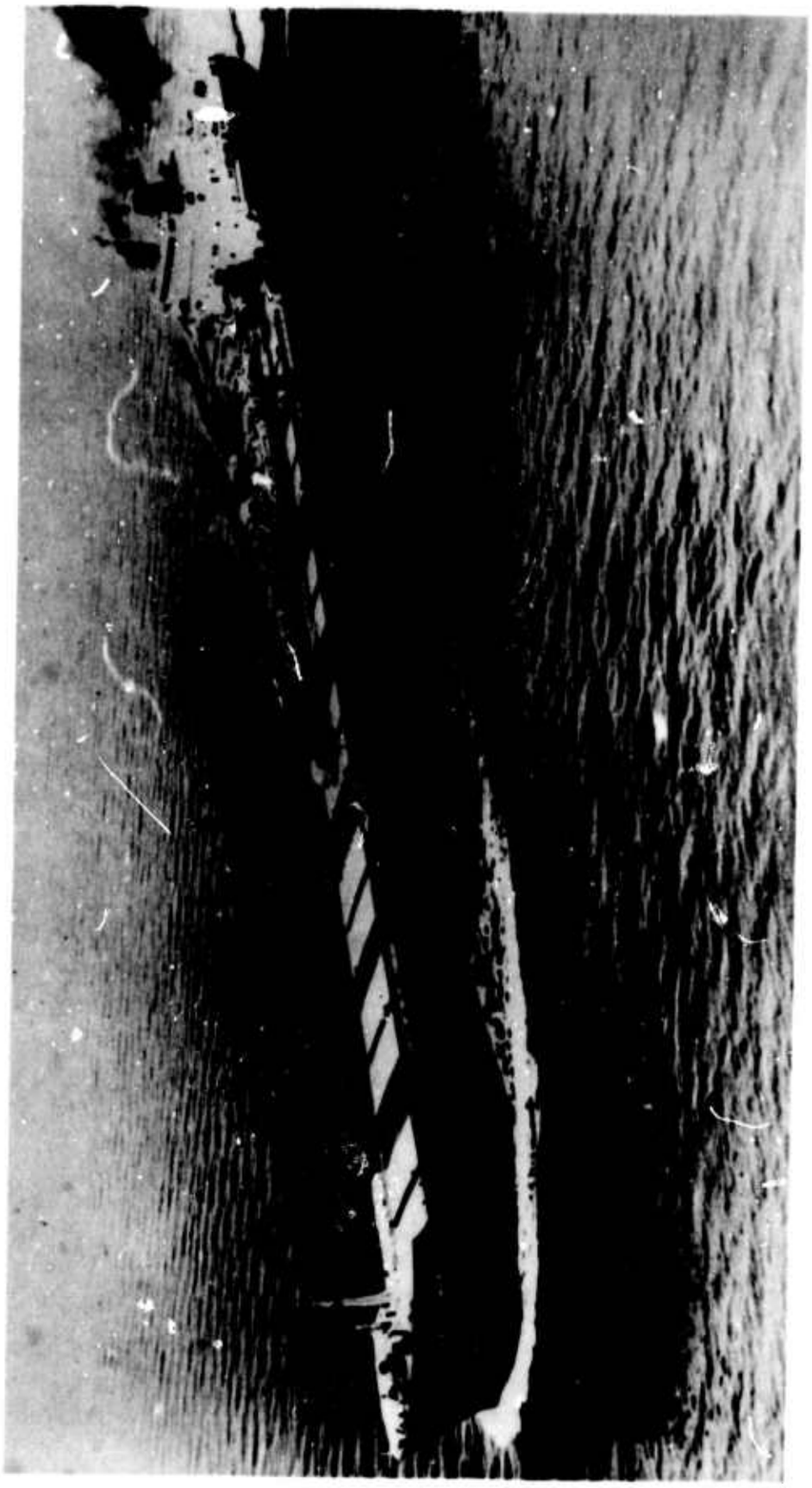

S.S. "ONTARIO POWER"

FIG. 1

of the length from forward and aft, and also at amidships. At each position a matched active gauge and a dummy gauge were placed on each side of the ship. The active gauges were on diagonally opposite sides of the bridge network in order to measure longitudinal stress. At amidships, extra active and dummy gauges were mounted on each side of the ship and connected to measure transverse stresses (longitudinal stresses due to transverse moments).

A stress gauge, as referred to here, is a matched combination of two conventional strain gauges mounted perpendicular to each other in one small element in order to compensate automatically for "Poisson's ratio" effects. The resultant output signal is then proportional to the stress along the axis of measurement.

Unlike most conventional large Lake vessels, the Ontario Power does not have fore and aft walkways under the decks at the sides, therefore gauges were mounted out on the open deck, and extreme precautions had to be taken to maintain waterproof connections. That this was successful is evident from the consistency of the model-ship correlation factors throughout the measurement period during the winter of 1965-66.

During a period of fine weather in Houston, Texas, in January, 1966, the gauges were renewed before Experiment 5.

Dockside experiments to compare actual stresses from the gauges with those obtained from the simple beam theory, using bending moments calculated as differences from buoyancy and weight moments, gave somewhat inconclusive results. The results from the stress gauges were of the same general order as from the simple beam theory, but were not such as to define a correlation factor. The actual measured stresses quoted in this article are based upon the gauge factors supplied by the manufacturer, which should be accurate within about 1 percent. The dockside experiments were carried out by shifting water ballast, and long delay times were involved. The technique has since improved, however, and more consistent results have been obtained with the Saguenay. A carrier amplifier system was used with the gauges and the outputs were recorded on a 14-channel analogue tape recorder. Records were also taken of the roll, pitch, and heaving motions of the ship, although this information is not presented here. Data signals were monitored in each experiment on a vacuum tube voltmeter and on paper tape recorders. There was always at least one NRC operator on board to operate the equipment and launch buoys; this latter operation required assistance from the crew.

Wave Buoys

Wave measuring buoys were used throughout the experiments for measuring sea state and this information also was recorded on the tape recorder. The wave buoys were equipped with free falling body type accelerometers, a system developed by Dr. R.L.G. Gilbert of the Bedford Institute of

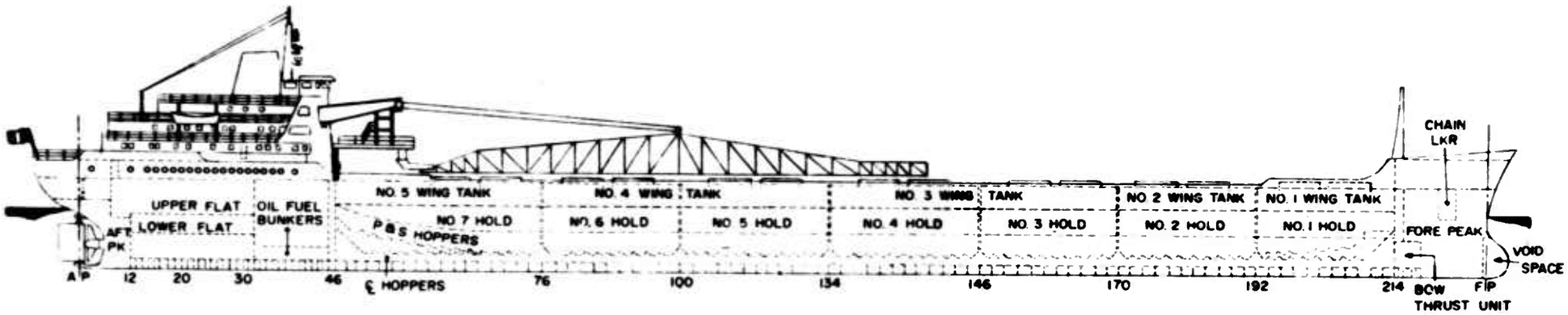

HOLD 1	5,500
HOLD 2	-
HOLD 3	5,350
HOLD 4	-
HOLD 5	7,200
HOLD 6	-
HOLD 7	7,600
	25,650 L/TONS

FUEL OIL	737
FEED WATER	65
LUBE OIL	24
DIESEL OIL	20
STORES	50
CREW EFFECTS	10
FRESH WATER	200
	1,106 L/TONS

CARGO	25,650	
OTHER	1,106	
D.W.T.	26,756	
LT. SHIP DISP.	10,661	
	37,417 L/TONS	29-00 MEAN
	READING	29-00 MEAN
	ADMID.	29-03 MEAN
	SAG	-03

S.W. DRAFT F27-05 A30-07 M29-00 ADMID 29-03

ONTARIO POWER

FIG. 2

LEAVING SEVEN ISLANDS JANUARY 27, 1966

Oceanography. In this type of accelerometer a free falling moving coil is oscillated vertically, and when the accelerometer is stationary the pulse rate is constant and corresponds to the acceleration due to gravity. The pulse rate is always proportional to the resultant acceleration field; therefore, when measuring waves the wave acceleration is proportional to the instantaneous pulse rate minus the static pulse rate. This system does not require the accelerometer to be mounted on a gyro-stabilized vertical axis, which is necessary for a normal inertial accelerometer, where the signal variations due to changes from the vertical of the gravitational bias signal are high. Simple telemetering of pulses gives a pulse frequency modulation system. The technique was developed for lowering the buoys on heaving lines over the stern with the ship under way, even in violent storm conditions. Many calibrations and comparisons with results from other instruments have been made, and the buoys are generally considered reliable. Transmission was good up to a distance of five miles, although quality fell off in the higher sea states.

Measurements and Analysis

Data were obtained during the normal voyages of the ship, and wave buoys were only launched in heavy weather conditions. Following original plans, no attempts were made to recover the buoys. Simultaneous data recording was carried out for each experiment for at least 20 minutes. A complete data summary for these experiments is given in Reference 1.

An experiment number was given to each recording period. In all, eight buoys were launched, corresponding to Experiments 1, 2, 5, 7, 11, 13, 16, and 19. The loading condition corresponding to Experiments 5, 7, and 11 are shown on Figure 2.

The highest static bending moments occur in the deep ballast condition and are hogging moments. The next worse condition is the alternate hold loading of ore cargo, which also gives rise to hogging moments. The grain cargo conditions produce sagging moments of lower values.

Typical monitoring paper tape stress records are shown on Figure 3. The vibration stresses occurring at frequencies higher than the main wave component encounter frequencies can be seen on the unfiltered records. Records with the vibration frequency stresses filtered out are also shown.

Log sheet records were kept in connection with each experiment. The speeds recorded correspond to the distance travelled between daily noon observations. Visual averages of stresses from voltmeter readings were also noted on the log sheet. The sea states data were estimated only. The magnetic tape recordings of stresses and wave accelerations were analyzed in the Analysis Laboratory of the Division of Mechanical Engineering, using hybrid computer equipment. The analogue stress records were automatically converted to digital data, and spectral analysis carried out and automatically

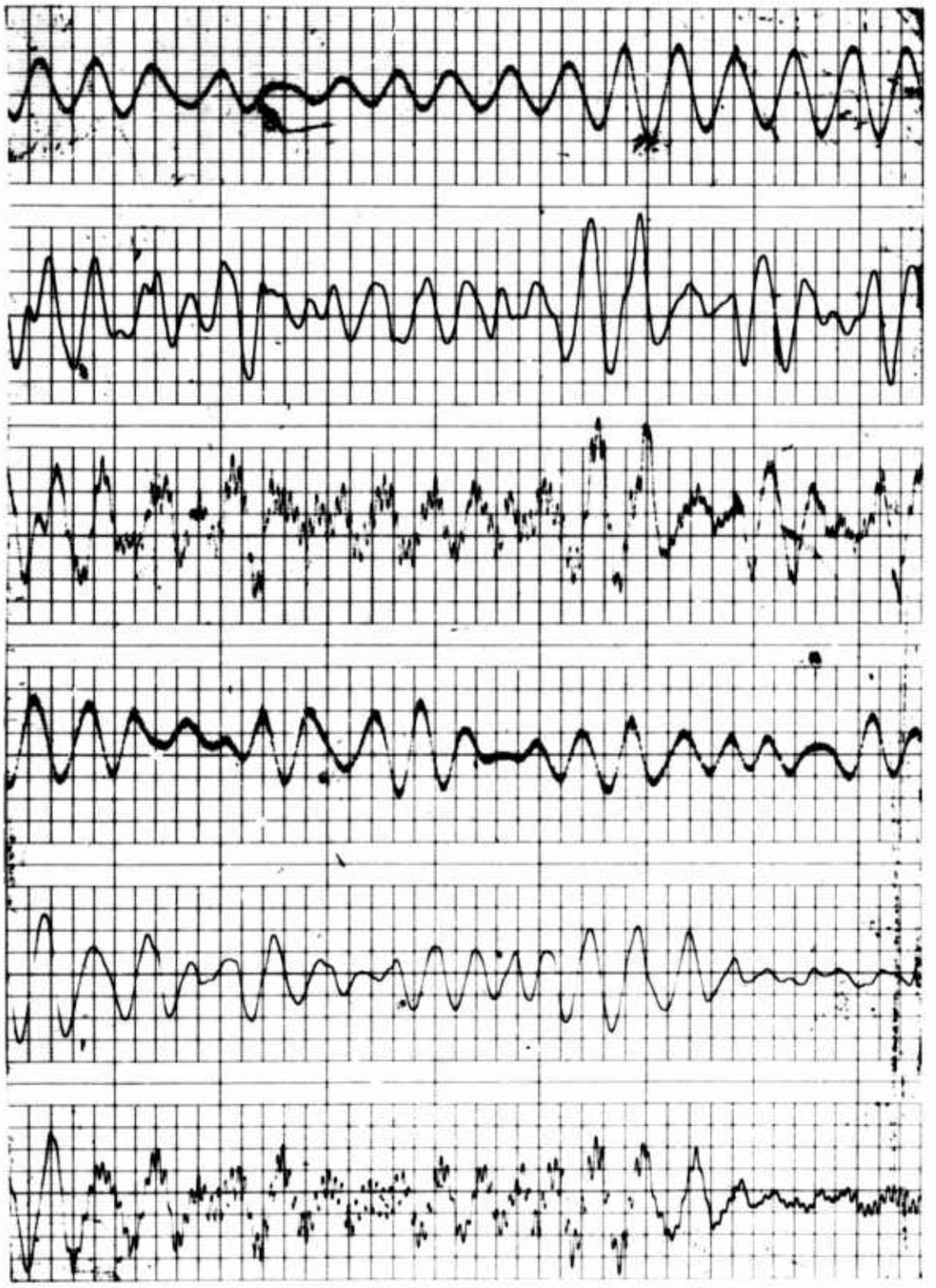

EXPERIMENT #16

PAPER SPEED = 1.25mm/sec

FIG. 3

plotted. The spectral analysis diagram for the midships longitudinal stress for Experiment 11 is shown on Figure 5. The area under the curve is the mean square profile deviation of stress for all frequencies. The stress associated with the vibration frequency of the ship should be noted. Printouts on the diagram are given for the root mean square (rms) profile deviation for all frequencies, and for the rms with the vibration frequencies filtered out. Statistical analyses show that the maximum stress single amplitudes in the recording periods are close to four times the rms deviations.

In the case of the accelerometer pulse recordings, the first analysis step was to automatically convert the pulses into a continuous record before carrying out the spectral analysis in the digital mode. The acceleration spectrum for Experiment 11 is shown on Figure 4. This spectrum includes information at the higher wave frequencies, which proved most useful in examining the mechanics associated with vibration stresses. Because of the low frequency noise (down to zero frequency) present in the acceleration records, it was decided to allow manual intervention in the analysis before obtaining the wave profile spectrum.

At this stage the acceleration spectra were examined and a decision made regarding the low frequency cutoff points, before the process of double integration of the acceleration spectra was carried out in order to produce the displacement spectra. This double integration was effected by dividing the acceleration spectra by the frequency raised to the fourth power.

The displacement spectrum for Experiment 11 is also shown on Figure 4. The area under this curve is the mean square profile deviation. A typeout of the rms deviation in feet is also given. For standardization purposes, and in order to discuss stresses in more meaningful terms, the significant single amplitude of stress is used, and for this article is defined as twice the rms deviation. The correct definition of significant amplitude is the average of the one-third highest amplitudes in a given sample, and for representative samples, in connection with ocean wave phenomena, these definitions lead to very similar values.

For the wave data, significant amplitude is defined in the same way. However, sea heights (double amplitudes) are discussed and significant sea height is therefore defined as four times the rms profile deviation.

Table 1 gives a summary of the ship speeds, conditions, and sea states for the various experiments. The speeds are estimates applicable at the time of each experiment and for the most part are obtained by comparing frequencies of encounter from pitch and stress spectra with the wave frequency corresponding to the peak of the displacement spectrum. The sea length is defined as the wave length corresponding to the frequency for the peak of the displacement spectrum. The relative sea directions are estimates only.

Table 2 gives a summary of the measured stresses. Those quoted in

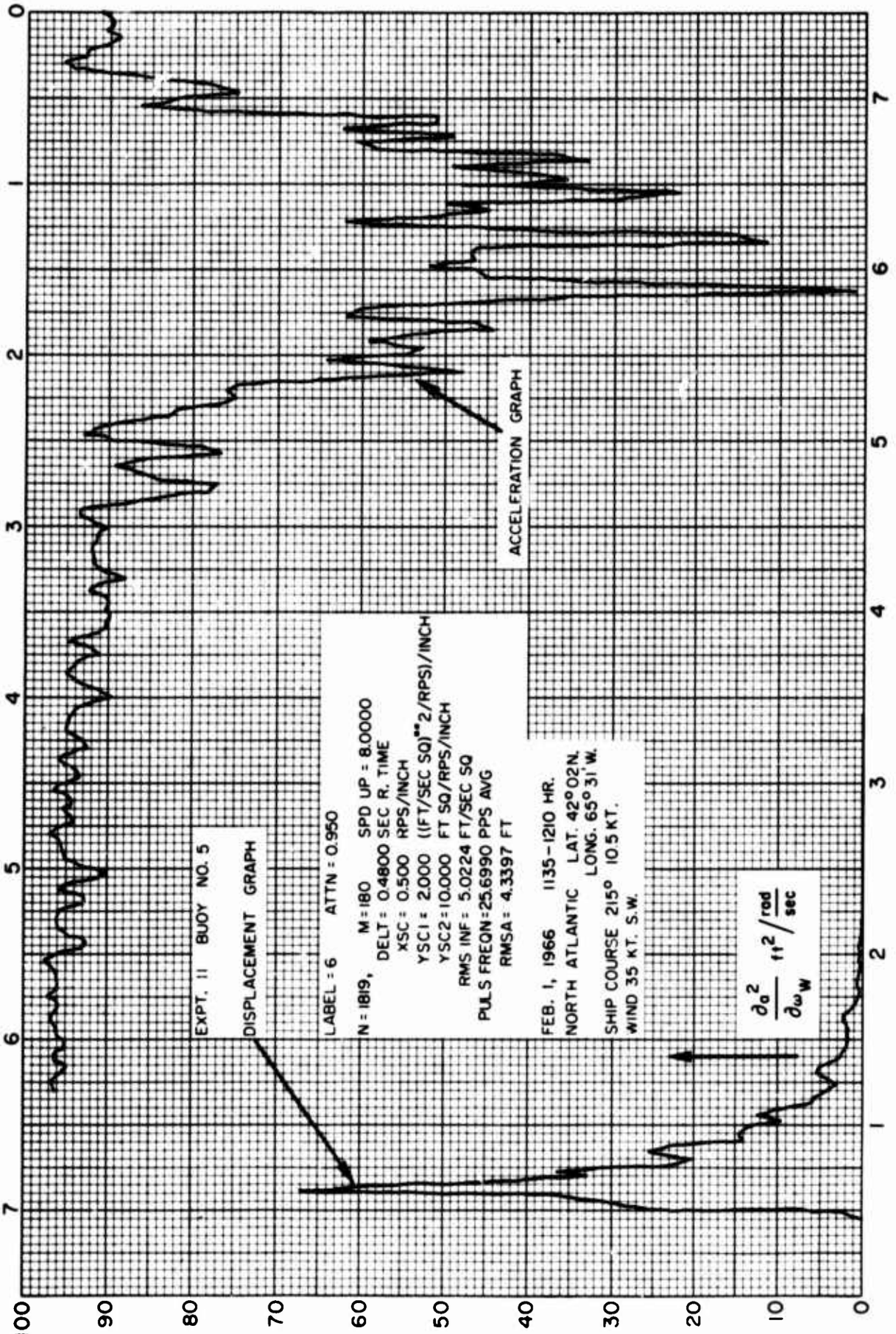

FIG. 4 TYPICAL WAVE SPECTRA

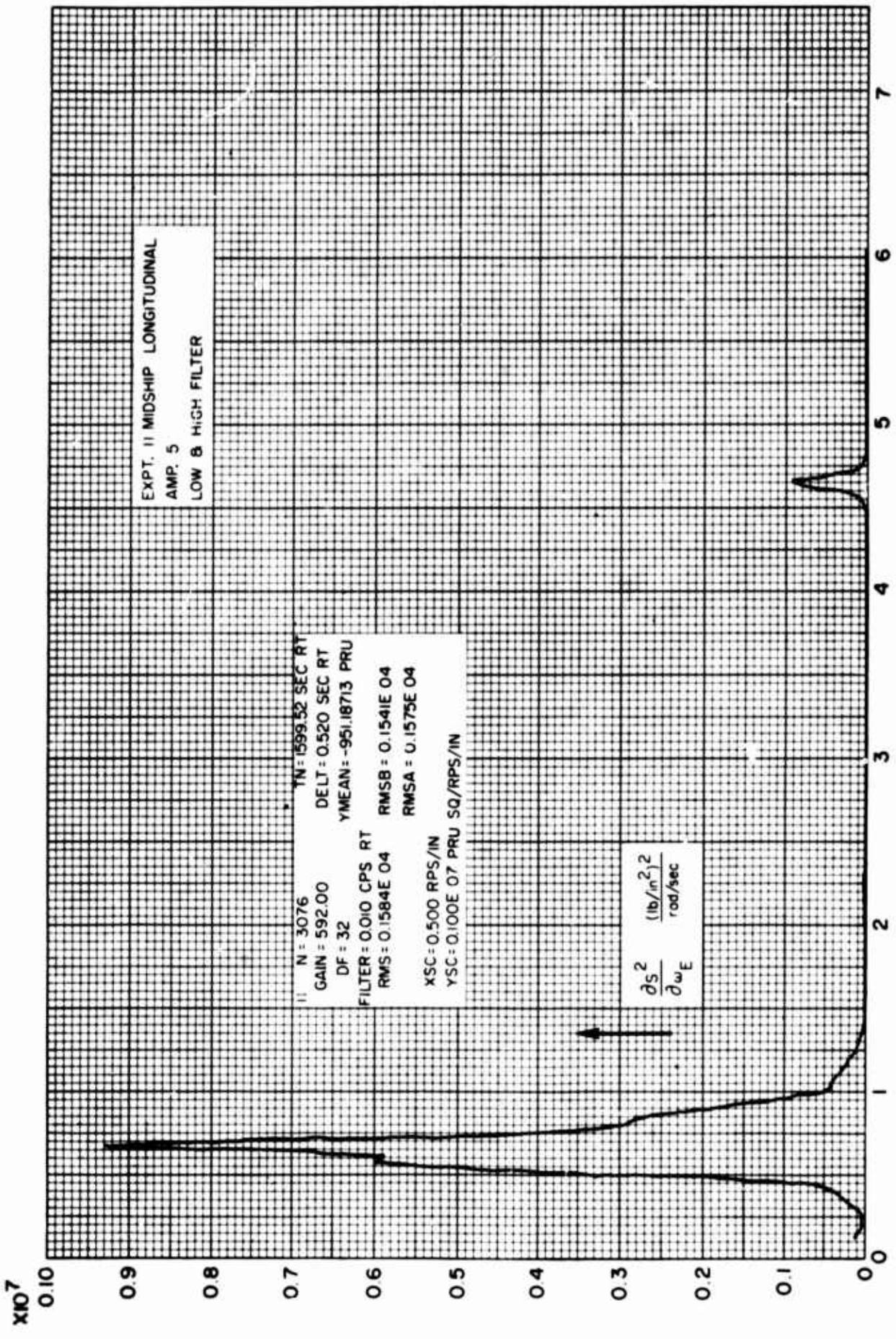

TYPICAL STRESS SPECTRUM
MIDSHIP LONGITUDINAL GAUGE

FIG. 5

TABLE 1

SHIP CONDITIONS AND SEA STATES

Expt. No.	Date	Cargo	Mean Draft, ft-in	Ship Speed, knots	Sea Height H_S, ft	Sea Length λ_S, ft	λ_S/H_S	Relative Sea Direction
1	12 Dec./65	Grain	29-03	13.37	23.6	653	27.7	Following
2	13 Dec./65	Grain	29-03	9.9	30.0	810	27.0	Following
5	28 Jan./66	Ore	29-00	5.58	25.6	598	23.4	45 deg Port (Bow)
7	29 Jan./66	Ore	29-00	4.28	28.2	719	25.5	22½ deg Stbd. (Bow)
11	1 Feb./66	Ore	29-00	3.74	17.4	545	31.3	Ahead
13	27 Mar./66	Grain	28-01	14.2	12.4	680	54.9	135 deg Port (Stern)
16	7 Apr./66	Deep Ball.	21-09	12.67	19.0	955	50.3	45 deg Port (Bow)
19	8 Apr./66	Deep Ball.	21-09	5.64	38.3	1000	26.2	Ahead

TABLE 2

SUMMARY OF STRESS MEASUREMENTS MIDSHIP GAUGES

lb/sq in units I/y = 78.59×10^3 sq in ft

	1	2	3	4	5	6	7	8
	Significant Longitudinal Wave Stresses							
Expt. No.	Long. MMT + -	Trans. MMT + -	Vibration + -	Resultant + -	Max. Sig.	Max. Long'l Wave Stress ±	Still Water Stress (Calculated)	Max. Total Stress (Derived)
1	4424	1617	266	4709	1.51	7110	1682 S	8,792 S
2	5186	(1895)	432	5521	1.63	9000	1682 S	10,682 S
5	3202	886	320	3321	1.92	6376	2736 H	9,112 H
7	3270	945	302	3403	1.71	5819	2736 H	8,555 H
11	3150	1399	651	3445	2.00	6890	2736 H	9,626 H
13	1979	306	201	2002	1.74	3484	1084 S	4,568 S
16	2924	461	809	2960	1.79	5298	7125 H	12,423 H
19	4866	832	723	4937	1.85	9134	7125 H	16,259 H

column 1 include the small vibration stresses shown in column 3. The figure for the transverse stress, column 2, for Experiment 2, was not recorded, and the 1895 psi value used is the same proportion of the longitudinal stress as for Experiment 1 where the ship was in the same loading and following sea condition. The resultant longitudinal stress of column 4 is the square root of the sum of the squares of columns 1 and 2. The factor

$$\frac{\text{maximum stress}}{\text{significant stress}}$$

for each experiment, column 5, was obtained from the means of the peaks and troughs maxima in the statistical analyses. Column 6 shows the maximum single amplitudes of stresses due to waves, by multiplying column 4 by column 5. Column 7 shows the still water stress obtained, from simple beam theory, by dividing the calculated static bending moments by I/y. In order to gain an appreciation for the magnitudes of the actual maximum stresses (column 8), the maximum wave stresses are added to the corresponding still water stresses. It should be noted that the still water stresses quoted here are the maximum values for each condition even though the maximum does not necessarily occur at amidships. Model tests have shown that there is a shift in the mean value of the wave stress that can be considered as modifying the still water stress; corrections for this effect are not made in Table 2.

Comments on Results

The maximum stresses, Table 1, column 8, are well within the elastic limit of the ship's high strength steel, and there was no evidence of any main structural damage as a result of the severe storms through which the vessel sailed. The worst still water stresses for the conditions considered occur in the deep ballast condition that give rise to hogging. Next in importance are the stresses for the ore cargo with alternate hold loading, which are also hogging stresses. The evenly distributed grain cargoes give the lowest still water stresses and for these conditions the ship sags. The very severe storm of Experiment 19 coincided with the ship in the deep ballast condition, and both the wave stress (±9134 psi), and the still water stress (7125 psi H), are the highest encountered during the ship's winter voyages. The maximum total stress for Experiment 19, derived as previously described, is 16,259 psi in the hogging mode.

When considering these stresses, it should be borne in mind that the midship section modulus of the Ontario Power is 1.84 times that of the Saguenay, which has the more conventional strength for this type of vessel. Sea states of the order of those in Experiments 5, 7, and 11 have been shown possible in recent measurements on the Great Lakes. The corresponding wave stresses for these vessels of more conventional strength, in connection with the hogging ballast condition of Experiment 19, could lead to maximum total stresses of the order of 25,000 psi.

Model Tests

A wooden model, 1/40 full size, was manufactured and statically and dynamically balanced for the condition shown in Table 3, corresponding to the 25.5-ft. draft. The model sheer and freeboard were correctly scaled, and it was decked in. A transverse hinge was fitted amidships, and a longitudinal strain-gauge type load cell was placed at the level of the model deck to measure the forces about this hinge. The small gap between the forward and after bodies of the model was made watertight with plastic tape. The load cell centre was 5 in. above the hinge line and its maximum range was ±1000 lb. for ±0.002 in. deflection.

TABLE 3

S.S. "ONTARIO POWER" HULL PARTICULARS

L.O. A.	711.42 ft	Depth	45.8 ft
L.B.P. (L)	675 ft	Seaway Draft (T)	25.5 ft
Beam (B)	75 ft	Seaway Δ (F.W.)	31,500 T

The model transducers were excited from constant voltage power supplies and recording was carried out on a galvanometer strip chart recorder.

Recordings of thrust, torque, shaft speed, model speed, pitch, heave, roll, and wave profile were made as well as longitudinal bending moment amidships. Only the bending moment and wave data are reported.

Tests were carried out in regular waves over a range of wave lengths from less than half to more than twice ship length. Tests were carried out in the 400-ft. × 25-ft. × 10-ft. tank, which is equipped with a pneumatic wave maker. The actual height-to-length ratio of the test waves was, on an average, 1/30. The tests were conducted in head, beam, and following seas at the 25.5-ft. draft. For the head and following sea conditions, at least five model speeds were tested for each wave length. This process, although more time consuming than irregular sea tests, does allow for a high degree of accuracy in obtaining data. The results of an experimental comparison (Ref. 2) of bending moment responses obtained in regular and irregular waves, show excellent agreement between the two methods. The linear theory (Ref. 3) is then used in connection with the model responses and wave spectra data, for full-scale predictions in irregular seas.

In the experiments the model was self-propelled and steered by its own rudder and was completely free of guides and constraints except for the electrical

connection leads that were suspended on a soft spring and led into the model at its centre of gravity so that their effect was negligible.

For each wave length, values of bending moment response coefficients (μ) were plotted against nondimensional frequency of encounter, in a large-scale diagram. The frequency of encounter varied as model speed was changed from one run to the next and was measured directly from the model bending moment recordings. For each wave length, the model was run over a speed range from zero to speeds corresponding to shaft speeds well in excess of the calm water maximum, in order to cover the largest possible range of encounter frequencies. The data obtained in head, following, and beam seas were later used for bending moment estimates at other headings.

A diagram for each heading at 15-deg. intervals between head and following seas was prepared, and curves of constant Froude number values of 0, 0.05, 0.10, 0.15, and 0.20 constructed on each diagram. The constant Froude number curves for each heading form the basic input data for a computer program that calculates bending moment response coefficients in irregular long crested and short crested seas.

Equipment to obtain data in waves at various headings in the 200-ft. × 400-ft. manoeuvring tank is now becoming available, so that some of the assumptions made here will not be necessary. There are, however, many problems regarding test techniques and automatic data processing to be solved if full use is to be made of this type of installation.

The assumptions made here on a rational basis lead to results that agree with the trend indicated by available published data regarding the effect of course changes, and may be considered as a special interpolation technique.

Some response coefficient curves for regular waves derived in this way are shown on Figure 6, together with some of the basic head, beam, and following sea data.

Standard Wave Spectra

The single parameter set of standard wave spectra, based upon the work of Reference 4 and recently adopted by the International

REGULAR WAVES $\mu \sim \omega^2_{WL}$ ——————

IRREGULAR WAVES { LONG CRESTED $\mu_L \sim \omega^2_{WLS}$ — — — — —
SHORT CRESTED $\mu_S \sim \omega^2_{WLS}$ ----------

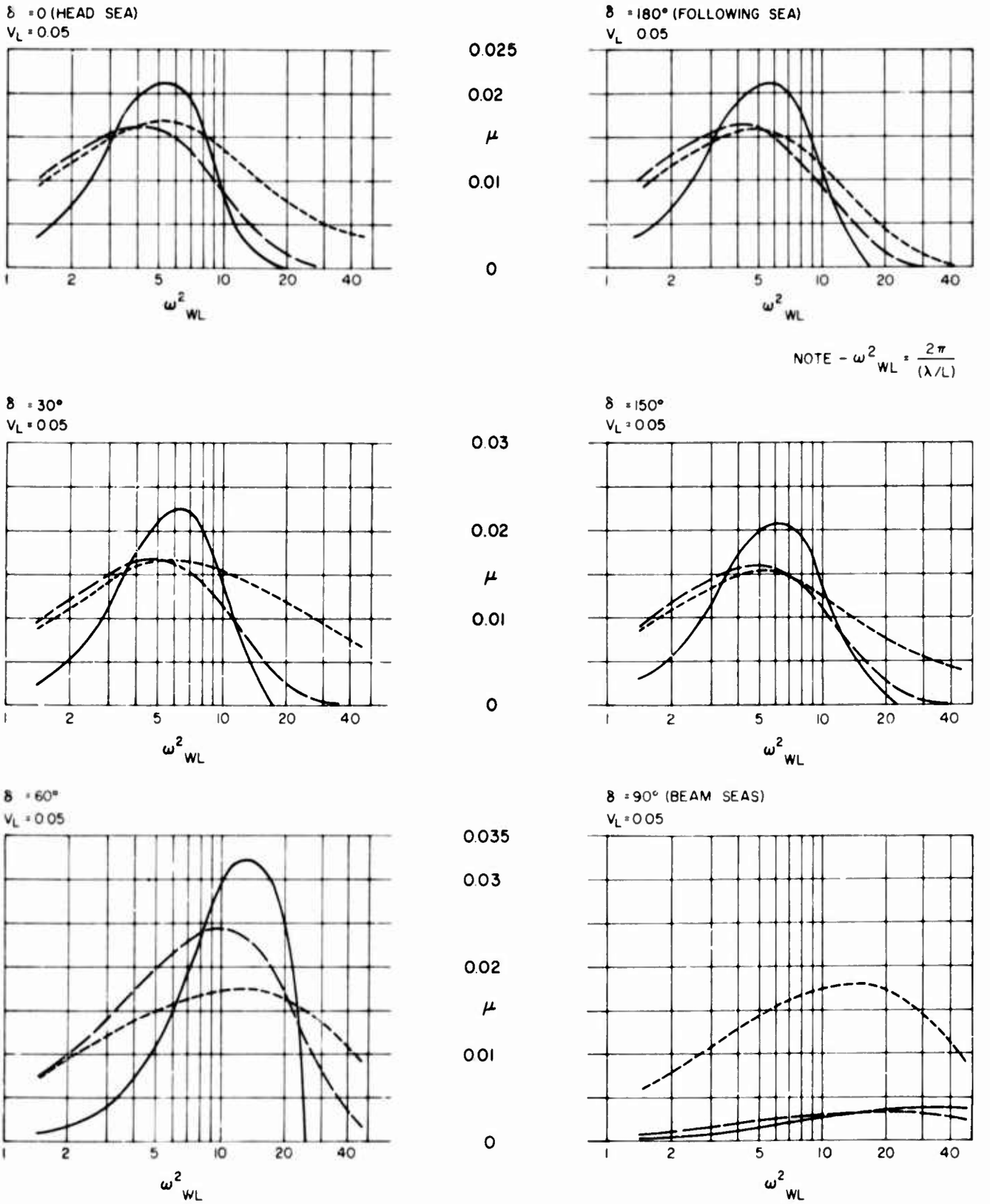

BENDING MOMENT RESPONSE COEFFICIENTS ~ WAVE FREQUENCY

AT VARIOUS WAVE TO COURSE ANGLES (δ)

FIG. 6

Towing Tank Conference, can be put in the following nondimensional form

$$\frac{\partial(a_\sigma^2)}{\partial\omega_{W\sigma}} = \frac{0.0081}{\omega_{W\sigma}^5 \cdot e^{0.002025/\omega_{W\sigma}^4}}$$

The area under the above nondimensional spectrum is necessarily equal to 1. The single parameter for the family of spectra defined by the formula is σ or wave height ($H_S = 4\sigma$). The resultant standard spectra are representations for "fully developed" seas and have been adopted for systematic investigation and comparison purposes. The value of $\omega_{W\sigma}$ corresponding to the nondimensional spectrum peak is: $\omega_{W\sigma S} = 0.200$. Considering the wave length (λ_S) corresponding to the spectral peak a reference wave length for any fully developed sea it follows from the formula that λ_S/H_S is constant and

$$\frac{\lambda_S}{H_S} = 39.2$$

From the wave measurements made during the Ontario Power experiments, values of λ_S/H_S in the range 23.4 to 54.9 were measured (see Table 1). These variations in sea slopes indicate the need for another parameter in the standard spectra formulation if realistic representation of the range of possible sea states is to be made. A parameter for this purpose is introduced here and is described below.

Modification of Fully Developed Sea Standard Spectra Formulation by Introduction of a Sea Slope Parameter

The formulation used corresponds exactly to that for the fully developed sea, and for all sea states is taken as

$$\frac{\partial(a_\sigma^2)}{\partial\omega_{Wk}} = \frac{0.0081}{\omega_{Wk}^5 \cdot e^{0.002025/\omega_{Wk}^4}}$$

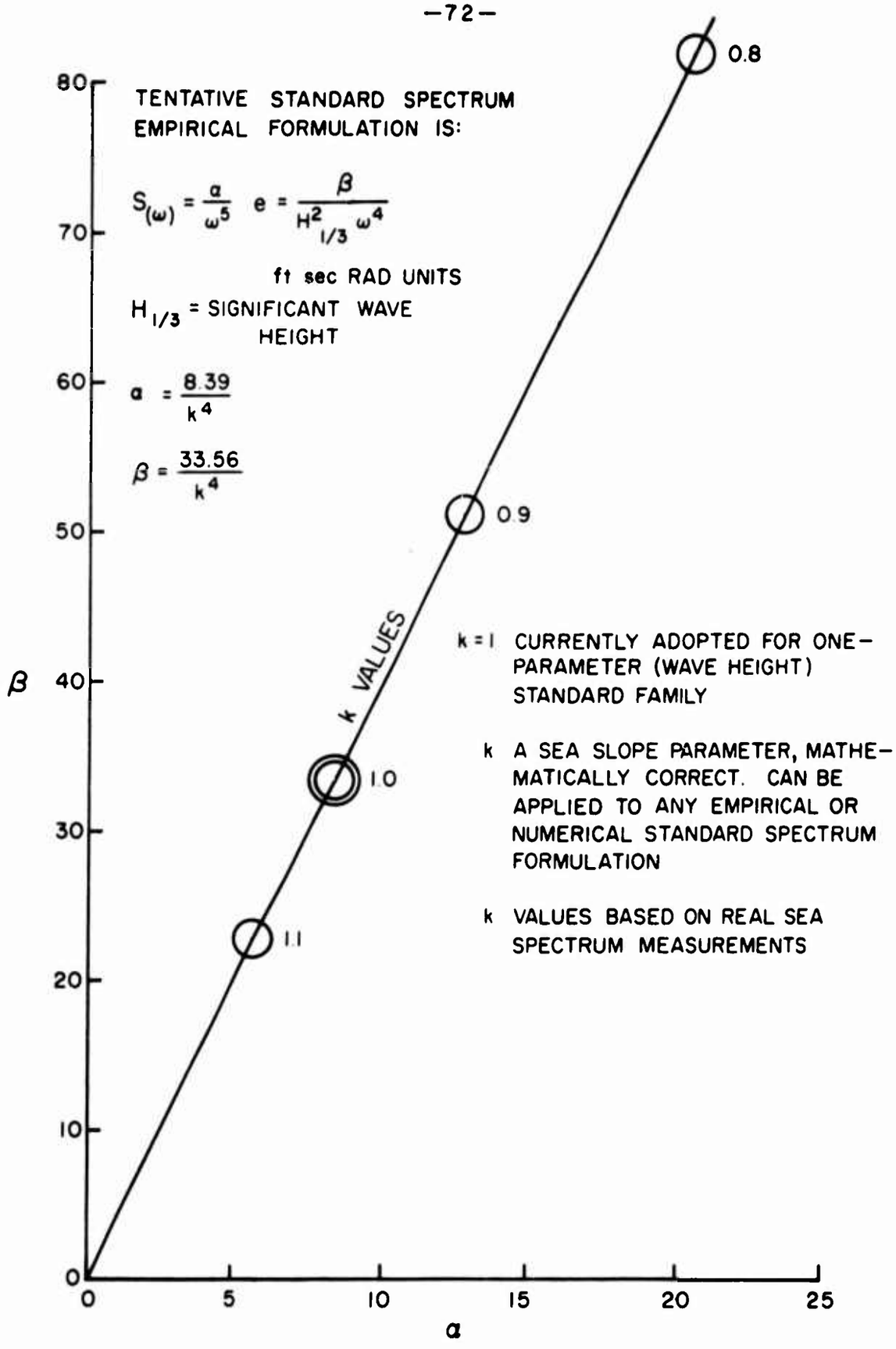

STANDARD SPECTRA CONSTANTS (α ; β)

VARIATION WITH k

FIG. 7

where

$$\omega_{Wk} = k\,\omega_W \sqrt{\frac{\sigma}{g}}$$

Figure 7 shows the connection with the standard spectrum in dimensional form. When this new parameter k is equal to unity, the preceding formula becomes exactly that for fully developed seas, previously described under "Standard Wave Spectra". The effect of changing the factor k from unity is to modify all the wave frequencies (ω_W) in inverse proportion to k. A value of k less than unity for a sea, produces a shift towards the higher frequencies when compared with fully developed spectra. The corresponding sea length-to-height ratios (λ_S/H_S) are then

$$\frac{\lambda_S}{H_S} = 39.2\,k^2$$

The smaller k values produce the shorter, steeper seas. Values of k greater than unity produce longer seas of smaller slope and can perhaps be thought of in connection with the presence of swell. In the experiments described in this article, k values obtained by comparing the frequencies for the peaks of the displacement spectra with that for the peak of the standard spectra, were in the range $0.78 \leq k \leq 1.17$ and led to the sea slopes shown in Table 1.

Bending Moment Responses in Irregular Waves

The regular wave responses obtained, as previously described, were used in connection with the two-parameter spectra formulation to examine bending moments in irregular waves. For the long crested wave calculations, the parameters were ship speed (V_L), course (δ), and the relative sea state parameter (σ_k). The regular wave responses for constant V_L values were drawn in on the basic $\mu \sim \omega_{EL}$ diagrams. For this the following relationship was used

$$\omega_{EL} = \omega_{WL} + V_L\,\omega_{WL}^2 \cos\delta$$

These V_L curves were then plotted against ω_{WL}^2 (Fig. 13) for the input of the computer calculations.

The responses in long crested irregular waves were then obtained for each heading and sea state σ_k (or ω_{WLS}^2) from the equation

$$\mu_L^2 = \int_0^\infty \mu^2 \frac{\partial(a_\sigma^2)}{\partial\omega_{Wk}}\, d\omega_{Wk}$$

NOTE - $\omega^2_{WLS} = \frac{2\pi}{(\lambda_s/L)}$

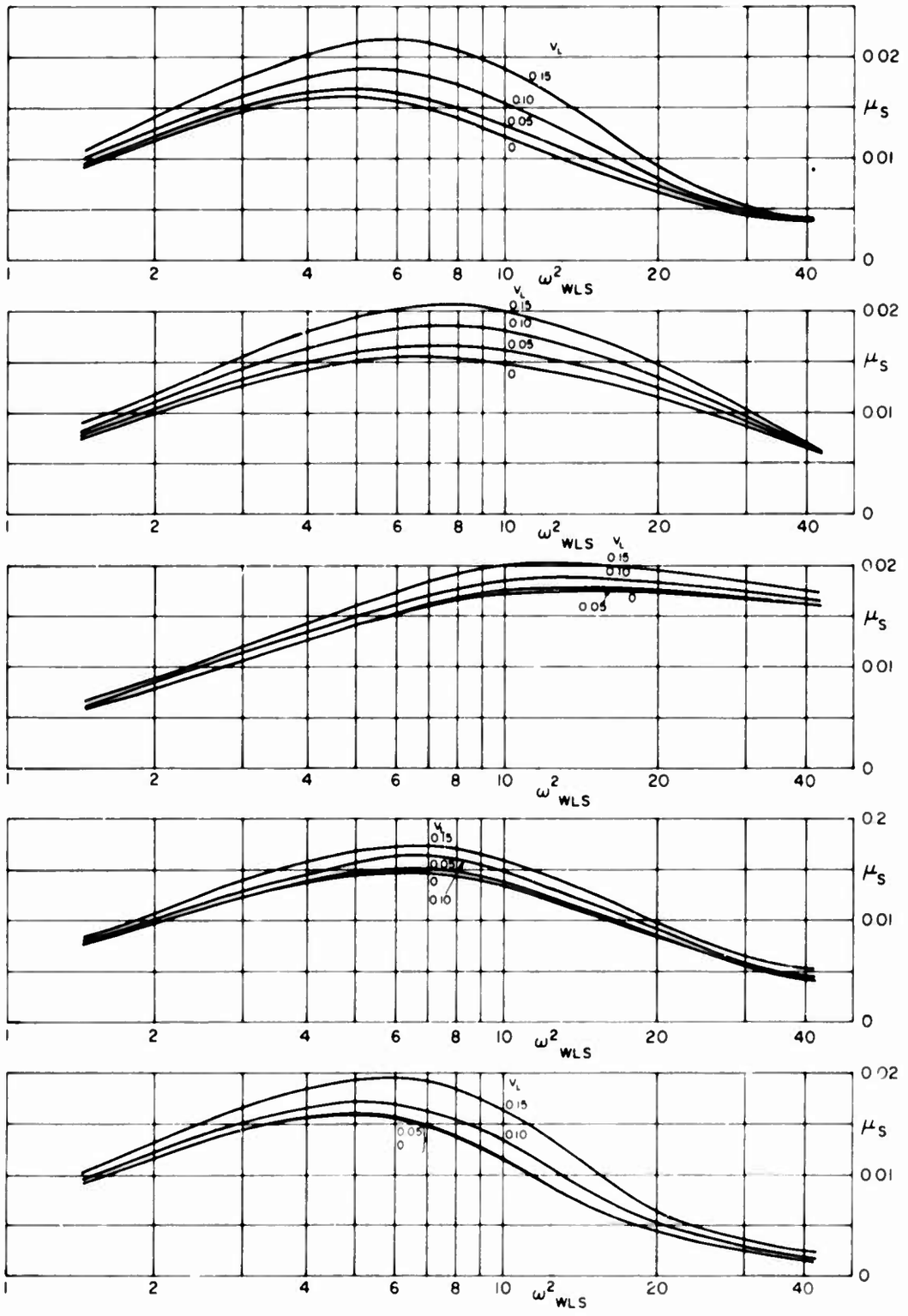

BENDING MOMENT RESPONSE COEFFICIENTS (μ_s) ~ WAVE FREQUENCY (ω_{WLS})

FOR VARIOUS SHIP SPEEDS (V_L) AND WAVE-TO-COURSE ANGLES (δ)
IN IRREGULAR SHORT CRESTED SEAS

FIG. 8

25.5-ft DRAFT

where ω_{Wk} is the independent variable, and ω_{WL} in the regular response diagrams is obtained from

$$\omega_{WL} = \frac{\omega_{Wk}}{\sqrt{\sigma_k}}$$

Some of these long crested irregular wave responses are also plotted on Figure 6, using ω^2_{WLS} as abscissa, and may be directly compared with the corresponding regular wave responses. It should be noted that the head, following, and beam sea results are based directly on the measured data without the assumption regarding apparent wave length for other headings.

Short Crested Seas

For the component waves emanating at angles α to the predominant direction (wind direction) of a real sea, it is assumed that the wave displacement energy is distributed in proportion to $\cos^2\alpha$, as suggested in Reference 3.

Use was made of all the bending moment response coefficients (μ_L) for long crested waves, which had been calculated for each wave-to-course angle (δ).

The short crested sea bending moment response coefficients (μ_S), for each wind direction relative to the ship (β), were, as a result, calculated from the following equation for each ship speed (V_L), and sea state σ_k (or ω^2_{WLS}). Note that $\beta + \delta = \alpha$.

$$\mu^2_S(\beta) = \frac{2}{\pi} \int_{-\frac{\pi}{2}-\beta}^{\frac{\pi}{2}-\beta} \mu^2_L(\delta) \cos^2(\beta + \delta)\, d\delta$$

Values of μ are plotted on Figure 8 for the various sea relative directions (β).

β, after the calculation, for purposes of comparison with long crested data, can be regarded as analogous to δ.

Some comparisons of regular wave bending moment responses with those for irregular long crested and short crested seas, for various relative headings, are shown on Figure 6. The most noticeable effect of short crestedness is to increase the low responses obtained in regular waves in beam seas.

The short crested data of Figure 8 are used for prediction purposes.

Predicted Midships Longitudinal Stresses in Waves from Model Tests

Wave stress predictions for the sea conditions, ship speeds, and wave-to-course angles of the full-scale experiments have been made from the following

$$\text{Significant stress} \qquad S_S = \pm \frac{\rho g B L^2 \mu_S \sigma}{I/y} \cdot 2$$

$$\text{For the Ontario Power} \qquad S_S = \pm 139.10^2 \mu_S \cdot H_S$$

where μ_S is read from Figure 8 for the experiment conditions given in Table 1.

Stresses predicted in this way were always higher than those measured at sea (Table 2).

The factor:

$$\frac{\text{actual stress measured at sea}}{\text{simple model prediction stress}}$$

had an average value of 0.65 for the eight full-scale experiments correlated.

For accurate, absolute prediction of stresses, account must also be taken of the changes in mean level of the oscillating bending moments in waves. It was found that this change in mean level, analogous to an electrical signal dc shift, also occurred in still water. These changes in mean level have been reported in Reference 2 and in other papers.

WAVE INDUCED VIBRATION STRESSES

Large Great Lakes bulk carriers when under way, even in low sea states, experience noticeable vertical vibration deflections. This phenomenon, often referred to as springing, is described in Reference 5, and in this latter report some values of the associated vibratory stresses measured on the Edward L. Ryerson are given. The maximum stresses recorded during the 1965 operating season for this ship, due to vibration alone, were ±5850 psi, and the observed periods of vibration were between 1.5 and 2 sec. Concern has been expressed regarding the magnitudes of these stresses, and the possible values for proposed large vessels.

From the stress recordings of the Ontario Power and the Saguenay, and especially from the spectral analyses, the presence of vibratory stresses has been noted. The maximum significant vibratory stress (defined as twice the rms deviation) measured on the Ontario Power was for Experiment 16, and the value was only ±809 psi. However, these vibration stress measurements were incidental to the main investigation for wave stresses, and larger vibration stresses might well have occurred during the period of the experiments. A vibration stress of ±794 psi was measured on the Saguenay when proceeding at full speed but in an extremely low sea state. For this latter recording, and a few others of similar type, the stress spectra showed only the vibration stress peak with no low frequency stress present except a very low level broad band of stress energy associated with machinery-induced hull vibration.

The general experience appears to be that the wave-induced vibration stress falls off with decreasing ship speed and in following seas, and so its additive effect towards the total stress in heavy sea conditions is not large.

By comparing the resonant frequencies at different draft conditions from the available records on the two ships, the nondimensional frequencies could be represented by the following formula

$$\omega_{ML} = C_1 \sqrt{\frac{I}{(0.01L)^3 B}} \cdot \frac{E/\rho g \cdot 10^6}{\sqrt{B.T.}}$$

Using ft. units

$$\omega_{ML} = C_1 \sqrt{\frac{I}{(0.01L)^3 B}} \cdot \frac{69.2}{\sqrt{B.T.}}$$

where

C_1 = 26.7 for the Saguenay (conventional bow) and

C_1 = 23.6 for the Ontario Power (bulbous bow).

Calculations were made for the vibration stress response coefficient

$$Y_M = \frac{\pm k^4 S}{C.E. \frac{y}{\sqrt{B.T.}}}$$

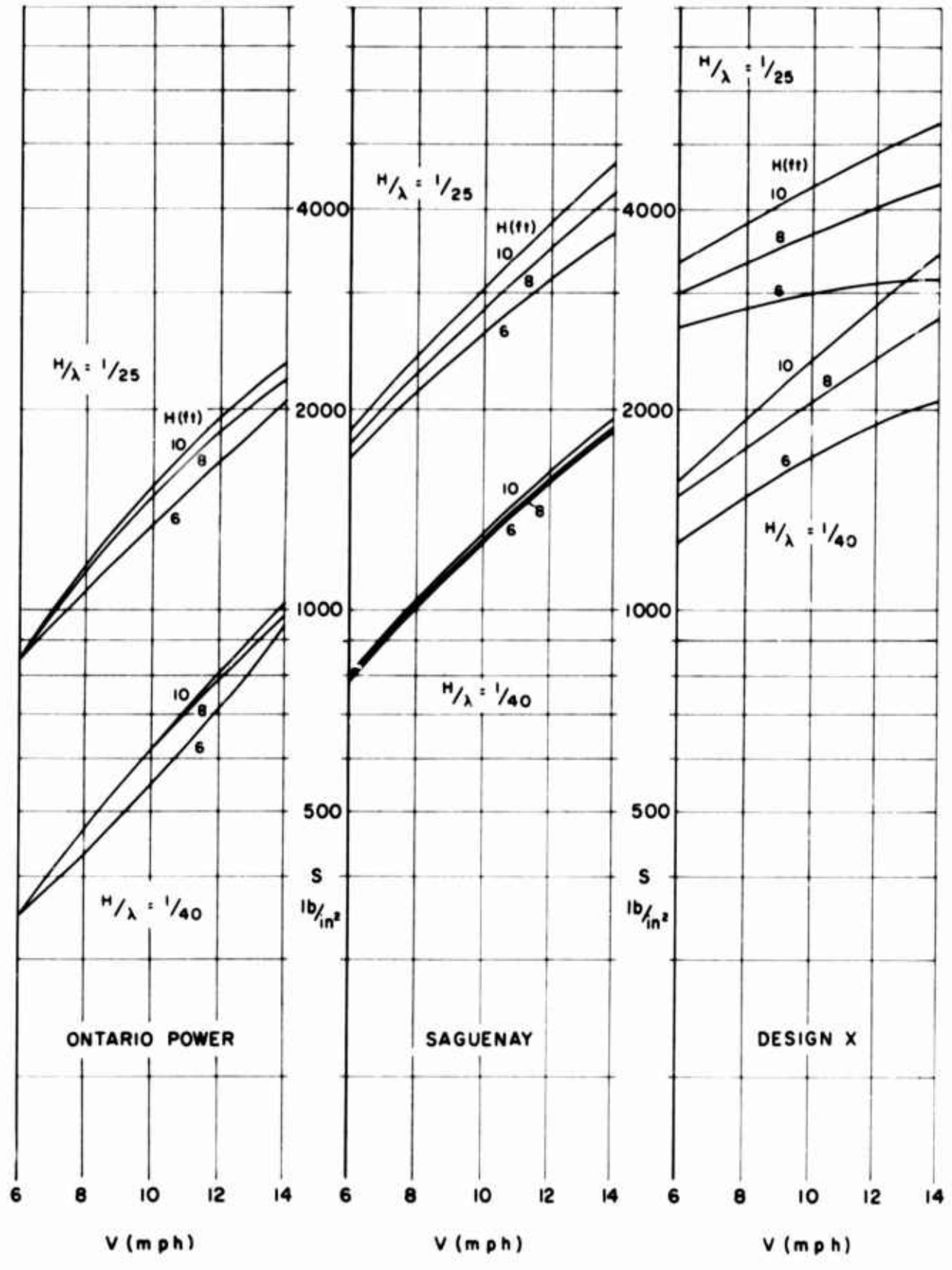

FIG. 9 RESONANT STRESSES (S) ~ SPEED (V)
HEAD SEAS

where C = 100 as derived by comparing the theoretical and full-scale data for seas in the bow quadrant. This response coefficient is defined in terms of the wave slope parameter (k^2). (The derivation and values of Y_M as a function of ship speed, natural frequency of vibration, and sea state are not given in this article.)

The correlation factor C was obtained by comparing measured values of vibration stresses, frequencies, and measured wave data.

TABLE 4

MAIN HULL DIMENSIONS, MIDSHIP STRUCTURE INERTIAS, AND RESONANT FREQUENCIES FOR THREE SHIPS

Item	Ontario Power	Saguenay	Design "X"
L ft (BP)	675	709	1,000
B ft	75	75	100
T ft	25.5	25.5	25.5
I ft^4	12,680	6430	14,750
y ft	23	21.5	23
t sec	1.31	1.80	2.93
WM r/s	4.80	3.50	2.15
WML	22	16.4	12

Vibration Stress Calculations for Three Ships

Calculations were made for three ships having the particulars shown in Table 4. The Saguenay has strength (I and y) typical of c[illegible]ntional large Lake vessels, and the Ontario Power has a vertical two-n[illegible]esonant frequency much higher than that of the Saguenay. The particulars of Design "X" have been chosen such that its resonant frequency is much lower; beyond this its dimensions have no significance other than to serve as a useful example. The results are plotted on Figure 9.

It is seen that reducing speed does not reduce stress for Design "X" as quickly as it does for the other two vessels, and the effect of sea height is

much more important for Design "X". For all three vessels, sea slope (H_S/λ_S) is of major importance.

The stresses at 12 mph in the steeper seas

$$\frac{H_S}{\lambda_S} = \left(\frac{1}{25}\right)$$

for seas of heights in the 6 to 10-ft. range, are on an average the same for Design "X" as for the Saguenay. The Design "X" stresses, however, are much larger than for the Saguenay, in the seas of lower slope

$$\frac{H_S}{\lambda_S} = \left(\frac{1}{40}\right)$$

The calculations also show that high stresses can be achieved, even in low sea states, when the vessels are operating at speeds well below the maximum attainable.

CONCLUDING REMARKS AND RECOMMENDATIONS

The present research programs for increasing knowledge of the strength of large Great Lakes vessels in service should be actively pursued.

Systematic model tests should be carried out at various wave-to-course angles and the effects of draft changes and changes in vessels' main proportions should be examined.

It should be noted that the model wave bending moment data in this article are presented nondimensionally, and therefore can be applied to vessels of all sizes having the same shape as the Ontario Power at the 25.5-ft. draft. For example, the results can be applied to a geometrically similar ship having a length (BP) of 850 ft., a beam of 94.5 ft. and a draft of 32 ft. Use of this nondimensional presentation for irregular seas, together with the sea slope parameter (k), allows for more complete data comparisons.

The model test results should include in the prediction data the effects of shifts of the mean levels of the oscillatory wave bending moments. Some work on this has already been carried out in the NRC Ship Laboratory.

Correlations of model and full-scale wave stresses should be made so that consistent trends, if they exist, can be revealed, and the factors for bringing about precise predictions investigated. In this connection the buoyancy changes associated with ship deflections, for these long flexible vessels, are possibly of importance.

More rigorous investigations of springing stresses for long flexible ships should be carried out, and the high vibration stress values associated with operation at speed, even in relatively low sea states, made known to ship operators.

Research should continue, and the data be published, regarding prevailing wave conditions on the Great Lakes and Gulf of St. Lawrence.

For the wave measurements carried out in connection with ship trials, further improvements in measurement techniques should be pursued and methods for obtaining directional spectra examined. Stereo-photography and other methods of wave measurement should be investigated.

Surveys of the problems associated with the large amounts of data involved in modern research on this subject should be undertaken, and methods developed, so that progress is not limited by data handling problems. This involves improved recording and analysis techniques and especially the development of automatic presentation and display methods. Speedier test techniques, with no decrease in accuracy if possible, must be developed if full use is to be made of the model research installations.

No mention has been made of theoretical bending moment calculations. When these become more reliable for prediction purposes, for the vessels under consideration, many of the experiments that are currently carried out will cease to serve a useful purpose.

The immediate task now facing the Great Lakes Shipping Industry is to formulate new strength standards for ships up to 1000 feet in length. All current research results should be used for this purpose and attention paid to static stresses, wave loads, and wave-induced vibration stresses.

ACKNOWLEDGMENTS

We are indebted to the Upper Lakes Shipping Company and to Canada Steamship Lines for making their ships available, and for their continued co-operation in this research program.

REFERENCES

1. Mathews, S.T.
   Kawerninski, L.I.
   Main Hull Girder Stresses - SS 'Ontario Power'. NRC, DME Mech. Eng. Report MB-266, National Research Council of Canada, October, 1967.

2. Moor, D.I.
   Longitudinal Bending Moments in Head Seas. R.I.N.A., 1966.

3. St. Denis, M.
   Pierson, W.J.
   On the Motions of Ships in Confused Seas. SNAME, 1953.

4. Pierson, W.J.
   Moskowitz, L.
   A Proposed Spectral Form for Fully Developed Wind Seas Based on the Similarity Theory of S.A. Kitaigorodskii. Journal of Geophysical Research, 1964.

5. Measurement of Seaway Stresses Aboard Great Lakes Ore Carrier 'Edward L. Ryerson' (1965 Operating Season Only). SNAME, T&R Report, January, 1966.

NOMENCLATURE

a^2	Component of sea variance in a frequency band	
B	Beam of ship	
E	Young's modulus of hull material	
H_S	Sea height defined as four times rms deviation	$H_S = 4\sigma$
I	Midship's structural inertia	
M	rms deviation of wave bending moment	
s	Single amplitude of vibration stress	2 × rms deviation
s_s	Single amplitude of wave stress	2 × rms deviation
J	Vertical structural stiffness of ship hull	
T	Draft of ship	
V	Ship speed	
V_L	Nondimensional ship speed	$V_L = \frac{V}{\sqrt{gL}}$
y	Depth of neutral axis from keel or deck	
Y_M	Vibration stress response coefficient	$Y_M = \frac{\pm k^4 S}{\text{C.E.} \frac{y}{\sqrt{\text{B.T.}}}}$
z	Vertical hull deflection in two-node vibration	
λ_S	Sea length corresponding to the frequency for the peak of the displacement spectrum	$\lambda_S = \frac{2\pi g}{\omega_{WS}^2}$
λ	Wavelength of a regular wave	$\lambda = \frac{2\pi g}{\omega_W^2}$
σ	rms deviation of a sea profile	

NOMENCLATURE (Cont'd)

σ_k	Relative sea length parameter associated with two-parameter wave spectra, and used for calculations	$\sigma_k = \frac{k^2\sigma}{L}$ Note: $\omega^2_{WLS} = \frac{40}{10^3\sigma_k} = \frac{2\pi}{\lambda_S\sqrt{L}}$
ρ	Density of water	1.94 slugs/cu ft (F.W.)
μ	Bending moment response, regular waves	$\frac{\partial M/\partial\sigma}{\rho g B L^2}$
ω^2_{WLS}	Relative sea frequency or sea length parameter	$\omega^2_{WLS} = \frac{2\pi}{\lambda_S\sqrt{L}}$

CURRENT PROJECTS

Much of the work in progress in the laboratories of the National Aeronautical Establishment and the Division of Mechanical Engineering includes calibrations, routine analyses and the testing of proprietary products; in addition, a substantial volume of the work is devoted to applied research or investigations carried out under contract and on behalf of private industrial companies.

None of this work is reported in the following pages.

ANALYSIS LABORATORY

AVAILABLE FACILITIES

Open-shop operation of an Electronic Associates 690 Hybrid computing system consisting of an EAI 640 digital computer (16^k memory, card input, disc), an EAI 680 analogue computer (60 amplifiers plus non-linear elements) coupled through an EAI 693 linkage and control system (32 analogue/digital and 10 digital/analogue channels plus logical control).

Open-shop operation of one 48-amplifier console of Electronic Associates 131R analogue computing equipment containing non-linear elements.

Open-shop operation of analogue statistical analysis equipment consisting of a Honeywell power spectral density analyzer, Bruel and Kjaer probability density analyzer, and associated instrumentation analogue tape recorders, counter, etc.

THEORETICAL STUDIES

Digital techniques for on-line statistical analysis of analogue data.

Investigation of the computer hardware and software requirements for an efficient problem-solving man-machine team.

Investigation of the detection of transient signals using adaptive filters.

Study of computing methods in optimal control problems.

Fibonacci search algorithms for function minimization.

Optimal control of linear stochastic systems.

Definition of a digital on-line control and data logging scheme for a hydraulic model of the St. Lawrence River.

COMPUTER BASED INVESTIGATIONS OF PARTICULAR PROBLEM AREAS

Computer production of random noise with specified output probability density and power spectral density.

Development of digital techniques for the analysis of pulse frequency modulated signals recorded from accelerometers, staff and pressure gauges, located in the Great Lakes.

Development of digital techniques for the analysis of wave noise measured by an airborne magnetometer.

In collaboration with the Department of National Defence, a hybrid computer simulation of the power plant of a proposed Navy destroyer.

In collaboration with the Department of Transport, a hybrid computer study of digital control schemes for the Mill Village satellite tracking station.

A general purpose hybrid computer technique is being developed to allow various configurations of gas generator free turbine engines to be simulated.

General purpose digital and hybrid techniques are being developed to describe the gas dynamics in a network of pipes and cylinders whose geometry varies with time, with application to the breathing of engines.

Evaluation of various numerical techniques for solving optimal control problems.

Curve-fitting, using gradient techniques to minimize mean square error.

Development of computer program for solving a class of optimal control problems.

Development of techniques for graphic input to analogue and digital computers.

Development of a data acquisition and data processing system for electro-encephlographic data.

CONTROL SYSTEMS LABORATORY

INDUSTRIAL CONTROL PROBLEMS

Investigation of industrial systems applications of fluidic circuits.

In collaboration with the Department of Energy, Mines and Resources, an investigation of the process dynamics and control characteristics of an electric arc furnace for processing iron ore.

Dynamic modelling of electric arc and oxygen steelmaking processes.

Investigation of the process dynamics and control characteristics of a copper converter.

LARGE SYSTEMS STUDIES

Investigation of the possible influence of fresh water outflow on climate.

Investigation of the properties and economies of large information systems.

HUMAN FACTORS ENGINEERING

A general program of research and development in the Human Factors Engineering field that includes the following:

Investigation of the control characteristics of the human operator and the basic phenomena underlying tracking performance.

Investigation of the nature of sensory interaction in human perceptual-motor performance.

Investigation of the factors involved in the presentation and processing of information, particularly in relation to simulator design.

BIOLOGICAL ENGINEERING

A general program of research and development in the biological engineering field that includes the following:

Investigation of the implementation of feedback control in living organisms.

Investigation of data transmission processes, with particular reference to nerve conduction characteristics.

Investigation of biological transducers (specifically pressure transducers) and their application to physical measurements.

Investigation of auditory methods of monitoring electrophysiological signals in general and the electroencephalograph in particular.

Development of depth probes for the study of electrical activity in the deep structures of the human brain.

Development of stereo-taxic and other apparatus for neurosurgical procedures.

Development of a phase memory filter for electroencephalograph studies.

Investigation of electroencephalograph data with a view to deriving a mathematical definition of the "normal" record.

PATTERN RECOGNITION

Investigation of the fundamentals of pattern recognition.

Development of techniques for the identification of biological cell populations, fingerprints etc.

BIRD DISPERSAL BY MICROWAVE RADIATION

Investigation of the effect of low-intensity microwave radiation on the behaviour of birds on the ground and in the air, to determine the practicability of using microwave radiation for dispersing birds on airfields and from the flight path of an aircraft.

ENGINE LABORATORY

FREE PISTON ENGINES

Study of the free piston engine and its applications, including various methods of power take-off. Mathematical study of the dynamic and thermodynamic processes in the engine, using computer simulation techniques, with a view to

elucidating starting and control phenomena. Experimental assessment of the operation and performance of the free piston engine in the laboratory. Study of the injection system most suitable for the peculiar requirements of the free piston engine, with possible application to all direct injection engines.

DUCTED FANS

Aerodynamic performance study of highly loaded ducted fans, with particular reference to inlet distortion phenomena as encountered typically by VTOL aircraft. The study comprises both analytical and experimental parts. Experimentally assessed performance of a fan-in-wing model in a wind tunnel over a range of inflow ratios and wing angle-of-attack settings for a family of inlets. Experimental examination of the aerodynamic characteristics of fan intakes on the upper surface of a wing with remotely placed suction machinery.

ENGINE CYCLE STUDIES

Performance calculations of gas turbine powerplant systems, with particular reference to VTOL aircraft. Extension of earlier rigorous design-point analysis to cover off-design point equilibrium operation, using analytically derived differential coefficients to generate rapidly converging trial parameters.

V/STOL NOISE STUDIES

Study of the mechanism of the generation and suppression of noise produced by ducted fans for VTOL aircraft. Identification of the noise sources and relating the strength of the sources to the physical parameters of the system.

CENTRIFUGAL COMPRESSORS

Design and performance investigation of centrifugal compressors, including study of flow phenomena in oversize model impellers. Detailed study of stability and distribution of flow in a single passage, in support of previous investigations of flow in a complete impeller.

LOCOMOTIVE DIESEL ENGINE PROBLEMS

In co-operation with the Canadian National Railway and the Canadian Pacific Railway, an investigation of locomotive diesel engine problems, including those arising from the use of Canadian crude oils as fuel. Studies of wear processes in the engine employing a specially developed, new method of spectrographic sampling of cylinder oil. Investigation of several new types of lubricating oil, different kinds of cylinder liners etc. with respect to engine wear.

FOAMED-CLAY MATERIALS

Investigation of novel light-weight foamed-clay building materials, with respect to chemical composition and physical properties.

BIRD HAZARDS TO AIRCRAFT

Work in support of, and arising from, the Associate Committee on Bird Hazards to Aircraft.

ENGINEERING LABORATORY

DYNAMIC BEHAVIOUR OF HELICAL GEARS

An improved method of recording dynamic measurements in gear tests, carried out in the 1000-hp gear test rig, has been developed. Previously, the signals that were monitored by electric resistance strain gauges and displayed on an oscilloscope were recorded by taking still photographs of the display at different gear speeds. This involved a large number of photographs and a considerable amount of rig operating time to cover the whole speed range adequately. In the new method, continuous records over the whole speed range were obtained by taking motion pictures of the display and an rpm meter while the speed was being increased continuously at a rate low enough to minimize distortion due to

acceleration. Synchronization of the camera shutter and the oscilloscope was achieved by driving the shutter from the test gear shaft that also drove the oscilloscope triggering device. The new method produces excellent records. It greatly reduces test rig operating time and reveals transient effects that otherwise might be missed.

A comprehensive investigation of dynamic loading of a pair of hobbed helical test gears has been completed. These gears had 6 pitch 20° full depth teeth, 10° helix angle, 3.25" face width, and a tooth number ratio of 46 to 46. Although the gear teeth were finished with a Grade AA finishing hob, the profile error was large enough to produce a very poor load distribution along the tooth helix. The cause of this error was traced to lack of sufficient stiffness in the hobbing machine and hob spindle thrust bearings. The investigation included recording the overall kinematic error when the gears were rolled together at very low speed and light load in the gear test rig.

The investigation also revealed that the gear body, which was of one-piece rim-and-central-web construction, was subject to widespread elastic deformation and vibration that was measurable even at very low gear speeds. At speeds of rotation approaching resonance, the mode of vibration was such that only a narrow band at the centre of the gear face was carrying any load.

Gear body vibration has also been studied with the aid of a full-size rubber model of the test gear. The model was subjected to forced vibrations and the relatively large deformations recorded by means of motion pictures, using stroboscopic illumination.

A set of very high precision, case-hardened and ground helical test gears were made in the Experimental Workshops. These gears have dimensions similar to those of the hobbed test gears, except that they have a heavy section instead of rim-and-web construction. Tests will include the effect of various degrees of profile modification, including zero modification, on dynamic loads and gear noise.

CIRCULAR PROFILE GEARS

An inspection instrument, required for measuring profile errors of circular profile gear teeth, is being designed.

A gear-cutting machine, capable of accurately cutting models of a new form of circular profile gear out of hard wax composition blanks, was built, and used in a study of this form of gearing.

FLIGHT RESEARCH LABORATORY

DESIGN AND DEVELOPMENT OF AN AIRCRAFT CRASH POSITION INDICATOR

A primary object of the present work is to provide basic information necessary for the design of CPI installations suitable for the CF-104 or other supersonic aircraft. Particular attention is being given to the flight behaviour of non-autorotating CPI aerofoils that are stable at large angles of attack. Studies are also being made of methods of adapting the CPI to helicopters.

MAGNETIC AIRBORNE DETECTION

Experimental and theoretical studies related to the use of Magnetic Airborne Detector equipment. The properties and application of optically pumped, atomic precession (rubidium vapour) magnetometers are being studied using a specially equipped North Star aircraft as a flying laboratory. Emphasis is being given to the use of digital techniques for data acquisition ..... analysis.

INVESTIGATION OF FLYING QUALITIES AND CONTROL SYSTEM REQUIREMENTS APPLICABLE TO V/STOL AIRCRAFT

Airborne simulation techniques, using helicopters equipped to provide variable stability and control properties, are being employed to explore the effects of the numerous parameters involved and to produce data that are directly applicable for design purposes.

FLIGHT INVESTIGATION OF AIRCRAFT TRAILING VORTICES

At the request of the Department of Transport, the T-33 turbulence research aircraft is being used to examine the magnitude and persistence of trailing vortices behind large transport aircraft at high altitudes.

INVESTIGATIONS OF GROUND EFFECT MACHINES

Studies relating to possible applications of air cushion vehicles in agriculture and in Northern transportation.

THE UTILIZATION OF AIRCRAFT IN AGRICULTURE AND FORESTRY

Studies relating to applications of aircraft in agriculture or forestry and investigation of problems arising in operations of this type.

RADAR ALTIMETER FOR FORESTRY USE

At the request of the Division of Radio and Electrical Engineering, a small helicopter is being used to test a new radar altimeter of potential use in preparing forest inventories.

INVESTIGATIONS RELATING TO FOREST FIRE CONTROL BY AERIAL METHODS

Studies of various factors determining the effectiveness of aerial fire suppression methods, including theoretical and experimental work on the behaviour of liquids released into an airstream, operational analyses and the investigation of aircraft design requirements. Data on aircraft behaviour and on liquid drop patterns are being obtained from flight experiments with a number of typical fire-bombing aircraft.

INVESTIGATION OF ATMOSPHERIC TURBULENCE

A T-33 aircraft, equipped to measure wind gust velocities, air temperature, wind speed and other parameters of interest in turbulence research, is being used for several investigations. These include measurements at very low altitude, in clear air above the tropopause, in the neighbourhood of mountain wave activity, and near storms. Records are obtained on magnetic tape to facilitate data analysis. Clear air turbulence detection methods are also being investigated.

CRASH INVESTIGATION OF DC-8F AIRCRAFT CF-TJM

At the request of the Department of Transport, assistance is being given in the analysis of the flight data recorded on magnetic tape and recovered from the wreckage of this aircraft.

INVESTIGATIONS OF FLYING QUALITIES OF LIGHT AIRCRAFT

Flight experiments on small aircraft to examine the adequacy of their flying qualities in relation to bush and other general operations.

FUELS AND LUBRICANTS LABORATORY

HYDROGEN-OXYGEN ENGINES

Experiments with small-scale equipment to obtain data on ignition at low pressures.

Theoretical studies aimed at producing the best design features for hydrogen-oxygen engines in multi-stage vehicles.

Investigation of heat transfer in a 500-lb. thrust rocket combustion chamber using a water-cooled chamber burning hydrogen and oxygen.

Experiments on cryogenic tankage.

FUNDAMENTAL STUDIES OF FRICTION, LUBRICATION AND WEAR PROCESSES

Analysis of friction and wear processes including the seizure of lubricated surfaces and the action of soft metal solid film lubricants.

Analysis of the mechanism of adhesion between non-conforming metallic surfaces.

PRACTICAL STUDIES ON LUBRICATION, FRICTION AND WEAR

Assessment of wear in shotgun barrels with shot manufactured from different materials.

Laboratory measurements of friction likely to occur between wire ropes and wheels in friction hoists in the presence of lubricants.

Laboratory cylinder liner and piston ring wear tests and their correlation with full-scale diesel engine results.

COMBUSTION RESEARCH

Experiments on fuel spray evaporation.

Development of laboratory procedure for establishing performance standards for power saw spark-arrester mufflers.

Development of a low-pressure propane gas heater.

STORAGE PROBLEMS

Evaluation of drum coating effectiveness and fuel deterioration in the long term storage of hydrocarbon fuels in coated steel drums.

EXTENSION AND DEVELOPMENT OF LABORATORY EVALUATION

Investigation of laboratory engine test procedures for evaluation of oxidation, dispersancy, and thermal stability characteristics of engine oils.

Development of laboratory full-scale axle procedures for the determination of the anti-score performance of hypoid gear oils.

Evaluation of methods for determining the electrical conductivity of aviation fuels.

PERFORMANCE ASPECTS OF FUELS, OILS, GREASES, AND BRAKE FLUID

Co-operative investigation covering used oil analysis and inspection of engines from Ottawa Transportation Commission buses to establish realistic oil and filter change periods.

Engine and bench test studies on the deterioration of engine crankcase oils with particular emphasis on the role played by oxides of nitrogen.

Studies on the use of vapour space rust inhibitors in steam turbine oils.

Investigation of the significance of Water Separation Index, Modified, in relation to filter/separator performance.

General research on lubricating greases including analytical methods and rheological studies.

Correlation of a simplified rig for the evaluation of the performance characteristics of hydraulic brake fluids with full-scale brake system performance.

Continuing studies of chain saw lubricants in the chain saw rig, and standard laboratory evaluation methods including correlation with field performance and wood cutting trials.

Development of a specification for high viscosity index hydraulic oils for marine use.

Examination and evaluation of some re-refined oils.

Study of the mercaptide gel forming tendencies of burner fuels.

Investigation of laboratory methods for predicting flow properties of engine and gear oils under low temperature operating conditions.

Investigation of laboratory methods for predicting low temperature flow properties of diesel and heating fuels and assessment of their suitability.

MISCELLANEOUS STUDIES

The preparation and cataloguing of infra-red spectra of compounds related to fuels, lubricants, and associated products.

Development of an empirical equation of state for carbon dioxide.

The application of Atomic Absorption spectroscopy to the determination of metals in petroleum products.

GAS DYNAMICS LABORATORY

V/STOL PROPULSION SYSTEMS

A general study of VTOL propulsion system methods with particular reference to requirements of economy and safety.

Investigation of a VTOL engine arrangement involving a shrouded fan driven by a partial admission turbine.

Experimental investigation of a pod-mounted VTOL fan for studies including the effects of flow distortion in cross-flow and shroud thrust effects.

Examination of wing intakes for VTOL propulsion systems with the objects of wing boundary layer laminarization and bird exclusion.

Examination of the pressure field associated with the efflux from a wing of a downward-directed air jet of variable cross-section and inclination.

INDUSTRIAL GAS TURBINES

Investigation of a gas turbine type suitable for geared turbine locomotives.

INTERNAL AERODYNAMICS OF DUCTS

An experimental study of the internal aerodynamics of ducts and bends, with particular reference to the effect of axial variation in cross-sectional shape.

HEAT TRANSFER STUDIES

The study of heat transfer within a vertical sealed tube (thermo-syphon) in which working fluid is boiled in the lower section and condensed in the upper section.

HIGH SPEED SHAFTING STUDIES

An investigation of the lateral vibration characteristics of shafting designed for high speeds of rotation.

HYDROSTATIC GAS BEARINGS

Studies of hydrostatic gas bearings to develop reliable methods of predicting bearing performance for a range of conditions and configurations, and to evolve suitable techniques for the satisfactory application of this type of bearing in situations where the special properties of gas bearings recommend their use.

ARC PRODUCED PLASMA STUDIES

A general investigation of the properties and flow behaviour of thermally ionized gases produced by arc heating on a continuous basis, together with the development of suitable diagnostic techniques for the study of such high temperature gases.

SHOCK PRODUCED PLASMA STUDIES

A general theoretical and experimental investigation of the production of high temperature plasma by means of shock waves generated by electromagnetic or gasdynamic means, and the development of diagnostic techniques suitable for a variety of shock geometries and the study of physical properties of such plasmas.

A theoretical and experimental study of strong converging and diverging shock waves, produced by chemical (explosive) and other means, and the development of experimental means to study the resulting transient plasma.

INDUSTRIAL PROCESS INSTRUMENTATION

The rapid measurement of SO_2 gas evolution of the electrical conductivity of the molten copper matte during various stages of the copper ore reduction process in a copper converter.

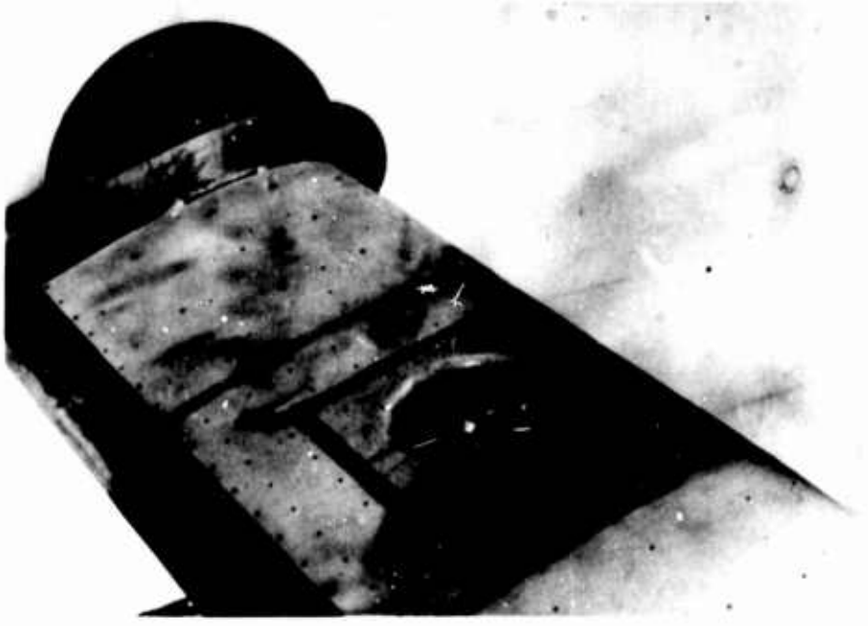

VIEW FROM TOP AND SIDE. INSTALLED INLET SHAPE HAS A LIP RADIUS-TO-FAN DIAMETER RATIO OF 0.09.

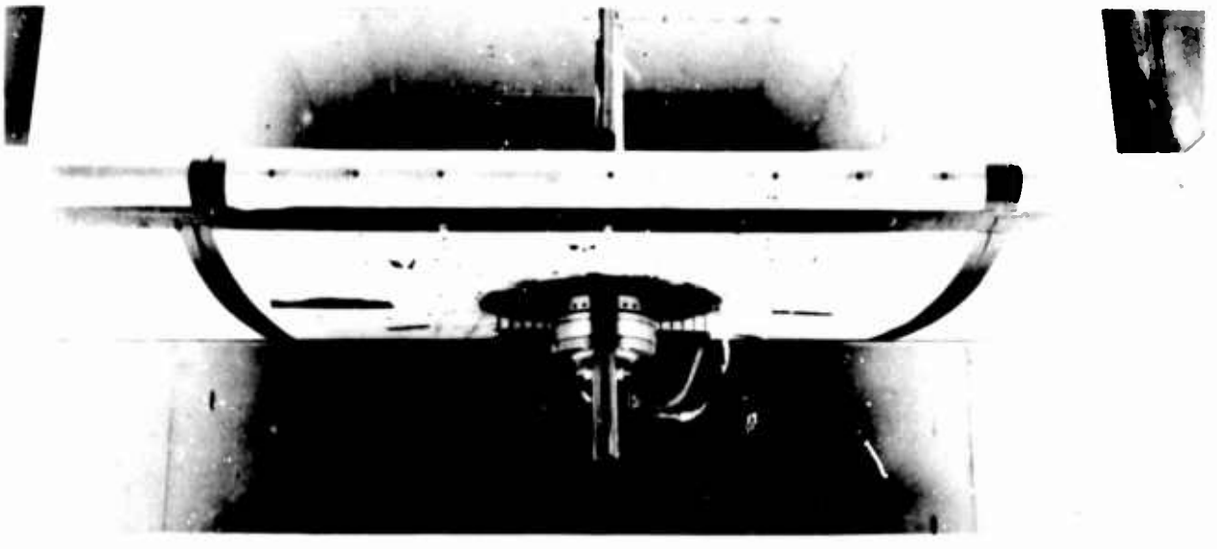

VIEW FROM FRONT AND UNDERSIDE. TEMPERATURE AND PRESSURE INSTRUMENT POD MOUNTED BELOW WING.

GEAR-DRIVEN 12-INCH FAN-IN-WING MODEL INSTALLED IN 10-FOOT x 20-FOOT PROPULSION WIND TUNNEL

GAS DYNAMICS LABORATORY
DIVISION OF MECHANICAL ENGINEERING

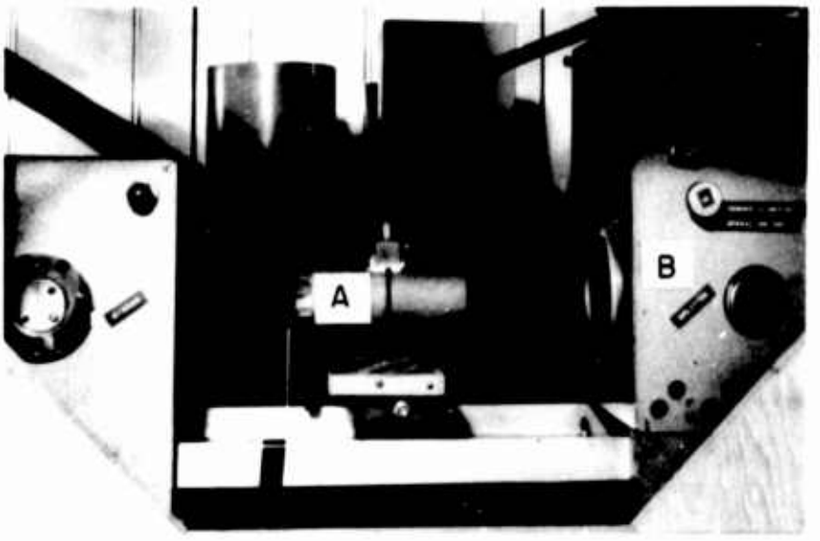

FIG. 1

FIG. 2

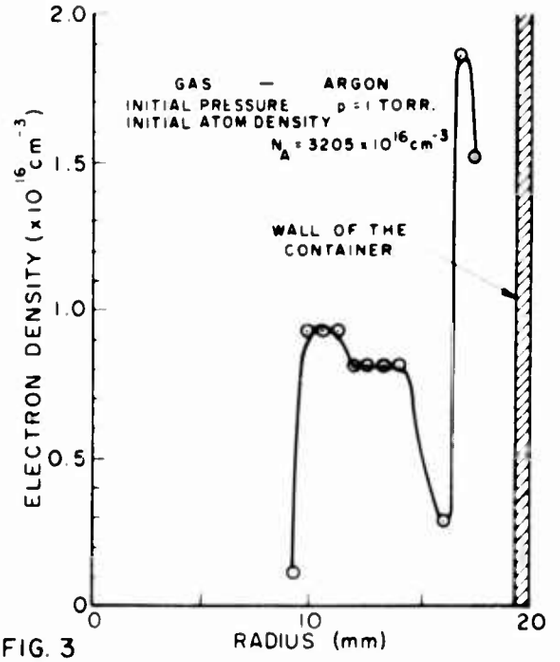

FIG. 3
ELECTRON DENSITY VERSUS RADIUS

A STRONGLY IONIZED, HIGH TEMPERATURE GAS IS PRODUCED BY MAGNETIC COMPRESSION OF A CURRENT RING GENERATED BY THE DISCHARGE OF A CONDENSER BANK IN A SINGLE TURN COIL (A, FIG 1); SOME PROPERTIES OF SUCH A PLASMA ARE INVESTIGATED BY MEANS OF AN INTERFEROMETER (B, FIG. 1). THE REGULAR PATTERN OF THE INTERFERENCE FRINGES IS DISTORTED WHEN THE PLASMA IS PRESENT AND A SIMPLE RELATION ALLOWS THE DETERMINATION OF THE ELECTRON DENSITY FROM THE FRINGE SHIFT IN INTERFEROGRAM (FIG. 2).

THE ANALYSIS OF THE INTERFEROGRAM OBTAINED FROM ARGON AT PRESSURE 1 TORR SHOWS THE SPACE DISTRIBUTION OF THE ELECTRON DENSITY (FIG. 3) AND THE HIGH DEGREE OF IONIZATION ACHIEVED. GAS TEMPERATURE AND NEUTRAL PARTICLE DENSITIES CAN ALSO BE DETERMINED FROM THE INTERFEROGRAMS.

OPTICAL INTERFEROMETRY FOR PLASMA MEASUREMENTS IN A THETA-PINCH DEVICE

GAS DYNAMICS LABORATORY
DIVISION OF MECHANICAL ENGINEERING

HIGH SPEED AERODYNAMICS LABORATORY

HYPERSONIC BOUNDARY-LAYER INTERACTIONS

Studies of the interaction of shock waves with hypersonic laminar boundary layers, of the interaction of suddenly applied, strong, favourable pressure gradients with hypersonic boundary layers, and of the interaction of surface temperature discontinuities with hypersonic laminar boundary layers.

HYPERSONIC THREE-DIMENSIONAL BOUNDARY LAYERS

Heat transfer measurements on two slender cones with half-cone angles at 15 deg. and 5 deg., at angles of attack in the hypersonic gun tunnel. Surface flow visualization experiments with oil dot technique. Theoretical study of three-dimensional boundary layers for this particular configuration is in progress.

HYPERSONIC VEHICLE STUDIES

Preliminary to more sophisticated studies, experimental measurements have been commenced on a simple caret wing to determine, in particular, the heat transfer distributions at design and various off-design conditions at Mach No. 10.4. At the same Mach number, tests on some conical or near conical intakes and recently, in co-operation with McGill University, testing at a Mach No. of 8.36 has commenced on some "modular" intakes derived from the so-called Busemann intake. These studies are being supported by theoretical work.

THREE-DIMENSIONAL BOUNDARY-LAYER FLOWS ON SEVERAL DESIGNS OF UPSWEPT FUSELAGE TRANSPORT AIRCRAFT

The flow about the upswept rear fuselage of a cargo transport aircraft may be modified to a considerable extent by the wing downwash field and three-dimensional flow separations produced near the junctions of the wing and fuselage, and undercarriage blister and fuselage.

An inviscid, attached flow, slender body theory is being used to calculate the fuselage pressures, and to account for the wing downwash field and body camber. An upswept fuselage model has been tested in the NAE 5-ft. × 5-ft. tunnel to investigate the vortex wake from the fuselage.

THEORETICAL RESEARCH ON THREE-DIMENSIONAL COMPRESSIBLE LAMINAR BOUNDARY LAYERS

The effect of blowing and suction on three-dimensional boundary layers is being examined. An approximate method for the solution of this problem with small cross-flow and arbitrary distributions of suction and blowing is being developed.

CONTROL OF A TURBULENT BOUNDARY LAYER IN A THREE-DIMENSIONAL SHOCK WAVE/BOUNDARY-LAYER INTERACTION

The 5-in. × 5-in. blowdown wind tunnel is being used to investigate the three-dimensional interaction between a glancing, oblique shock wave and a turbulent boundary-layer flow along a flat wall.

In a second phase the boundary-layer flow in the three-dimensional interaction region will be re-energized by tangential air blowing.

FLOW FIELDS ABOUT CONES

Theoretical work on methods for predicting the inviscid flow field and turbulent boundary layer growth on cones is continuing to support the experimental measurements made in the 5-ft. × 5-ft. wind tunnel at both subsonic and supersonic speeds.

SEPARATED FLOW OVER LONG BODIES OF REVOLUTION

Earlier force measurements and surface flow visualization have been complemented by further 5-ft. × 5-ft. wind tunnel tests to measure the surface pressure distribution. Tests were conducted at both subsonic and supersonic speeds at incidences up to 28 degrees with a range of nose shapes, and show that above a certain incidence, which depends on the nose shape and Mach number, large side forces may develop indicating the occurrence of asymmetric flow separation.

WIND TUNNEL TESTS ON ROLLING MODELS

Additional tests at subsonic, transonic, and supersonic Mach numbers with the Black Brant II and V configurations. The main emphasis was to determine the roll lock-in angle of attack and roll orientation for low initial roll rates (~ 7 cps).

WIND TUNNEL TESTS ON FLEXIBLE BODIES OF REVOLUTION

Deflectional and aerodynamic characteristics of a series of models with 10 diameter-long flexible nose sections were

determined at M = 2.5. Nose flexibility increases the normal force above the 'rigid' model value, and moves the centre of pressure forward by as much as 0.5 diameter. Maximum slope and deflection measured at the nose tip at an incidence of 15 deg. were 2 deg. and 0.75 inch.

METEOROLOGICAL ROCKET WIND TUNNEL TESTS

Six-component measurements with a full-scale model of a meteorological rocket were performed.

TWO-DIMENSIONAL AUGMENTOR WING STUDIES IN THE 5-FOOT WIND TUNNEL

The augmentor wing is a system, related to the well-known blown flap and jet-flap techniques, to allow the operation of aircraft at the high lift coefficients required for short take-off and landing. An air ejector, utilizing air available from a jet engine, is incorporated into the wing structure and is controlled and directed by the variable passage formed by elements of the flap system. A two-dimensional model is being prepared for the transonic test section of the NAE 5-ft. wind tunnel. Tests will determine the two-dimensional aerofoil characteristics of the augmentor wing at landing and cruising speeds.

THEORETICAL STUDIES OF TWO-DIMENSIONAL AUGMENTOR WINGS

In support of the experimental studies of the augmentor wing, a theoretical analysis of the performance of the wings is being initiated. The presence of the wind tunnel walls in actual testing conditions will also be considered in the theoretical model.

SQUARE FLARE WIND TUNNEL TESTS

An aerodynamically improved version of the conical flare, preferred to fins as rear stabilizing surface for high speed rockets, is the so-called square flare. This has a cross-section that changes from circular at the body intersection to square at the base. Comparative wind tunnel tests have been made on a model with a 10-deg. conical flare and a 10-deg. circumscribed square flare at M = 2.5 to 4.25.

HYDRAULICS LABORATORY

WAVE CLIMATE STUDY

Under the sponsorship of the Department of Transport, and in conjunction with the Bedford Institute of Oceanography and the Meteorological Branch of the Department of Transport, a study of wave statistics of the Great Lakes and the Gulf of St. Lawrence.

ICE FORMATION AND MOVEMENT

Field observations to determine the heat budget and mechanism of freeze-up on the St. Lawrence River from Kingston to Three Rivers.

WAVE RECORDER DEVELOPMENT

Development of a staff gauge wave recorder, either to be mounted to a fixed mast in shallow water or floating in deep water. Evaluation of other types of wave recorders: accelerometers, pressure transducers, etc.

ST. LAWRENCE SHIP CHANNEL

Under the sponsorship of the Department of Transport, a study of navigation, water levels, tide and ice problems.

DYNAMIC MODEL OF LAKE ONTARIO

A fundamental study of the wind and thermally induced circulations in Lake Ontario.

INSTRUMENTS LABORATORY

FREIGHT CAR STUDIES AND TRAIN DYNAMICS

Continuation of analysis of force/displacement/time relationships of typical production and development draft gears under controlled impact conditions, and of consideration of means for the relative rating of draft gears.

Computer studies on the simulation of train actions, comparison of the coupler forces resulting from braking action in trains consisting of standard freight cars, empty and loaded, and the new heavy (100-ton) car, loaded.

Evaluation of the effectiveness of various forms of lading restraints used with particular loading patterns and of the protection afforded by a new form of T.O.F.C. hitch.

ST. LAWRENCE RIVER MODEL

Design and development of integrated tide level and flow control system for the entire model.

MECHANICAL AIDS TO SURGERY

Evaluation of two new forms of mechanical aids, viz., in clinical surgery, a device for the intradermal injection of pigment and, in experimental surgery, a vascular suturing instrument for the anastomosis of body vessels 6-12 mm in diameter.

Evaluation in experimental surgery of various treatments of blood vessel prostheses to improve their anti-thrombogenic properties.

TRANSIENT PHENOMENA RECORDER

Aircraft installation and preliminary flight tests for the evaluation of a prototype 7-channel recorder to be used for recording of atmospheric gust data.

IMPACT RECORDER

Development of a new concept in impact recording, using correlation of lading damage with velocity/acceleration spectra of the environment.

BOARD THICKNESS MEASURING GAUGE

Field tests of a prototype non-contacting device for continuous measurement of thickness of boards during log-sawing process. Laboratory tests of a second, much cheaper, and compact arrangement.

LOW SPEED AERODYNAMICS LABORATORY

AERODYNAMIC CHARACTERISTICS OF V/STOL PROPELLERS

Investigation of six components of force and moment on a tilted propeller and of flow characteristics in the slipstream.

THEORETICAL AND EXPERIMENTAL STUDY OF PROPELLER-WIND INTERACTIONS

Detailed measurements of forces, moments, pressure distributions on a half-model of variable span, with flaps, and boundary-layer control by flap blowing.

V/STOL MOMENTUM THEORY

Comparison of power measurements on V/STOL models in transition regime with idealized momentum theory predictions.

WIND TUNNEL TESTS FOR OUTSIDE ORGANIZATIONS

Tests in the 6-ft. × 9-ft. horizontal wind tunnel, 15-ft. diameter vertical wind tunnel, and 10-in. × 13-in. water tunnel have been conducted for Canadair Limited, DeHavilland Aircraft of Canada, Limited, and Spear, Northrup and Associates.

THE NRC 30-FOOT V/STOL WIND TUNNEL

Four of five construction contracts, and that for the 6-component balance, have been awarded. A call for tender on the buildings and the data system will be issued shortly.

STUDIES OF FLUID DYNAMICS OF FLUID AMPLIFIERS AND OTHER FLUID STATE DEVICES

Water flow visualization studies in large models of fluidic devices.

PRESSURE, VELOCITY, AND DIRECTION MEASUREMENTS

Survey of the literature on pressure, velocity, and direction measurements in subsonic flow, and development of special probes to fill certain gaps.

WIND TUNNEL WALL INTERFERENCE ON A V/STOL MODEL

Investigation of the use of slotted and other "ventilated" test sections to reduce wall interference.

LOW TEMPERATURE LABORATORY

LOW TEMPERATURE PROBLEMS IN RAILWAY OPERATIONS

Analytical and experimental work, conducted under the auspices of the Associate Committee on Railway Problems, Sub-Committee on Climatic Problems, including the low temperature performance of air brake systems, aftercooler design and development, an investigation into rail switch malfunctions under severe climatic conditions, and refrigeration problems at low temperature. The heating of an insulated container for rail service has been investigated.

HELICOPTER DE-ICING

A study of helicopter icing protection involving the evaluation of various systems (thermal, fluid, and self-shedding materials) and the development of de-icing control systems including ice detectors.

ABSORPTION REFRIGERATION

The design and development of experimental prototype absorption refrigeration units based on the Platen-Munters cycle that requires no moving parts, with special reference to applications in remote areas and transportation.

LOW TEMPERATURE APPLICATIONS IN MEDICAL ENGINEERING

The investigation (in co-operation with the Department of Neurosurgery, University of Ottawa) of selective brain cooling, and the development of medical engineering equipment allowing the quick connection of an in-line arterial heat exchanger.

An investigation into control of anti-coagulation in the extracorporeal equipment connected to the arterial system.

The design, development, and evaluation of cannulae for temporary connections between arteries and extracorporeal blood circuits.

An investigation into boundary-layer thermal flow measurement in pulsatile non-Newtonian flow.

AIRCRAFT INSTRUMENTATION

The investigation of possible modes of failure for aircraft pitot heads under icing and snow conditions.

FLUID AMPLIFIERS

An investigation of the operating characteristics of various models of turbulent reattachment fluid amplifiers to determine, primarily, the feasibility of applying the turbulent reattachment fluid amplifier to the direct control of high power fluid streams.

MISCELLANEOUS ICING INVESTIGATIONS

Analytical and experimental investigations of a non-routine nature, and the investigation of certain aspects of icing simulation and measurement.

SHIP LABORATORY

WAVE STUDY AND SHIP STRENGTH

Rough water trials were continued in the Gulf of St. Lawrence and the Great Lakes on bulk carriers. A large amount of computer analysis was completed.

FISHING VESSELS

Some existing model seakeeping test data were prepared for a more generalized treatment by computer.

DREDGING

A study was made of the relationships between dredges and their associated dump barges, to establish a basis for optimizing the design of the latter.

CATAMARANS

An extensive series of model tests of a catamaran buoy vessel with asymmetric hulls at different spacings was completed.

TANKERS

Two models were tested for resistance and propulsion.

CAVITATION

Alternative blade designs for a controllable-pitch propeller were tested in the cavitation tunnel.

TOWED BODIES

Model tests to investigate the dynamic depression of towed echo-sounder bodies were initiated.

HYDROFOILS

Hull tests to relatively high speeds on a model of a hydrofoil test vehicle were undertaken.

STRUCTURES AND MATERIALS LABORATORY

FATIGUE OF METALS

Fatigue strength of welded maraging steel plate; characteristics of structural grade steel bolts under fatigue loading; effects of environment on fatigue strength of light alloys; development of test methods for variable amplitude loads and investigation of effects of such loads; certification tests on aircraft components.

RESPONSE OF STRUCTURES TO HIGH INTENSITY NOISE

Study of excitation and structure response mechanisms; study of panel damping characteristics and critical response modes; investigation of fatigue damage laws; industrial hardware evaluation; investigation of jet exhaust noise.

HIGH TEMPERATURE AIRCRAFT HYDRAULICS

Study of bulk modulus of hydraulic fluids, including emulsions and mixtures in relation to temperature and pressure; studies of seal performance and high pressure, high velocity phenomena.

OPERATIONAL LOADS AND LIFE OF AIRCRAFT STRUCTURES

Instrumentation of aircraft for the measurement of flight loads and accelerations; fatigue life monitoring and analysis of load and acceleration spectra; full-scale fatigue spectrum testing of airframes and components; investigation of rough ground operations.

FRACTURE MECHANICS AND FRACTOLOGY

Investigation of crack formation and propagation in gradient stress fields; correlative electron microscope studies of fracture surfaces; notch sensivitity and fracture toughness; resistance of materials to high strain rate and impact loading.

RESEARCH ON PROTECTIVE COATINGS FOR REFRACTORY METALS

Investigation of coating compounds for protection of refractory metal substrates at high temperatures; methods and techniques of coating deposition; study of interface diffusion rates and products; development of methods of evaluation of physical properties of coated test coupons.

MECHANICS AND THEORY OF STRUCTURES

Review of the static and dynamic conditions of the suspension of a rigid body by a system of springs; study of coupled flexural-torsional vibration of structural members; development and application of finite element methods; investigation of non-linear flutter of a circular cylindrical shell; investigation of motion of a particulate separator driven by an inertial unbalance; development of transmission matrices; extension of beam theory to include effects of transverse curvature.

CONSTRUCTION AND DEVELOPMENT OF BIRD CARCASS ACCELERATING GUN

Development of Canadian facility; analysis of national needs and co-ordination of utilization; hardware evaluations.

CALIBRATION AND CERTIFICATION OF FORCE MEASURING DEVICES

Facilities available for the calibration of government, university, and industrial equipment include deadweight force standards up to 100,000 lb., back-to-back calibration of accelerometers, and limited calibration of fluid pressure-type transducers.

COMPOSITE AND NON-METALLIC MATERIALS

Studies of material properties, types of composites, fabrication procedures, structural efficiency, etc.

STRUCTURAL TESTING OF A HELICOPTER SKI

STRUCTURES AND MATERIALS LABORATORY
NATIONAL AERONAUTICAL ESTABLISHMENT

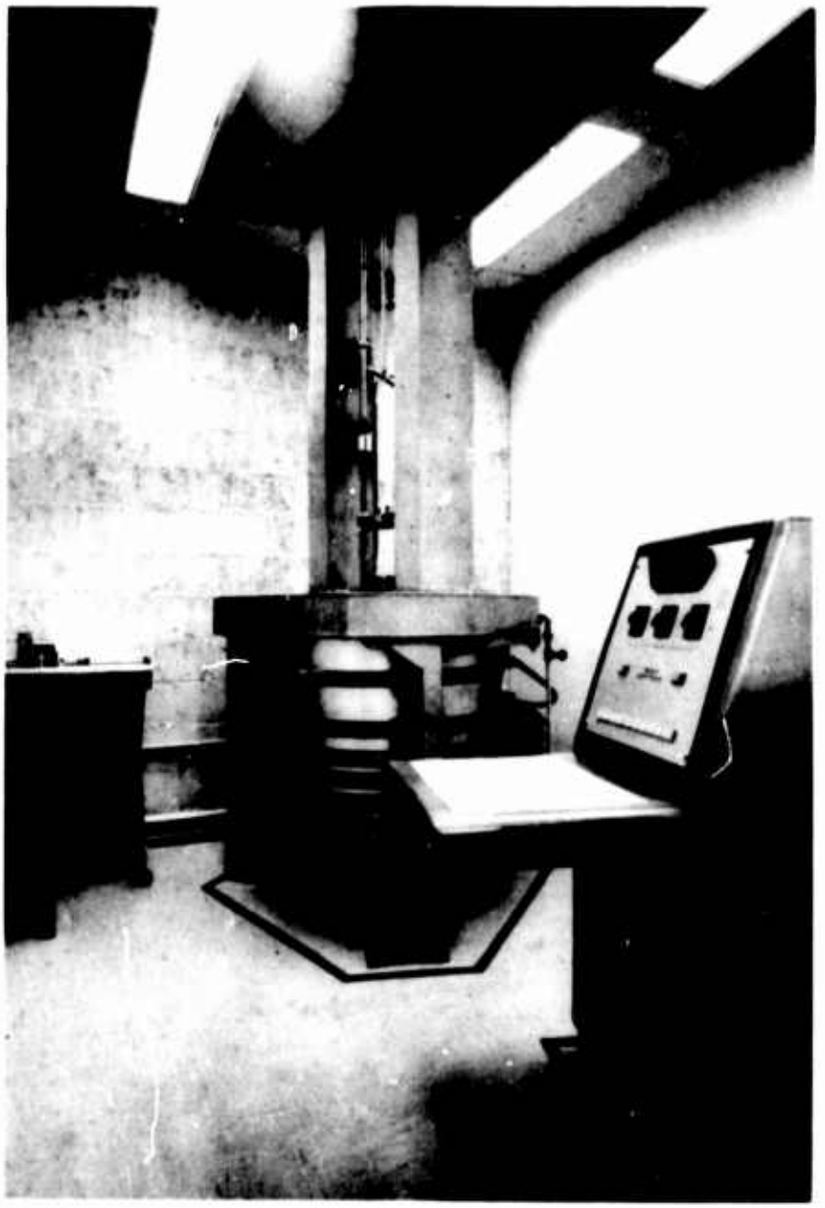

GENERAL VIEW OF 3,000-LB DEADWEIGHT MACHINE
FOR FORCE STANDARDS CALIBRATION

UNSTEADY AERODYNAMICS LABORATORY

BASIC STUDY OF OSCILLATORY PHENOMENA IN HYPERSONIC FLOW

Hypersonic flow around oscillating two- and three-dimensional bodies is investigated. Analytical methods are developed to determine effects of viscosity and leading edge (or nose) bluntness on static and dynamic stability derivatives. Supporting experiments consist of pressure distribution measurements on steady and oscillating models, derivative measurements on oscillating models, and optical studies of the relative motion between model and shock wave. All experiments are performed in helium at Mach No. 9 and 17.

HELIUM HYPERSONIC WIND TUNNEL

The existing helium blowdown wind tunnel is continuously developed. Conversion to a closed jet test section, installation of a heater, and addition of a third nozzle are improvements considered. The tunnel is operating in a closed loop using a helium recovery system, which includes a cryogenic purifier. A 3-in. diameter usable core is available in uniform flow nozzles at Mach No. 9 and 17 and at Reynolds No. per foot up to 50 million and 16 million respectively. Instrumentation for most types of aerodynamic investigations is available.

GAS PHASE REACTION KINETICS

A physico-chemical study of the reactions of some constituents of the upper atmosphere, viz. O, N, and H atoms. An objective of these studies is to provide the rate parameters and light emission characteristics of chemiluminescent reactions appropriate for rocket seeding experiments.

TECHNIQUE OF FREE-FLYING MODELS

A new experimental technique is being developed for the hypersonic wind tunnel that will permit obtaining aerodynamic data from observation of the behaviour of free-flying models in the tunnel test section. The model is pneumatically launched upstream into the test section and a high speed camera record is made of its flight upstream as well as its return, when it is carried downstream with the flow. This technique eliminates sting interference effects and permits studies of models at high incidence or at large amplitude, which would be impossible with conventional mechanical suspension.

PUBLICATIONS

The following unclassified reports were released during the quarter:

Aeronautical Reports

LR-490 AIRBORNE INSTRUMENTATION FOR A CLOUD PHYSICS RESEARCH PROJECT.

K.G. Pettit, National Aeronautical Establishment, October 1967.

During the period from 1959 to 1963, the National Research Council, in co-operation with a number of other agencies, participated in an experimental study of the physics of precipitation. Although an immediate objective of this study was the determination of the efficacy of silver-iodide seeding of clouds as a means to augment rainfall over the forest regions of western Quebec, the long-range objective was the advancement of the knowledge of fundamental precipitation mechanisms by the measurement and correlation of rainfall and of the basic properties of cloud and atmospheric parameters.

Temporal and geographic control of the dissemination of the silver-iodide seeding material and in-flight measurements of cloud and atmospheric parameters were obtained by the use of a specially instrumented aircraft provided by the Flight Research Section of the National Research Council.

This Report describes the airborne instrumentation and assesses the accuracy of the measurements.

LR-491 LONGITUDINAL AERODYNAMIC CHARACTERISTICS OF BLACK BRANT V AT MACH NUMBER 7 IN HELIUM.

J.G. LaBerge, National Aeronautical Establishment, December 1967.

Two slightly different configurations of the Black Brant V rocket were tested at Mach number 7 in the NAE helium hypersonic wind tunnel. Static longitudinal characteristics were measured at two Reynolds numbers differing by a factor of 8 over a nominal incidence range of ±5 degrees. The helium results were converted to equivalent air results and compared with those of the NAE 5-foot air wind tunnel, in which the maximum Mach number reached was 4.25. The results from both tunnels were compared with calculated values.

LR-492 VIBRATION MODES AND RANDOM RESPONSE OF A MULTI-BAY PANEL SYSTEM USING FINITE ELEMENTS.

G.M. Lindberg and M.D. Olson, National Aeronautical Establishment, December 1967.

A finite element approach to the dynamic analysis of continuous skin-stringer panels is presented. The method is illustrated in the calculation of vibration modes and random response of a five-bay stringer-stiffened panel with all outer edges clamped. The panel skin is represented by finite plate elements and the stringers, which are assumed infinitely stiff in bending, are represented by beam torsional elements.

Results are presented for the first 35 panel vibration modes. These modes occur in distinct groups with five similar modes in each, the number five corresponding to the number of panel bays. The response of the panel to plane wave propagation of acoustic noise (propagating normal to the stringers) is also calculated. The resulting response power spectral densities were found to be fundamentally different from those associated with single span panels. These power spectra did not have widely separated peaks, but rather the peaks tended to be squeezed into groups corresponding to the groupings of natural frequencies for the panel.

LR-493 GROUND DISTRIBUTION CONTOUR MEASUREMENTS FOR FIVE FIRE-BOMBERS CURRENTLY USED IN CANADA.

J.I. MacPherson, National Aeronautical Establishment, November 1967.

This Report presents the results of the fire-bomber ground distribution tests made at Uplands Airport during the spring, summer, and fall of 1967. A total of 37 contour patterns are presented for five of the major existing fire-bombers currently used in Canada; the Turbo-Beaver, the Otter, the Twin Otter, the TBM Avenger, and the Canso. Pertinent meteorological data, speeds, altitudes, and recovery percentages are included with each contour pattern, and contour lengths and enclosed areas are calculated for each drop distribution. The effects on the ground distribution of using long-term retardant and a water-thickening additive are also discussed.

Mechanical Engineering Reports

ME-224 DATA REDUCTION PROGRAM FOR FREE PISTON ENGINE TESTS.

F. Rueter, Division of Mechanical Engineering, December 1967.

A program written in Fortran IV for the IBM 360 computer, for the reduction of data from free piston engine tests is described, along with a brief description of the engine and its instrumentation, and the derivation of the various equations used.

Input data are in the form of punched cards, and output, in tabulated form, is on the standard line printer. At the option of the user, some of the more important output data may, in addition, be plotted on the EAI dataplotter.

ML-1 A MATHEMATICAL MODEL OF ISOLATED FROG SCIATIC NERVE.

R.W.J. Ford and J.A. Tanner, Division of Mechanical Engineering, November 1967.

The search for a reversible method of opening neuro-muscular control loops led to the investigation of the effect of high frequency a.c. excitation on nerve conduction processes. Experiments conducted on isolated frog nerve revealed that the amplitude of the compound action potential evoked by a pulse stimulus decreases in a specific manner when a high frequency a.c. signal (5-30 kc/s) of increasing intensity is applied to the nerve. To establish the underlying mechanism a mathematical model has been developed, in the form of a digital computer program, and matched to the living nerve. Although used to describe largely non-physiological states of nerve conduction, this model affords a different viewpoint of the conduction processes and one from which to explore such problems as interaction between adjacent fibres and random excitability.

Miscellaneous Papers

BIRTA, L.G. The Concept of Generativity in General Systems Theory. Proc. 1967 IEEE Systems Science and Cybernetics Conference, Boston, October 1967.

BIRTA, L.G. and TRUSHEL, P.J. Conjugate Gradient Search in Initial Costate Space. IEEE Trans. on Automatic Control, Vol. AC-12, No. 6, December 1967 (Correspondence).

CLOUTIER, L.J. and TORDION, G.V. Analyse du Contact d'Engrenages du Type W.-N. aux Axes Concourants. S.E.I.E. Bulletin No. 53, Paris, September 1967.

DICK, T.M. Limits to Navigation by Ice in Port of Churchill. Journal of the Waterways and Harbors - Vol. 93, No. WW4, November 1967.

GIBBS, C.B. Impairment, Dangerous Driving and the Law. Paper presented to American Association for Automotive Medicine, 11th Annual Meeting, 21 October 1967 (To be published).

KLEIN, G.J. Design of a Contour Milling Machine. Product Design and Value Engineering, September 1967.

OLSON, M.D. Finite Elements Applied to Panel Flutter. AIAA Journal, Vol. 5, No. 12, 1967, pp. 2267-2270.

PELLEG, J. and HEINE, W.R. Linear Contraction as a Method for Studying Surface Defects in Iron Castings. Modern Castings, Vol. 52, No. 6, December 1967, pp. 102-108. Also in Transactions AFS 1967, pp. 394-400.

SANDRI, R. Some Considerations on the Use of a Pressurized Tank System for a Rocket Engine. Can. Aero and Space J., Vol. 13, No. 8, October 1967, pp. 369-372.

SCHAUB, U.W. Fan-in-Wing Aerodynamics: Experimental Assessment of Several Inlet Geometries. AIAA Paper No. 67-746, presented to 10th Anglo American Aeronautical Conference, Los Angeles, California, 18 October 1967.

SEWELL, R.T. Low Altitude Flight Load Spectra for Light Aircraft. CASI Journal, Vol. 13, No. 8, October 1967, pp. 373-380.

TANNER, J.A., ROMERO-SIERRA, C. and DAVIE, S.J. Non-Thermal Effects of Microwave Radiation on Birds. Nature, Vol. 216, No. 5120, 23 December 1967, p. 1139.

TYLER, R.A. and WILLIAMSON, R.G. Diffuser Performance with Distorted Inflow. Proc. Inst. of Mech. Eng. Symposium on Subsonic Fluid Flow Losses in Complex Passages and Ducts, 3-5 October 1967.

Correction to DME/NAE 1967(3)

MCLANE, P.J. and MUFTI, I.H. (not GRAEFE) On Plant Parameter Variation in the Scalar Linear Optimal Regulator Problem. IEEE Trans. on Automatic Control, Vol. AC-12, No. 5, October 1967.

Unpublished Papers and Lectures

CAMPBELL, W.F. Highway Safety: Common Sense and/or the Facts. Presented at Queen's University, Kingston, Ont., 15 November 1967.

DICK, T.M. Some Comments on the Estimation of Littoral Drift. Presented to 1st Marine Engineering Seminar, Department of Public Works, December 1967.

FEIR, J.E. Some Results from an Investigation on the Instability of Progressive Waves on Deep Water. Presented to NRC DME-NAE Science Association, December 1967.

GAGNE, R.E. and WRIGHT, E.J. Generalized Simulator for Turbo-Jet Engine Studies. Meeting of the Eastern Simulation Council, Buffalo, New York, 18 October 1967.

GAGNE, R.E. Some Characteristics of Hybrid Computers. Seminar on Computer Applications for Engineers, University of Ottawa, 8 December 1967.

GIBBS, C.B. Human Performance under Stress. Paper presented to Deep River Science Association, 15 December 1967.

MATHER, G.K. and GOULD, D.G. A Note on Turbulence Measurements and Models, and Their Applications with Respect to Structural Loads, Flying Qualities and Crew and Passenger Environments. Paper presented at CAARC Meeting on Turbulence held at R.A.E., Bedford, England, October 1967.

OLSON, M.D. Structural Response to Acoustic Noise. Lecture presented to Graduate Seminar, Carleton University, Ottawa, 15 November 1967.

PLOEG, J. Use of Hydraulic Models in Coastal Engineering. Presented to 1st Marine Engineering Seminar, Department of Public Works, December 1967.

RINGER, T.R. Low Temperature Effects on Material and Man. Presented to Ottawa Chapter of R.S.E.S., 23 November 1967.

AERONAUTICAL LIBRARY

Statistical Summary of Library Operations for the Quarter October - December, 1967

Documents accessioned (including duplicates)	3,016
Documents accessioned (first copies only)	2,749
Cards added to the catalogue	15,979
Books received	351
Bound periodicals received	105
Loans to NRC staff (including Periodical circulation and Xerox and Microfiche copies supplied in lieu of loans)	7,095
Loans and distribution to outsiders	1,596
Total circulation	8,691

Statistical Summary for 1966 and 1967

	1966	1967
Documents accessioned (including duplicates)	15,039	14,337
Documents accessioned (first copies only)	11,856	11,195
Cards added to the catalogue	60,038	64,075
Books received	1,415	1,454
Bound periodicals received	475	483
Loans to NRC staff (including Periodical circulation and Xerox and Microfiche copies supplied in lieu of loans)	24,589	28,122
Loans and distribution to outsiders	7,967	7,057
Total circulation	32,556	35,179

NOTE: These summaries include statistics for the Uplands Branch of the Aeronautical Library.

PROPRIETARY PROJECTS DURING 1967

Part of the work of the two Divisions covers proprietary projects, and, for this reason, has not been reported in these Bulletins.

Following is a list of Industrial Organizations, Government Depart and Universities for whom work was done during 1967.

INDUSTRIAL ORGANIZATIONS

Advanced Dynamics Corporation Ltd., Montreal, P.Q.
Aero Photo Inc., Quebec City
Air Canada, Montreal, P.Q.
A.J. Simpson Marine Ltd., Brockville, Ont.
Aluminium Laboratories Ltd., Kingston, Ont.
American Society for Testing Materials, Philadelphia, Pa., U.S.A.
Amoco Chemical Corp., Chicago, Ill., U.S.A.
Amoco Chemical Corp., Whiting, Indiana, U.S.A.
Avian Aircraft Limited, Georgetown, Ont.
Aviation Electric Ltd., Montreal, P.Q.

Babcock and Wilcox Canada Ltd., Galt, Ont.
Bach-Simpson Ltd., London, Ont.
Barnes Engineering Co., Stamford, Conn., U.S.A.
Bell Helicopter Company, Fort Worth, Texas, U.S.A.
Bingham Pump Company Ltd., Burnaby, B.C.
Boeing of Canada, Arnprior, Ont.
Bourns (Canada) Ltd., Toronto, Ont.
B.P. Canada Ltd., Oakville, Ont.
B.P. Canada Ltd., Montreal, P.Q.
Bristol Aerospace Ltd., Winnipeg, Man.
Bristow Instruments Company, Edmonton, Alta.
British American Research & Development Co., Sheridan Park, Ont.
British American Research & Development Co., Toronto, Ont.

CAE Industries Ltd., Montreal, P.Q.
Canadair Limited, Montreal, P.Q.
Canadian General Electric, Scarborough, Ont.
Canadian Ice Machine Co., Toronto, Ont.
Canadian International Paper Company, Gatineau, P.Q.
Canadian Pacific Railway Company, Montreal, P.Q.
Canadian Petrofina Ltd., Pointe-Aux-Trembles, P.Q.
Canadian Vickers Ltd., Montreal, P.Q.
Capital Air Surveys Ltd., Ottawa, Ont.
Castrol Limited, Bracknell, Berkshire, England
Century Air-Ground Services Limited, Montreal, P.Q.
Cistric Filerosis Association of Quebec Inc., Montreal, P.Q.

Computing Devices of Canada Ltd., Ottawa, Ont.
Co-Ordinating Research Council, New York, N.Y., U.S.A.
Cowley Consultants Limited, Toronto, Ont.
C.R. Snelgrove Co., Ltd., Don Mills, Ont.
CTS of Canada Limited, Streetsville, Ont.

De Havilland Aircraft of Canada Ltd., Downsview, Ont.
Dominion Forge Company, Windsor, Ont.
Dupont of Canada Ltd., Kingston, Ont.

Elco Corporation, Cleveland, Ohio, U.S.A.
Emco Ltd., Gas Division, Weston, Ont.
Engineering Research Associates Ltd., Toronto, Ont.
Enjay Additives Laboratory, Linden, N.J., U.S.A.

Fairey Canada Ltd., Dartmouth, N.S.
Falconbridge Nickel Mines, Ltd., Falconbridge, Ont.
Ferranti-Packard Electric Ltd., Toronto, Ont.
Field Aviation Co., Ltd., Malton, Ont.
Found Brothers Aviation Ltd., Grand Bend, Ont.
Free Piston Development Company Ltd., Kingston, Ont.

Gaspe Copper Mines, Murdochville, Que.
General Electric Company, Waterford, N.Y., U.S.A.
Goodyear Tire & Rubber Co., Akron, Ohio, U.S.A.

Hauts-Monts Inc., Quebec City, P.Q.
Hawker Siddeley Canada Limited, Trenton, N.S.

Imperial Oil Enterprises Ltd., Dartmouth, N.S.
Imperial Oil Enterprises Ltd., Montreal, P.Q.
Imperial Oil Enterprises Ltd., Sarnia, Ont.
Irving Refinery Ltd., St. John, N.B.

Keystone Lubricating Co., Scarborough, Ont.

Ladouceur's Garage, Alexandria, Ont.
Laurentide Aviation Ltd., Montreal, P.Q.
Leigh Instruments Ltd., Carleton Place, Ont.
Levy Auto Parts, Toronto, Ont.
Levy Industries Ltd., Toronto, Ont.
Litton Industries Limited, Toronto, Ont.
Lockwood Survey Corp., Ltd., Toronto, Ont.
Lockwood Survey Corp., Ltd., Vancouver, B.C.
Lubrizol Corporation, Don Mills, Ont.
Lubrizol Corporation, Cleveland, Ohio, U.S.A.

Manning, Bruce, Paterson & Ridout, Toronto, Ont.
McDonnell & Ryan Insurance Adjusters, Ottawa, Ont.
Measurement Control Engineering, Arnprior, Ont.
Milne, Gilmore & German, Montreal, P.Q.

Montreal Transportation Commission, Montreal, P.Q.
Muirheads Ltd., Carleton Place, Ont.

Noranda Copper Refining Industries Ltd., Montreal, P.Q.
Noranda Research Centre, Pointe Claire, P.Q.
Northern Canada Power Commission, Ottawa, Ont.

Orenda Ltd., Toronto International Airport, Ont.
Ottawa Civic Hospital, Ottawa, Ont.
Ottawa Transportation Commission, Ottawa, Ont.

Pioneer Chain Saws, Peterborough, Ont.
Precision Electronics Components Ltd., Toronto, Ont.

Quebec Hardwoods Inc., Hull, P.Q.

Range Aerial Survey Ltd., Calgary, Alta.
Renfrew Electric Co., Ltd., Renfrew, Ont.
Rolls-Royce (Montreal) Limited, Montreal, P.Q.
Royalite Metal Furniture Co. Ltd., Smiths Falls, Ont.

Dr. George Sander, Ottawa, Ont.
Sandia Corporation, Albuquerque, New Mexico, U.S.A.
Schofield de Vries Ltd., Breslau, Ont.
Sheldons Engineering Ltd., South Galt, Ont.
Shell Canada Ltd., Montreal, P.Q.
Shell Canada Ltd., St. Boniface, Man.
Shell Canada Ltd., Toronto, Ont.
Shell Canada Ltd., Vancouver, B.C.
Sheridan Controls Limited, Oakville, Ont.
SPAR Aerospace Products Ltd., Toronto International Airport, Ont.
Spartan Air Services Ltd., Ottawa, Ont.
Sperry Gyroscope Company, Ottawa, Ont.
Sperry Gyroscope Company, Montreal, P.Q.
Survair Limited, Ottawa, Ont.
Sun Oil Canada Ltd., Toronto, Ont.

Taylor Instruments Co. Ltd., Toronto, Ont.
Terra Surveys Limited, Ottawa, Ont.
Timmins Aviation Ltd., Dorval, P.Q.

Union Carbide Canada Ltd., Montreal East, P.Q.
United Aircraft of Canada Ltd., Longueuil, P.Q.

Vale Enterprises, Montreal, P.Q.
Vapor Heating Ltd., Montreal, P.Q.

Williams Research Corporation, Walled Lake, Michigan, U.S.A.

GOVERNMENT DEPARTMENTS

Admiralty Underwater Weapons Establishment, Portland, England.
Atomic Energy of Canada, Ottawa, Ont.

Canadian Armed Services (AETE) Uplands, Ont.
Canadian Broadcasting Corporation, Ottawa, Ont.
Canadian Government Specifications Board, Ottawa, Ont.
Canadian National Railways, Montreal, P.Q.
Canadian Wildlife Service, Ottawa, Ont.
Corporation of the City of Ottawa Limited, Ottawa, Ont.

Defence Research Board, CARDE, Valcartier, P.Q.
Defence Research Board, Ottawa, Ont.
Department of Defence Production, Ottawa, Ont.
Department of Energy, Mines & Resources, Ottawa, Ont.
Department of Fisheries, Ottawa, Ont.
Department of Forestry, Forest Products Research Branch, Ottawa, Ont.
Department of Forestry and Rural Development, Ottawa, Ont.
Department of Industry, Ottawa, Ont.
Department of Justice, Ottawa, Ont.
Department of National Defence, (AIR), Ottawa, Ont.
Department of National Defence, (ARMY), Ottawa, Ont.
Department of National Defence, (NAVY), Ottawa, Ont.
Department of National Defence, Quality Assurance Branch, Ottawa, Ont.
Department of Public Works, Ottawa, Ont.
Department of Transport, Ottawa, Ont.
Department of Transport, Prescott, Ont.

Federal Aviation Agency, Washington, D.C., U.S.A.

Geological Survey of Canada, Ottawa, Ont.

Hydro-Quebec, Montreal, P.Q.

National Capital Commission, Ottawa, Ont.
National Film Board, Montreal, P.Q.
National Harbours Board, Montreal, P.Q.
National Space and Aeronautical Museum, Ottawa, Ont.

Ontario Department of Lands and Forests, Toronto, Ont.

Royal Aircraft Establishment, Bedford, England
Royal Australian Air Force, Australia

United States Navy Washington, D.C., U.S.A.
USAF CL-84 Tri-Service Evaluation Team, Fort Eustis, Virginia, U.S.A.

UNIVERSITIES

Carleton University, Ottawa, Ont.
McGill University, Montreal, P.Q.
Ottawa University, Ottawa, Ont.
Queen's University, Kingston, Ont.
University of Alberta, Edmonton, Alta.
University of Toronto, Toronto, Ont.
University of Western Ontario, London, Ont.